THE UNIVERSITY of EDINBURGH

A NOVEL SYNTHESIS OF TRIPODAL BORATE LIGANDS

ALEJANDRO SANCHEZ PERUCHA M.Sc.

A Thesis Submitted for the Degree of

Doctor of Philosophy

The University of Edinburgh

January 2007

DECLARATION

I hereby declare that this thesis has been entirely composed by myself and that the work described herein is my own except where clearly mentioned either in acknowledgement, reference or text. It has not been submitted, in whole or in part, for any other degree, diploma or other qualification.

Alejandro Sánchez Perucha

ACKNOWLEDGEMENTS

Three years have passed by since I first arrived in Edinburgh. During this time I have had the chance to meet different people from all over the world without whom this thesis would be completelly different. I would like to acknowledge first my supervisor Dr. Philip Bailey for his encouragement and always polite treatment towards me and my work. The freedom I have experienced in the lab has given me the chance to learn a lot not only about chemistry but more important, about myself. Thank you Phil. I also would like to thank the people I have been working with in the Bailey´s lab during these three years, in special Michele Melchionna for sharing the "same boat" during all this time; Felix Rudolphi for all his hard work during the summer of 05; Robert and Andrea Pfeifer for their hospitality and always interesting conversations; and past and present members who are too many to be all mentioned here. I have been really lucky of being part of the European Network AC3S which has given me the possibility of meeting outstanding researchers from Europe. I would like to express my more sincere acknowledge and respect to the whole School of Chemistry staff that have always been ready to help me during this time with special thanks to John Millar. This thesis would not be the same without the International community of the Edinburgh University who welcome me when I first arrived and made these three years the happiest ones of my life. Dr. Metal Mike, Abraha, Alessandro, Andrea, Chiara and Davide, Daniela, Chris and Elaine, Emiliano, Irene, Laurent, Maraki, Pekka and Rosa, Anestis, Thanasis, Gggiorgos, Matinaki mou… thanks for everything. I owe a special mention to my Spanish community. Ana, Catione, Chimooo, Laia y Diego, Isa y Rafferty, Javi y Spartacus, Albi y Luis, Iria y el Gondoliere, Pilar, Pepe, Tere y Pablo, gracias a todos, os voy a echar de menos.

Last but not least, I want to thank my parents and my sister for their unconditional support throughout these three years. I know it has not been easy at all; two new members, Sofía and Martina, have joined us in the meantime, friends have left… without your support I would have not been able to stand all this time.

ABSTRACT

Poly(azolyl)borate ligands have proven to be extremely popular ligands since their introduction by Trofimenko in the late 60´s. The basic skeleton of these ligands involves usually three heterocycle units linked to a central boron apex via the azole nitrogen atoms. These ligands have been applied in diverse research areas such as homogeneous catalysis, materials science and bio-inorganic chemistry. More than 2000 papers, including books and reviews regarding the properties of these compounds, have been published. However, only a few synthetic methods for the preparation of such ligands have been reported and only a few examples of chiral borate-centred ligands are known. This thesis deals with the development of a novel synthetic route to tripodal borate ligands using $B(NMe_2)_3$ as the boron source. The mechanism of the reaction of this borane with azole heterocycles has been established by exploring the reactivity of a range of azoles. One of the major features of this new synthetic protocol is that it allows the formation of chiral tripodal ligands where the chiral groups are located either at the forth position at the boron atom or at the azole heterocycles. Coordination studies of the ligands have been undertaken and the metal complexes have been studied by a combination of spectroscopic and X- ray diffraction techniques. Preliminary application of the most representative ligands in the Asymmetric Transfer Hydrogenation (ATH) of prochiral ketones has been undertaken in collaboration with Prof. Dieter Vogt at the Technical University of Eindhoven.

TABLE OF CONTENTS

ABBREVIATIONS

Ar, ar	Aromatic
ATH	Asymmetric Transfer Hydrogenation
Bn	Benzyl
BINAP	2,2´-dihydroxi-1,1´-binaphtyl
BINOL	2,2´-bis(diphenylphosphino)-1,1´-binaphtyl
br	Broad
BuLi	Butyllithium
^{n}Bu	Butyl
COE	Cyclooctene
Cp	Cyclopentadiene
Cy	Cyclohexyl
D	Doublet
d.e.	Diastereomeric excess
DBU	1,8-diazabicyclo[5.4.0]undec-7-ene
DCM	Dichloromethane
DFT	Density Functional Theory
DABCO	1,4-diazabicyclo[2.2.2]octane
DMF-DMA	Dimethylformamide-dimethylacetal
DMAP	Dimethylaminopyridine
DMSO	Dimethylsulphoxide
e.e.	Enantiomeric excess
ES-MS	Electrospray Mass Spectrometry
Et	Ethyl
Et_3N	Triethylamine
Et_2O	Diethylether
FAB-MS	Fast Atom Bombardment Mass Spectrometry
fac	Facial
Hpz	Pyrazole
Hz	Hertz
H	Hydrogen
IPA	Isopropylalcohol
IR	Infrared
J	spin-spin coupling constant
K	Kelvin
Kj mol^{-1}	Kilojoule per mol

LADH	Liver alcohol dehydrogenase
LDA	Lithium diisopropyl amide
m	Multiplet
M	Molar (mol l^{-1})
m	*Meta*
M.p.	melting point
Me	Methyl
MeCN	Acetonitrile
MeLi	Methyllithium
Methimazole, mt	2-mercapto-1-methylimidazole, 3-methyl-1-imidazolyl-2-thione
Mmol	Millimoles
MPV	Meerwein-Ponndorf-Verlay reduction
NMR	Nuclear Magnetic Resonance
NMe_2	Dimethylamine
o	*Ortho*
p	*Para*
p-cym	*para*-cymene
Ph	Phenyl
ppm	parts per million
^{i}-Pr	Isopropyl
q	Quartet
Ru_{MeCN}	$Ru(MeCN)_4(Cl)_2$
Ru_{pcym}	$[Ru(p\text{-cymene})Cl_2]_2$
s	Singlet
S_{N1}	Nucleophilic Substitution 1
S_{N2}	Nucleophilic Substitution 2
t	Triplet
TH	Transfer Hydrogenation
THF	Tetrahydrofuran
TLC	Thin layer chromatography
Tm	hydrotris(2-mercapto-1-methylimidazolyl)borate
TMEDA	Trimethylethylenediamine
$Tp^{Me}{}_2$	hydrotris(3,5-dimethylpyrazolyl)borate
Tp	hydrotris(pyrazolyl)borate
TRISPHAT	[Tris(tetrachlorobenzenediolato)phosphate(V)] anion
Tt	hydrotris(thioxotriazolyl)borate
ZTm	Zwitterionic Tm ligand
ZTp	Zwitterionic Tp ligand

CHAPTER I

SYNTHESIS OF BORATE-CENTRED LIGANDS

1.1 INTRODUCTION

Borate ligands were first studied by the Dupont chemist Jerry Trofimenko in 1966.[1] He was dedicating his own part-time research to the study of boron-pyrazole chemistry when he synthesised the tetrapyrazolyl borate $[B(pz)_4]^-$ anion upon bubbling BCl_3 into molten pyrazole. Addition of this ligand to a solution of $FeCl_3$ yielded crystals of the composition $Fe[B(pz)_4]_2^+[FeCl_4]^-$ where the $B(pz)_4^-$ moiety is coordinating the Fe centre with three pyrazolyl groups in a κ^3-fashion. This was the very first example of a family of ligands known as *Scorpionates* which, since their inception, have been reported in more than 2000 papers and complexed to around 70 elements of the periodic table. The most extensively studied member of the family is the hydrotris(pyrazolyl)borate ligand (**1.1**), abbreviated as Tp (Fig. **1.1**). The name scorpionate derives from the way the ligand coordinates to metal centres. Two pyrazole rings form a deep boat conformation upon complexation whilst the third ring, rotates forwards like a scorpion's tail to "sting" the metal atom.

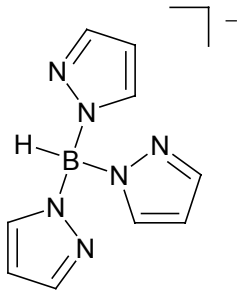

1.1

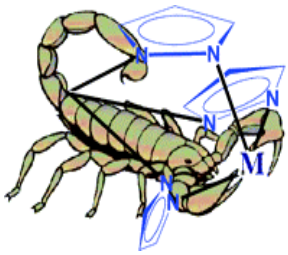

Fig. 1.1. *Tp ligand* (**1.1**) *and illustrative picture of their resemblance to a scorpion.*

This ligand resembles the anionic, facial-capping, six electron donor (ionic model) cyclopentadienyl ligand (Cp), but with a strong tendency to forming *fac*-octahedral complexes. An important advantage of these ligands compared to Cp is that they are highly tunable. It is possible to modify them in various ways by introducing different substituents on the pyrazole rings which has been found to influence the coordination behaviour of the resulting ligands (**1.2**). Also by using different azole heterocycles other than pyrazole, like methimazole or imidazole, to

yield ligands with alternative donor groups (**1.3**). The third way of modification is by replacing the boron central atom by phosphorus, carbon, or silicon to yield analogous neutral ligands (**1.4**).[2]

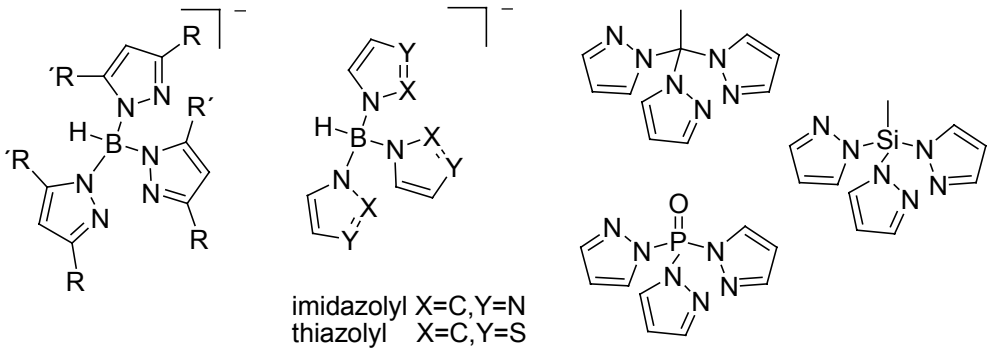

1.2 **1.3** **1.4**

Fig. 1.2. *Different modifications of the Tp framework.*

1.2. BOROHYDRIDE ROUTE

Due to all the possible modifications, a lot of attention was given to these ligands. The first improvement was in their synthesis; heating together a borohydride salt and pyrazole at the melting temperature (T_1) of the latter, it was possible to synthesise bis, tris or tetra-pyrazolyl borates by controlling the temperature of the reaction (Scheme **1.1**). High temperatures induce pyrazolyl substitution at the boron centre. This reaction is carried out in a solvent-free environment and it is known as the *melt reaction*. This procedure remains nowadays the general route to the synthesis of anionic borate ligands, but it has been found to be of limited applicability since it depends on the pK_a and the melting point of the heterocycle.[3]

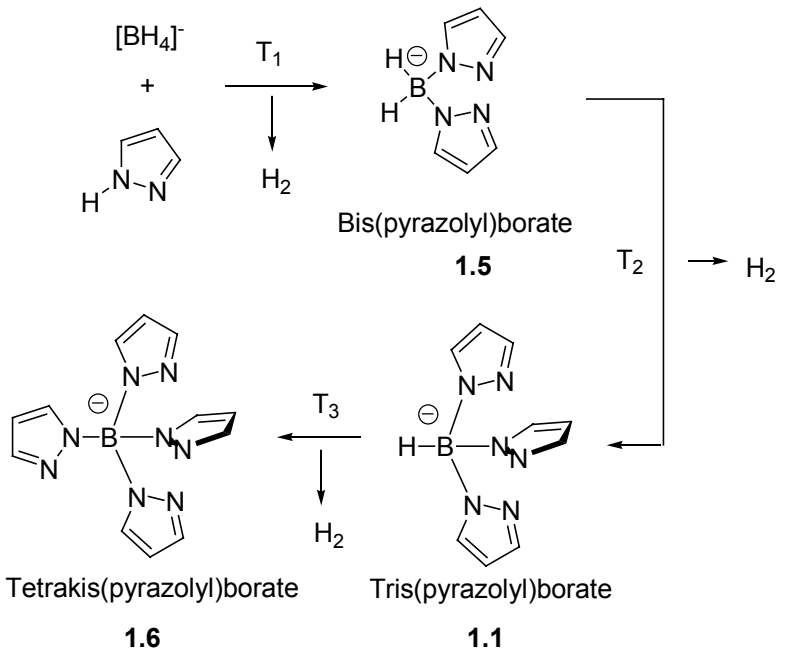

Scheme 1.1. *Synthesis of poly(pyrazolyl)borates by temperature control of the reaction.*

More than 200 different poly(azolyl)borates have been efficiently synthesised by heating tetrahydroborate salts with the chosen heterocycle in a melt reaction. It is a convenient route since the release of H_2 as by-product can be used to follow the progress of the reaction. The use of a high boiling point solvent like xylenes or diglyme has also been reported in the synthesis of these ligands.

Some interesting examples of tripodal ligands synthesised using this methodology are discussed next. In Fig. **1.3**, tripodal ligands where the pyrazolyl rings have been replaced by imidazolyl, methimazolyl, thioxotriazolyl and triazolyl groups are shown. These ring modifications have lead to a set of novel ligands that have been applied in different research areas from bioinorganic to materials science, due to their special coordination properties.

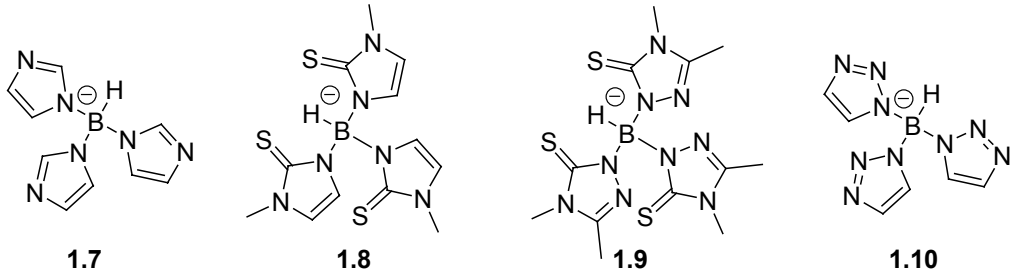

1.7 **1.8** **1.9** **1.10**

Fig. 1.3. *Tris(azolyl)borates from imidazole, methimazole, thioxotriazole and triazole.*

An interesting example is the hydrotris(methimazolyl)borate ligand (Tm) (**1.8**) reported by Reglinski in 1996.[4] It can be regarded as an analogue of Tp, but presenting softer sulphur donor atoms. It has been mainly used in bioinorganic chemistry to mimic zinc metalloproteins which are known to present sulphur-rich active centres, like the liver alcohol dehydrogenase (LADH) or the thiolate alkylating enzymes.[5] When this ligand coordinates the metal atom in a κ^3-fashion, three eight-membered chelate rings are formed contrasting with the six-membered rings formed by Tp as shown in the Fig. **1.4**. The reason for this difference is the presence of a diatomic unit (N-C) between the central boron (E) and the sulphur donor atoms (D), whilst the Tp system contains just a single nitrogen linking atom (L). The two ligands can thus be categorized as $E(L_2D)_3$ and $E(LD)_3$ respectively. This difference affects the geometry and symmetry of the resulting metal complexes. While the Tp ligand forms a bicyclo[2.2.2]-cage with ideal C_{3v} symmetry, the Tm forms a bicyclo[3.3.3]-cage that undergoes a twist to relieve angle strain, thus forming C_3-symmetric complexes.

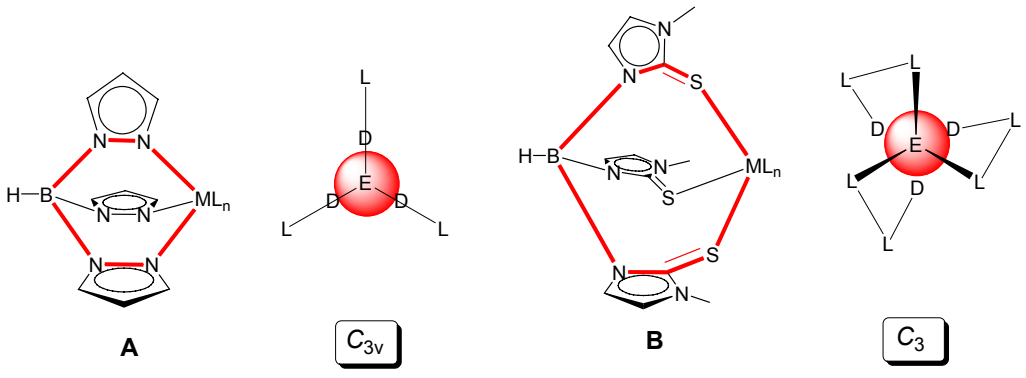

A C_{3v} **B** C_3

Fig. 1.4. *Tp and Tm ligand form six (A) and eight (B) membered chelate rings that result in different complex geometries.*

This propeller-like ligand conformation of the Tm ligand around the metal centre confers helical chirality to the resulting complex. The two possible enantiomers (Λ and Δ) are displayed depending on the direction of helical rotation, (Λ = anticlockwise twisting, Δ = clockwise twisting) as is shown in the figure below.

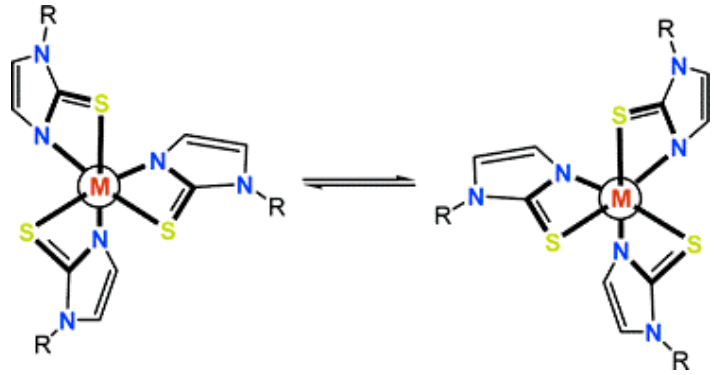

Fig. 1.5. Λ and Δ *enantiomers formed upon complexation of Tm to a metal centre.*

An interesting example that links both Tp and Tm families is the case of the hydrotris(thioxotriazolyl)borate (Tt) ligand (**1.9**).[6] Since the azole heterocycle contains both the hard nitrogen and the soft thione donor atoms this ligand is considered as a highly flexible ligand that potentially offers either N_3, S_3 or intermediate coordination modes depending on the steric and electronic requirements of the metal. Therefore, complexation to the hard sodium cation was found to be preferred through the nitrogen groups whilst the three thione groups were used to coordinate softer cations like bismuth (III) (Fig. **1.6**).

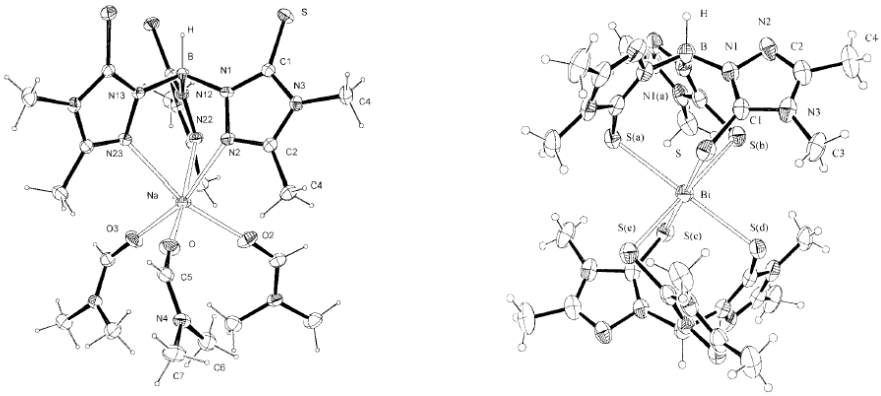

Fig. 1.6. *Na and Bi complexes of Tt showing the different coordination behaviour.*

The Tt ligand coordinates to the relatively soft manganese(I) cation through the nitrogen donors indicating a crossover point between hard nitrogen and soft sulphur coordination where thermodynamic issues regarding the eight versus six membered chelate rings are also considered to influence the observed coordination mode.

Using the melt reaction methodology Tolman and coworkers reported the first chiral pyrazolyl borate ligand in 1994.[7] The chiral pyrazoles were synthesised from chiral ketones such as *R*-(+)-camphor, or *R*-(+)-pulegone as starting materials. Melt reaction between three equivalents of the enaniopure pyrazole and potassium, borohydride yielded the chiral tripodal ligands in relative good yields (70%) (Fig. **1.7**).

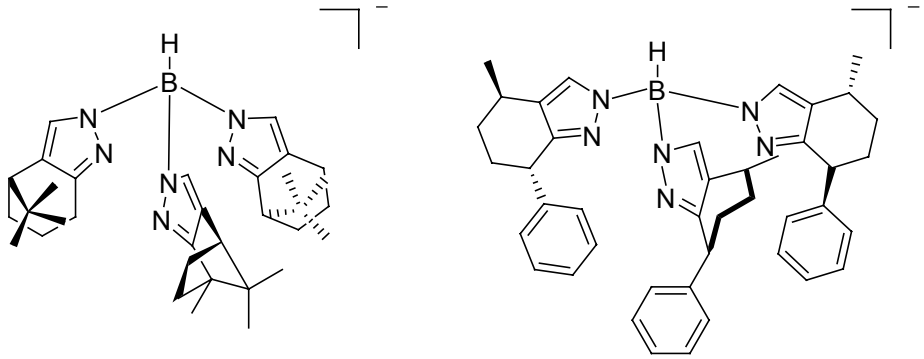

1.11 **1.12**

Fig. 1.7. *Selected examples of chiral Tp ligands reported by Tolman.*

The ligand derived from *R*-(+)-pulegone (**1.12**) has been applied in the copper catalysed asymmetric cyclopropanation of styrene with ethyldiazoacetate, this being the first case reported of a Tp system inducing high enantioselectivities in a catalytic reaction (81% ee trans, 85% ee cis) (Scheme **1.2**).

Scheme 1.2. *First reaction catalysed by a Scorpionate complex.*

When using KBH_4 as the boron source for the synthesis of tripodal ligands, the forth position at the boron remains always occupied with a hydrogen atom. There are no reports in the literature of ways to substitute this hydrogen; therefore, to synthesise tripodal borate ligands bearing different groups at the forth position, another boron starting source must be used. The use of $^t BuBH_3Li$ for the synthesis of scorpionates using the melt procedure has recently been reported, where the fourth position at the resulting borate ligand is occupied by a tertbutyl group.[8] This group at the boron centre is able to increase the solubility of the ligand in apolar solvents and prevents possible ligand degradation at the B-H bond.

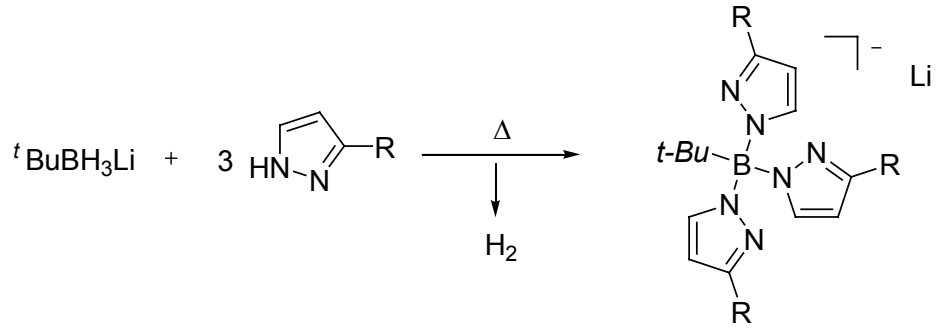

1.13 **1.14**

Scheme 1.3. *$^t BuBH_3Li$ has also been used in the melt reaction.*

Although several tripodal borate ligands have been synthesised by melting the chosen heterocycle with a borohydride salt, this synthetic procedure has been found to be quite limited.[3] Both the melting point and the acid pK_a of the azole heterocycle must be within a specific range for the reaction to occur. The next section will cover alternative synthetic procedures for the synthesis of poly(azolyl)borate ligands reported to date.

1.3. FROM BORON HALIDES

1.3.1 $BF_3{\cdot}Et_2O$

Boron trifluoride etherate has rarely been used in the synthesis of borate ligands, although a couple of examples are reported in the literature. The difluorobis(3,5-dimethyl-1-pyrazolyl)borate salt (**1.16**) was synthesised by reacting 3,5-dimethylpyrazolide freshly prepared from 3,5-dimethylpyrazole and sodium hydride, with boron trifluoride etherate (**1.15)** in refluxing THF during 12 hours. After workup, the anion was isolated in the form of its cobalt or nickel chelates (**1.17**).[9]

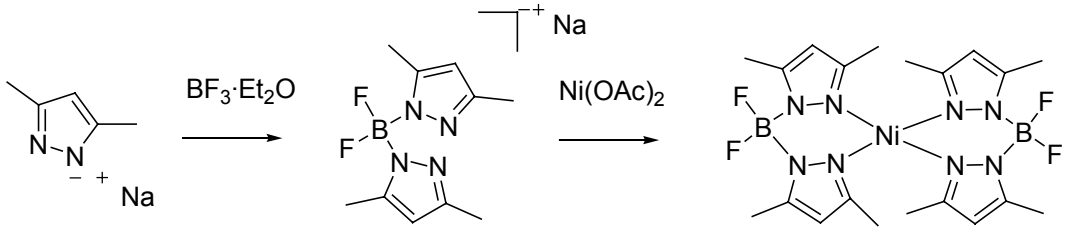

Scheme 1.4. *Synthesis of difluorobis(3,5-dimethyl-1-pyrazolyl)borate salt.*

The second example is the cesium salt of tetrakis(2-thienyl)borate (**1.18**) reported by Moore and Pacey from the reaction of 2-thienyllithium with boron trifluoride etherate followed by aqueous workup with cesium chloride to precipitate the salt.[10]

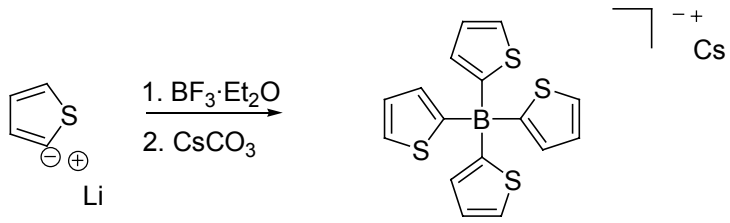

1.18

Scheme 1.5. *Synthesis of the cesium salt of tetrakis(2-thienyl)borate.*

Curiously, this ligand was found to be unable to coordinate to any metal centre and Riordan and coworkers have studied the reason through an elegant molecular orbital analysis.[11] They reported that the coordination behaviour of this ligand was related to the localization of the electronic charge density in the sulphur lone pair orbitals and that the coordination strength was proportional to the amount of electron density donated from the ligand onto the metal. Delocalization of the sulphur lone pair charge density through conjugation with the adjacent π-bonds was found to dramatically reduce the Lewis basicity of the ligand preventing the formation of stable metal complexes.

1.3.2 BBr_3

The synthesis of scorpionates using **boron tribromide** has recently been reported by Reger and coworkers.[12] Treatment of BBr_3 with a trimethylsilane derivative caused the substitution of bromide to form (**1.19**). This resulting dibromoborane was then reacted with three equivalents of pyrazole to form the tripodal ligand. In-situ reaction with ^{t}BuONa finally formed the sodium salt (**1.20**). Complexation to $FeCl_2$ in a 2:1 ratio yielded the octahedral iron (II) complex (**1.21**) where all pyrazole groups are occupying the six coordination sites at the metal centre.

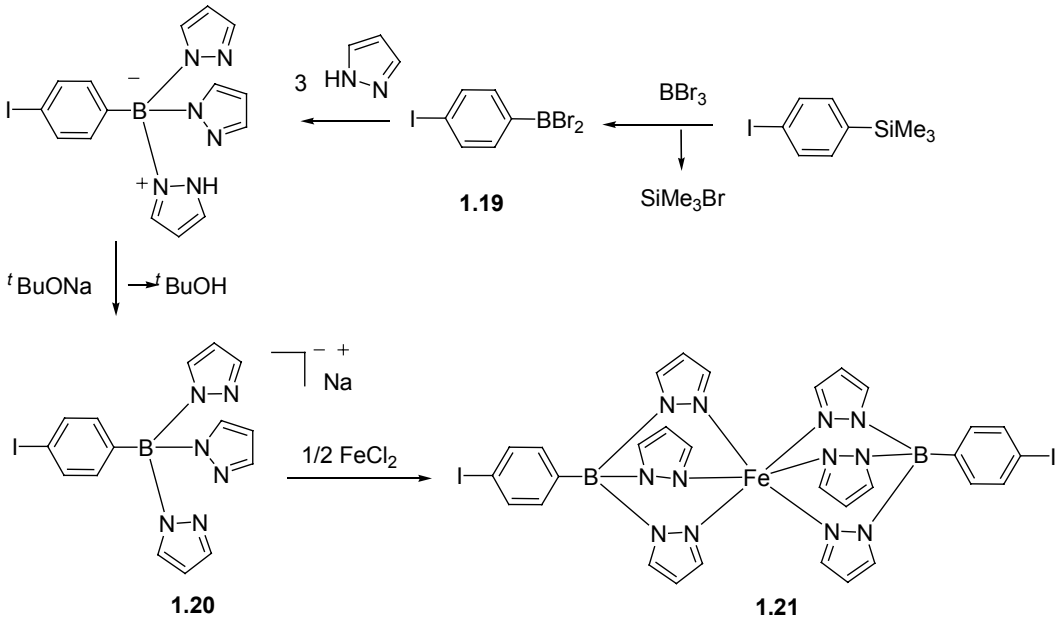

Scheme 1.6. *Synthesis of the scorpionate* **1.20** *and formation of an iron (II) complex.*

The iodine group of the aromatic ring that occupies the forth position at the boron in **1.20** can be used to functionalise these complexes. Sonogashira coupling with terminal alkynes catalysed by Pd(II) allowed the introduction of different groups at this position which are known to influence both the electronic and the magnetic properties of the resulting complexes.[12]

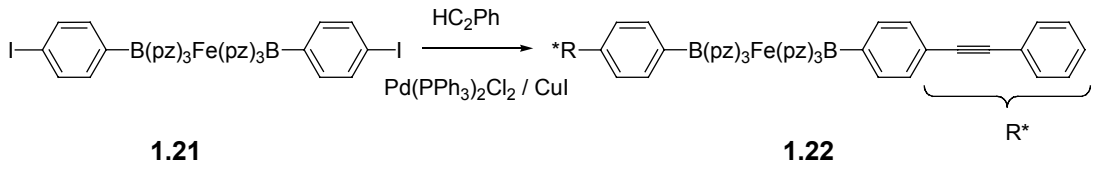

Scheme 1.7. *Sonogashira coupling functionalises the "back" non-coordinating position of the scorpionate complexes.*

1.3.3 $PhBCl_2$

Substituted chloroboranes like **dichlorophenylborane** have also been used in the synthesis of tripodal borate ligands where the phenyl group ends up occupying the forth position at the boron centre. Slow addition of $PhBCl_2$ to a solution of excess pyrazole in toluene formed the tripodal ligand (**1.23**) that was found to coordinate in a κ_3-fashion to a wide range of transition metals like Mn, Fe, Co, Ni, Cu and Zn.[9]

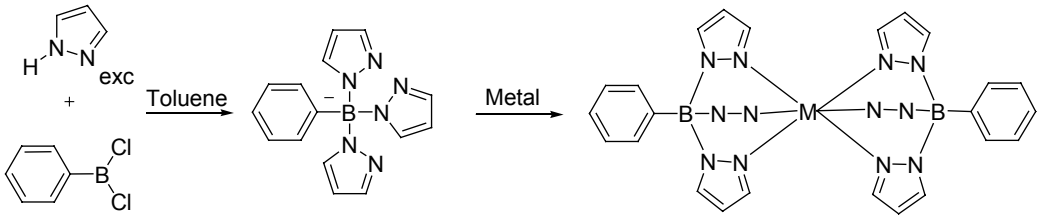

1.23 **1.24**

Scheme 1.8. *The forth position at the boron is now occupied by a phenyl group.*

This starting material has also been used in the synthesis of anionic tripodal borate ligands with alkyl or aryl substituted phosphino[13] and thioether[14] donor groups. The synthesis of both kinds of ligands is similar, starting with the deprotonation of the appropriate methylphosphine or methylsulfide with BuLi in the presence of TMEDA. The resulting anion was then added to a solution of dichlorophenylborane to form the tripodal anionic ligands in very good yield. These borate ligands could be isolated or reacted *in situ* with metals to form complexes where the substituents at the phosphorus or sulphur donor arms serve to encapsulate the metal centre. Due to the negative charge at the boron atom, these metal complexes exist in a zwitterionic form. Complexes of this type have shown to be a promising approach to novel homogeneous catalysts.[15]

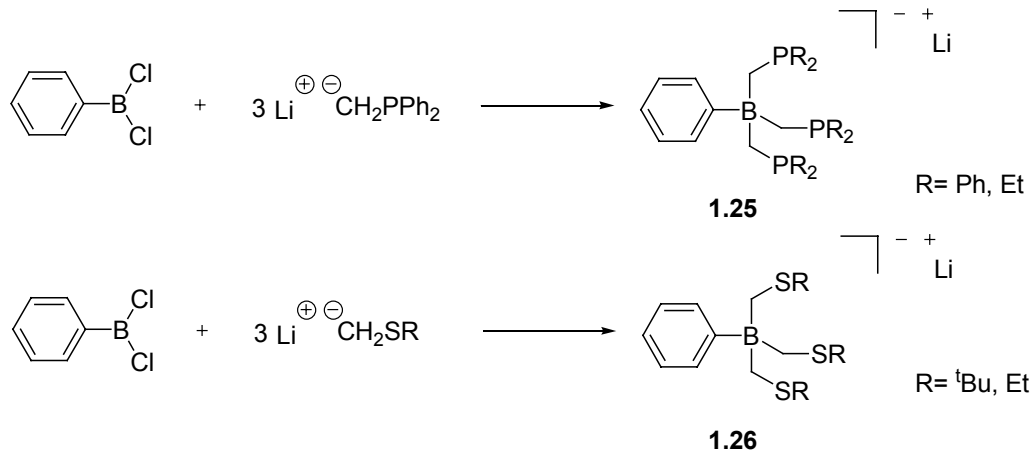

Scheme 1.9 *Synthesis of tripodal ligands from dichlorophenylborane.*

1.3.4 Ph_2BCl

Nitrogen donor tripodal ligands analogous to those above have yet to be reported. However, the use of **chlorodiphenylborane** led to the synthesis of bipodal ligands with nitrogen donor groups.[16] The methodology is quite similar in concept; the nucleophilic carbanion $BH_3Me_2NCH_2Li$ was synthesised from the BH_3NMe_3 adduct by deprotonation with BuLi. On reaction with half equivalent of the chloroborane source a bidentate ligand was formed where both nitrogen atoms remained protected with BH_3 groups. Deprotection with DABCO finally yielded the bipodal borate ligand (**1.28**).

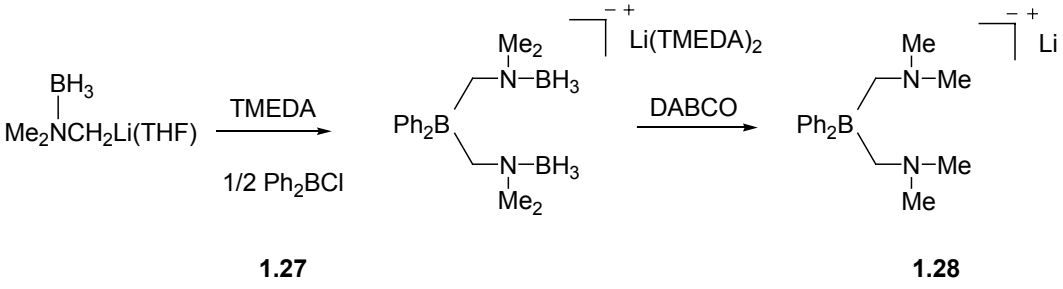

Scheme 1.10. *Bipodal ligands are also available from disubstituted boranes.*

1.3.5 (Ipc)BCl_2

Using an enantiopure boron halide source like **isopinocampheylboron dichloride**, our lab reported in 2003 the first example of a tripodal scorpionate with a chiral group attached directly to the boron atom.[17] The isopinocampheylboron dichloride was reacted with sodium pyrazolide in dry THF to yield sodium isopinocampheyltris(pyrazolyl)borate (**1.30**). This hygroscopic salt was then used to synthesise transition metal complexes of manganese and ruthenium. The chiral group at the boron, although far from the metal centre, was found to interact with the 3 positions of the pyrazolyl rings leading to distortion of the angles around the B-C bond.

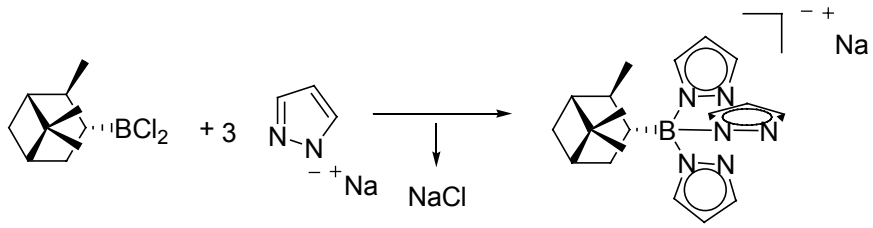

1.29 **1.30**

Scheme 1.11. *Enantiopure borane for the synthesis of a chiral scorpionate.*

1.3.6 $MeBBr_2$

Dibromomethylborane is another boron halide source for the synthesis of tripodal ligands where the methyl group will finally occupy the forth position at the boron centre. In a one pot reaction and under very mild conditions (toluene, room temperature), the synthesis of the thallium tris(pyrazolyl)borate (**1.32**) salt was reported.[18]

There are two main advantages in the use of this methodology; the reaction conditions allow the use of thermally unstable pyrazole heterocycles as starting azoles and second, this route directly yields the thallium borate salts which are known to be versatile reagents for pyrazolylborate ligand transfers to other metals.[19]

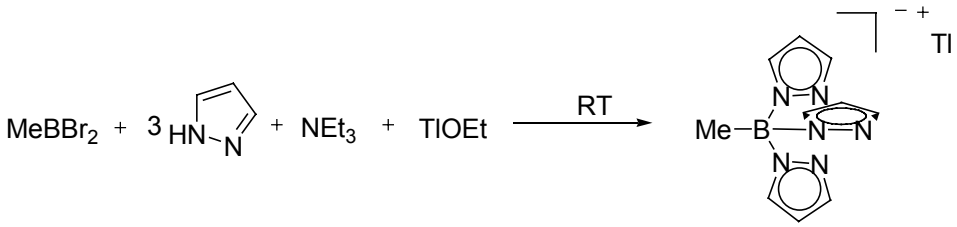

1.31 **1.32**

Scheme 1.12. *One pot synthesis of a thallium scorpionate under mild reaction conditions.*

1.3.7 $FcBBr_2$

An analogous precursor, **dibromoferrocenylborane**, has also been reported for the synthesis of redox active-ferrocene based scorpionates.[20] Ferrocene is an ideal starting material since it can be borylated up to four times and it shows a reversible one-electron redox process. The dibromoferrocenylborane was transformed into the dimethylamine derivative as shown in Scheme **1.11**. This borane was further reacted with one equivalent of lithium pyrazolide and two equivalents of pyrazole to form the ferrocenyl tris(pyrazolyl) borate salt (**1.35**) in almost quantitative yield.

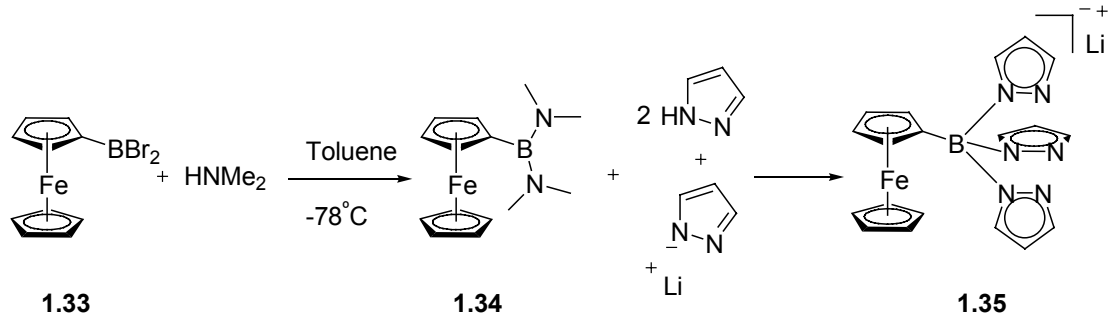

1.33 **1.34** **1.35**

Scheme 1.13. *Synthesis of a Ferrocene scorpionate.*

This ligand (**1.35**) has been reported to coordinate to a variety of metal complexes in the expected κ^3-mode. However, the thallium complex is an exception to this, being the first scorpionate to adopt a polymeric structure in the crystal lattice and therefore will be discussed next. Each thallium coordinates to two pyrazolyl rings of one scorpionate ligand and to one pyrazolyl group of another ligand generating the polymeric structure. This special coordination must be due to the bulky ferrocenyl group attached to the boron centre since for the hydrotris(pyrazolyl)borate thallium salt, a monomeric structure has been reported. This higher degree of steric crowding is visible in the X-ray structure (Fig. **1.8**). The asterisk (*) shows an unfavourable intramolecular short distance between the ferrocene and a pyrazole ring. A neighbouring pyrazole group stays away from the ferrocene to avoid a similar interaction and this is the reason why it does not coordinate the same thallium atom.

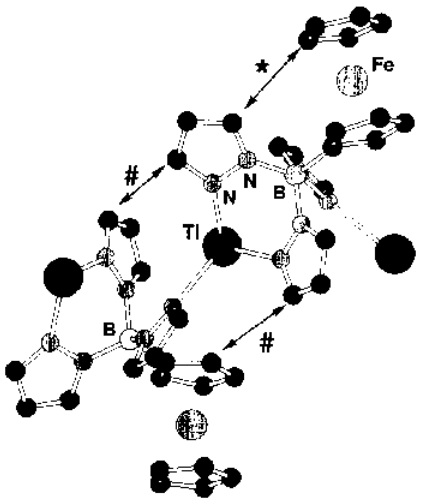

Fig. 1.8. *X-ray structure of theTl ferrocenyl scorpionates.*

1.3.8 PhB(Br)(NMe$_2$)

The same group has reported the synthesis of an interesting ligand using **bromo(dimethylamine)phenylborane** as starting material.[21] Hydrolysis of this compound with half equivalent of water in the presence of triethylamine led to the

1,3-diboroxane which was further reacted with pyrazole and lithium pyrazolide to form the anionic tridentate (N, N, O) chelator (**1.35**) shown in Scheme **1.14**.

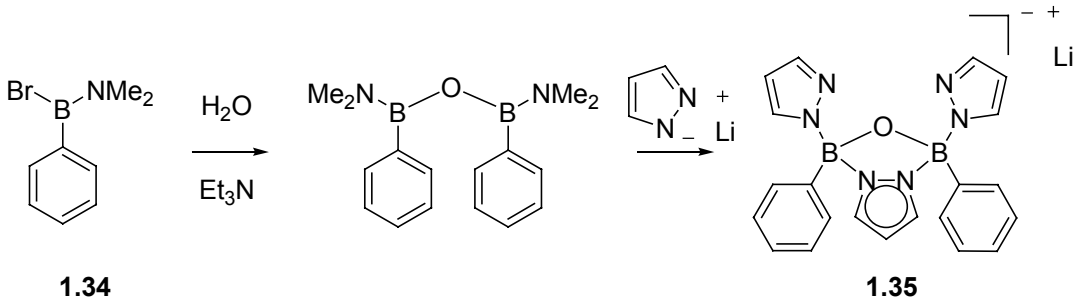

1.34 **1.35**

Scheme 1.14. *Synthesis of the first "trans"-scorpionate.*

The most interesting feature of the pyrazolyl ligand (**1.35**) is that it is the only example reported of an almost *trans*-coordinating scorpionate ligand. When coordinated to Fe(II), Fe(III), and Cu(II), the (pz)N-M-N(py) bite angle values reported lie between 118° and 150° whilst in the case of *cis*-coordinating scorpionates the bite angles are always lower than 104°. However, when compared (**1.35**) to known *trans*-coordinating ligands like $[(ArNCH_2CH_2)_2]^{2-}$, which form metal complexes with bite angles close to 180°, it is clear that the ligand (**1.35**) is not able to coordinate in a truly *trans* fashion. The reason was reported to be the simultaneous presence of a sp^3 oxygen, two sp^3 boron atoms and the pyrazolyl six-membered ring that prevents a fully planar coordination mode of the ligand upon metal complexation.

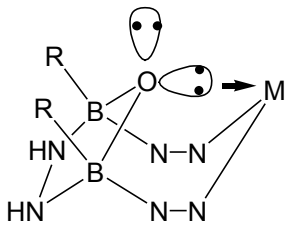

Fig. 1.10. *The ligand can not coordinate "trans" to the metal.*

1.3.9 $Me_3N:BHBr_2$

Borate ligands incorporating *N*-heterocyclic carbene donors (NHC) have been reported in the literature by Fehlhammer and coworkers.[22] Using the melt procedure, hydrotris(imidazolyl)borate **1.7** was synthesised from imidazole and KBH_4. Methylation at the imine nitrogen atoms, followed by deprotonation at the 2-position with BuLi yielded the tripodal carbene (**1.36**). This ligand reacts with $FeCl_2$ to form a complex where two ligand molecules are simultaneously coordinating the iron centre. The saturation at the metal does not allow further reactivity studies of this complex. A way to avoid this situation would be the insertion of bulky groups at the nitrogen 3 positions to impede the coordination of two ligand molecules to the iron centre due to steric hindrance.

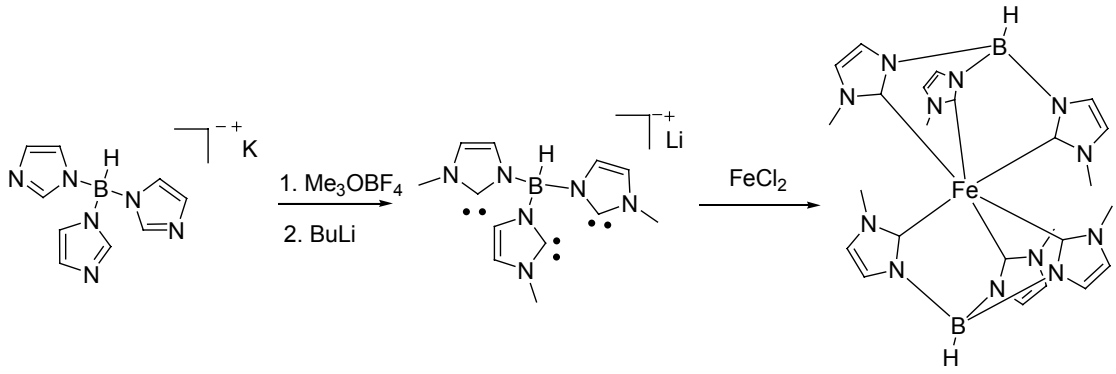

1.7 **1.36** **1.37**

Scheme. 1.15. *NHC´s scorpionate* **1.36** *forms the saturated iron complex* **1.37**.

Recently, the group of Smith has reported a synthetic route to bulky tripodal carbene ligands using **$Me_3N:BHBr_2$** as the boron source.[23] This borane adduct was reacted with three equivalents of tert-butylimidazole in refluxing chlorobenzene to yield the bromo salt (**1.38**). Deprotonation at the 2 position could be performed using one equivalent of MeMgBr to form (**1.39**) which was used as a ligand transfer reagent for the synthesis of the unsaturated four coordinated metal complexes.

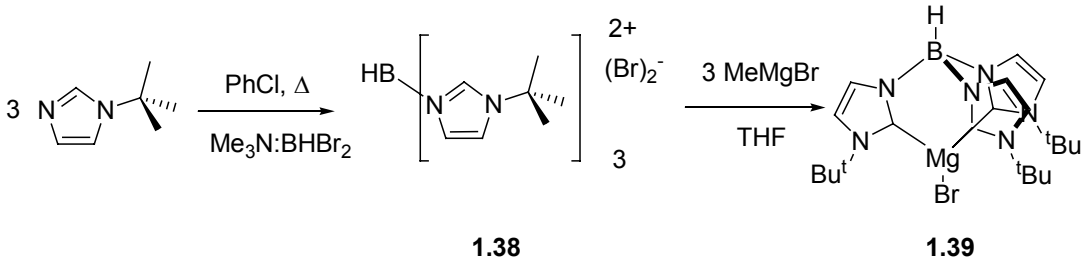

1.38 **1.39**

Scheme 1.16. *Formation of the tripodal carbene complex* **1.39**.

1.4. FROM $B(NMe_2)_3$

Dimethylamino substituted boranes are versatile reagents in the synthesis of scorpionate ligands. Their use was first reported by Niedenzu in 1981.[24] **Tris(dimethylamino)borane** $[B(NMe_2)_3]$ was reacted at room temperature with pyrazole leading to a transamination reaction with liberation of dimethylamine gas to form the zwitterionic [(dimethylamido)tris(1-pyrazolyl)] borate (**1.41**).

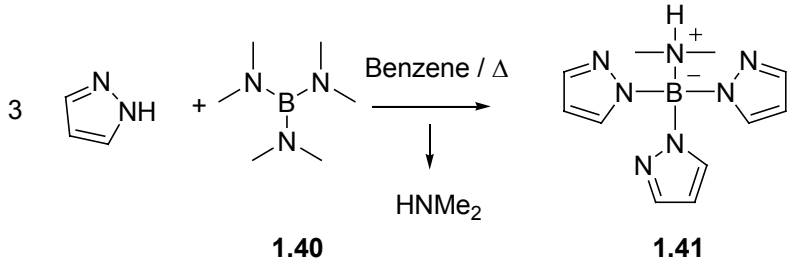

1.40 **1.41**

Scheme 1.17. *Transamination reaction to form the zwitterionic scorpionate* **1.41**.

The forth position at the boron is now occupied by dimethylamine the proton of which undergoes site exchange to the pyrazole nitrogen atoms at room temperature. The borate was readily deprotonated with MeLi to form the anion $[(Me_2N)B(1\text{-pyrazolyl})_3]^-$ that coordinated to the molybdenum precursor $[(MeCN)_2Mo(CO)_2Cl(\eta_3\text{-}CH_2CCH_3CH_2)]$ in a quite unexpected way.

Instead of coordinating to the metal through the three pyrazolyl groups (κ^3-N_{pz},N_{pz},N_{pz}) as observed with the hydrotris(pyrazolyl)borate Tp ligand, the NMe_2 group now competes with a pyrazolyl ring for the coordination. The available lone pairs of the NMe_2 make this group more basic and thus more nucleophilic than the pyrazole; therefore its coordination to the metal is preferred.

Recently Wagner and coworkers have reported the solid-state structures of the alkali metal salts $M[(NMe_2B(pyrazol\text{-}1\text{-}yl)_3]$ (M = Na^+ or K^+) where this unusual (κ^3-N_{pz},N_{pz},N_{NMe}) coordination fashion can be observed (Fig **1.11**).[25]

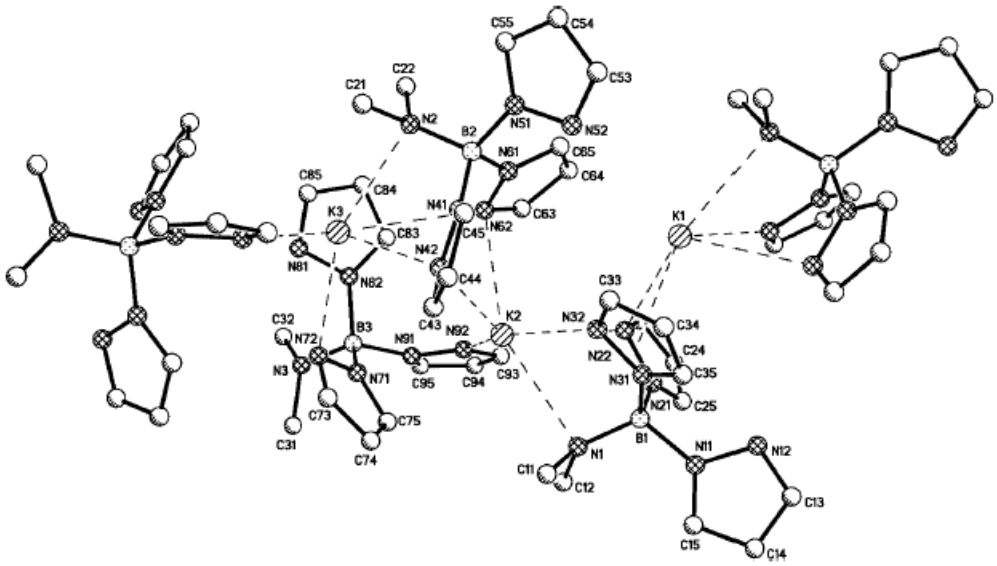

Fig. 1.11. *X-ray structure of* **1.41** *where the ligand adopts a* (κ^3-N_{pz},N_{pz},N_{Nme}) *coordination mode.*

Our group has reported a study of the reaction of $B(NMe_2)_3$ with different azole heterocycles. It was found that the Lewis basicity of the azole influences the reaction outcome.[26] For weakly basic heterocycles like pyrazole, the transamination reaction discussed above takes place to form the dimethylamino adduct of the tris(azolyl)borate $[(HNMe_2)B(azolyl)_3]$.

On the other hand, for more strongly basic heterocycles such as imidazoles, the homotopic tetraazolyl system H[B(azolyl)$_4$] is the only product of the reaction, and furthermore this product is also formed when sub-stoichiometeric ratios of azole and B(NMe$_2$)$_3$ (< 4:1) are used. A mechanism will be proposed which is based on preliminary coordination of the heterocycle to the B(NMe$_2$)$_3$ which transforms its reactivity. If the azole is basic enough (e.g. imidazole) it can coordinate to the free *p*-orbital of the borane and the subsequent transamination reaction yields the homoleptic products. However, if the azole is not basic enough (methimazole, pyrazole) this pathway does not occur, yielding the observed dimethylamine adducts. The results will be covered in detail in the following Chapter.

1.5. TRIALKYLBORANES

Trialkylboranes (alkyl = Me, ^{n}Bu) have also been employed as the boron source in the synthesis of borate ligands.[27] The reaction between the appropriate trialkylborane with sodium pyrazolide followed by heating with excess pyrazole yielded the disubstituted dialkylbis(pyrazolyl)borate ligands (Scheme **1.17**). Even under forcing conditions, it was not possible to substitute the remaining alkyl groups. Since alkyltris(pyrazolyl)borates are known to be stable, the reason must be kinetic in origin. If a S$_N$2 mechanism is proposed, the substitution of a third alkyl chain is not favoured due to steric reasons, and considering an S$_N$1 mechanism, the resonance-stabilized pyrazolide ion would always be a better leaving group than the anionic alkyl chain.

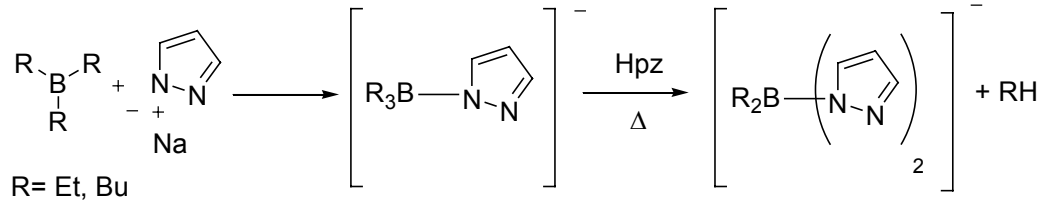

1.42 **1.43**

Scheme 1.18. *Trialkylboranes yield only bis(pyrazolyl) ligands.*

1.6. BORONIC ACID AND BORONIC ESTERS

The elusive alkyltris(pyrazolyl)borates could be synthesised using the starting boron source **trimethoxyborane** [$B(OMe)_3$] as reported by Tarquini and Reger.[28] The borane was reacted with a Grignard reagent (^{i}PrMgBr or ^{n}BuMgBr) followed by acidic workup to synthesise the alkyl substituted boronic acid (**1.45**) which was then reacted with sodium pyrazolide and excess pyrazole to form the borate salt (**1.46**) where the forth position at the boron is occupied with the alkyl chain.

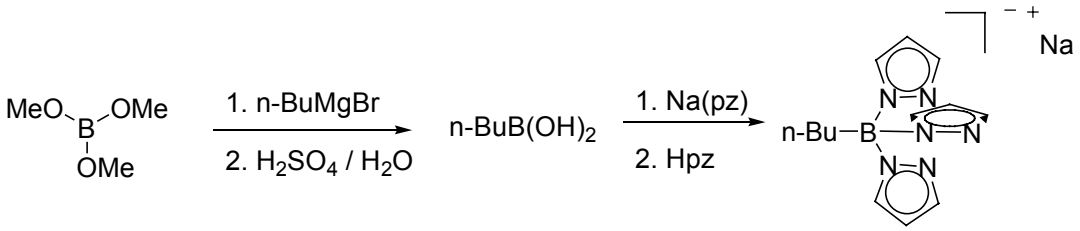

1.44 **1.45** **1.46**

Scheme 1.19. *Alkyl substituted scorpionates are available from boronic esters.*

Boronic acids and boronic esters can also be reduced by $LiAlH_4$ to yield borohydride salts as reported by Brown *et al*.[29] This procedure provides a high yielding general route to the synthesis of lithium monoorganylborohydride salts (**1.47**) to use as starting materials for the synthesis of scorpionates through the melting procedure.[30] (Scheme **1.20**).

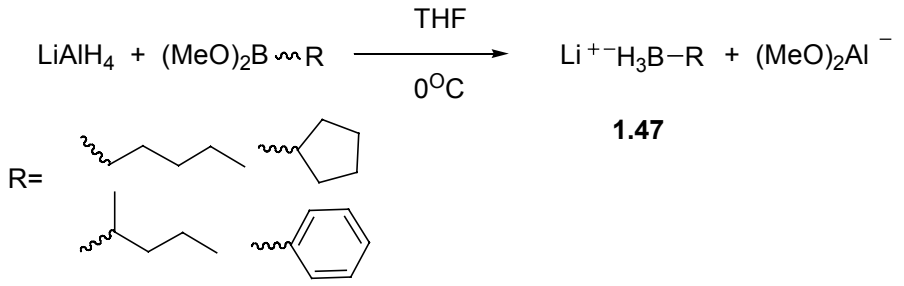

Scheme 1.20. *Synthesis of organylborohydride salts from alkyl boronic esters.*

The direct use of boronic esters has been reported for the synthesis of tripodal borate ligands by the group of Oro.[31] Treatment of triisopropyl borate (**1.48**) with allylmagnesiumbromide yielded the allyl borate salt (**1.49**) which was then reacted with benzoyl chloride to form the diisopropylallyl borate (**1.50**).

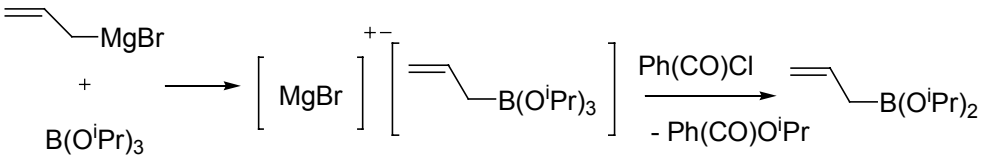

1.48 **1.49** **1.50**

Scheme 1.21. *Synthesis of allylbis(isopropyl)borane.*

This borate was then reacted with two equivalents of pyrazole and one of potassium pyrazolide to form the scorpionate (**1.51**) where the forth position is occupied by the allyl group.

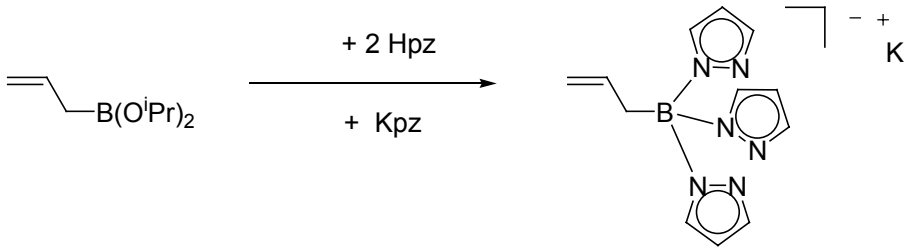

1.50 **1.51**

Scheme 1.22. *Synthesis of allytris(pyrazolyl)borate* **1.51**.

The allyl moiety allows the attachment of the tris(pyrazolyl)borate groups to carbosilane dendrimers with the ultimate goal of preparing stable neutral metallodendrimers as the group has published this year.[32] Using the same methodology they have also recently reported the synthesis of the hybrid scorpionate (**1.52**).

The lithium salt of diphenylphosphinomethane was reacted with the allylboronic ester and the resulting borate was heated with two equivalents of pyrazole in refluxing toluene to form the ligand **1.52**. This ligand forms rhodium and iridium complexes adopting the expected *fac* disposition in a κ^3-mode.

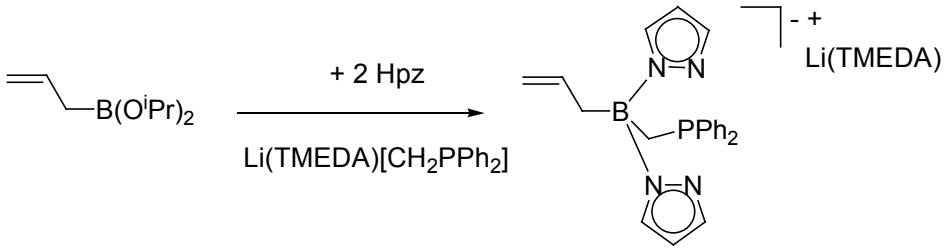

1.50 **1.52**

Scheme 1.20. *Hybrid scorpionate synthesised from a boronic ester.*

1.8. DITOPIC SCORPIONATE LIGANDS

1.8.1 FROM $B_2(NMe_2)_4$

Dinuclear metal complexes are important in different areas such as bioinorganic chemistry [33a], catalysis [33b] and materials science.[33c] Many examples have been reported where the two metal centres cooperate together to enhance the reactivity of the whole system. The design of multinuclear complexes using tripodal borate ligands was considered introducing ditopic scorpionate moieties within the ligand framework.

In 1988, Niedenzu reported the first dinuclear scorpionate (**1.54**) which was synthesised from **tetrakis(dimethylamino)diborane** (**1.53**) and pyrazole.[34] (Scheme **1.21**). The new bidentate ligand has been shown to coordinate to diverse metal centres such as lanthanides, molybdenum or palladium to form bimetallic complexes, thus acting as a bis(polydentate) ligand.

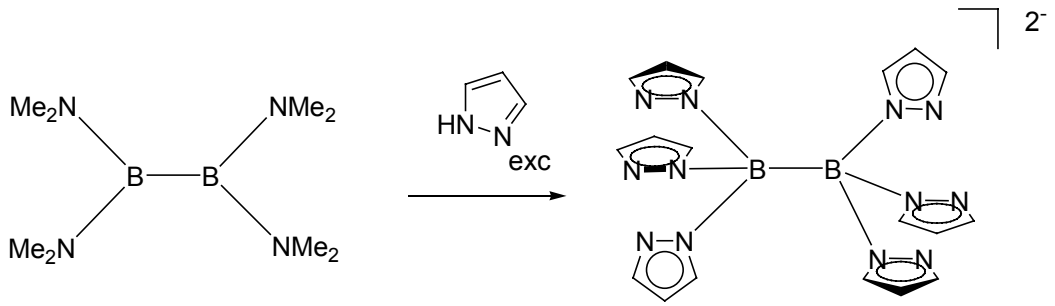

1.53 **1.54**

Scheme 1.21. *Ditopic homoscorpionate.*

1.8.2 FROM $FcB_2(Me)_2(pyr)_4$

Wagner and coworkers reported in 1996 a ferrocene based ditopic scorpionate used to generate a variety of heterotrinuclear complexes and also to act as a model system for organometallic coordination polymers.[35]

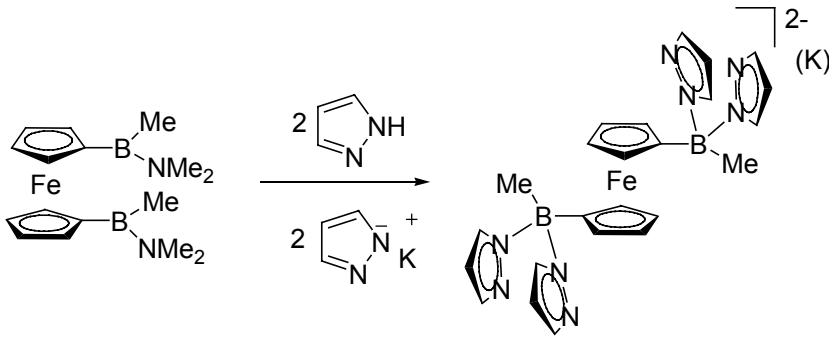

1.55 **1.56**

Scheme 1.22. *Ditopic ferrocenyl scorpionate.*

Complexation of the ditopic ligand (**1.56**) to transition metals has also been reported. The presence of different metals in these trimetallic molecules has an influence on the redox activity of the ferrocene units, although the degree of electronic communication within the system is generally low.

The authors explain this as being due to the binding of the three pyrazolyl groups to the metal in a conformation where it is always as far away from the iron centre as possible. Therefore ditopic scorpionates with one only pyrazole group per ferrocene unit were synthesised with the expectation that the lack of the third σ-donor site would force the complexed metal to interact directly with the Cp of the ferrocene, thus enhancing the communication between metals. This presumption was confirmed upon isolation of (**1.57**) where the lithium ion is coordinated to both the pyrazole groups and the cyclopentadienyl ring forming a multiple-decker sandwich arrangement in the solid state. However, studies regarding the level of chemical communication between the metal atoms are yet to be reported.

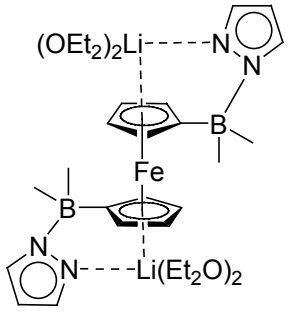

1.57

Fig. 1.12. *The complexed metal interacts with both the pyrazole and the cyclopentadienyl rings.*

1.9. CONCLUSIONS

This chapter has reviewed diverse reactions for the synthesis of borate-centred ligands using a variety of boron precursors. The original borohydride route involves a solvent-free reaction between a borohydride salt with the azole heterocycle at high temperatures. Although it is still the most widely used procedure for the formation of such ligands, it has been reported to be not applicable in all cases due to its dependence on the melting point and acid pK_a of the heterocycle. Moreover, using the melt methodology, the final borate ligand does not allow further modifications once formed. The use of alternative boron precursors allows the synthesis of borate ligands with enhanced features, although a general procedure for the synthesis of a wide range of borate ligands is yet to be reported. It is worth noting that almost all the synthetic protocols discussed were directed towards the synthesis of pyrazolyl borate ligands, whilst the application of such protocols to the synthesis of ligands featuring other azole heterocycles has received very little attention. Also surprising is the almost paucity of synthetic routes to chiral borate ligands reported to date.

1.10 REFERENCES CHAPTER I

1. S. Trofimenko, *J. Am. Chem. Soc.,* 1966, **88**, 5588.
2. C. Pettinari, R. Pettinari, *Coord. Chem. Rev.,* 2005, **249**, 525.
3. J. F. Ojo, P. A. Slavin, J. Reglinsky, M. Garner, M. D. Spicer, A. R. Kennedy, S. J. Teat, *Inorg. Chim. Acta,* 2001, **313**, 15.
4. D. D. Lecloux, C. J. Tokar, M. Osawa, R. P. Houser, M. C. Keyes, W. B. Tolman, *Organometallics*, 1994, **13**, 2855.
5. M. M. Ibrahim, M. Shu, H. Vahrenkamp, *Eur. J. Inorg. Chem.,* 2005, 1388.
6. M. Garner, J. Reglinski, I. Cassidy, M. D. Spicer, A. R. Kennedy, *Chem. Commun.,* 1996, 1975.
7. P. J. Bailey, M. Lanfranchi, L. Marchió, S. Parsons, *Inorg. Chem.,* 2001, **40**, 5030.
8. O. Graziani, P. Hamon, J-Y. Thepot, L. Toupet, M. Tilset, J-R. Hamon, *Inorg. Chem.,* 2006**, 45**, 5661.
9. S. Trofimenko, *J. Am. Chem. Soc.,* 1967, **89**, 6288.
10. G. E. Pacey, C. E. Moore, *Anal. Chim. Acta,* 1979, **105**, 353.
11. A. L. Sargent, E. P. Titus, C. G. Riordan, A. L. Rheingold, P. Ge, *Inorg. Chem.,* 1996, **35**, 7095.
12. D. L. Reger, J. R. Gardinier, W. R. Gemill, M. D. Smith, A. M. Shahin, G. J. Long, L. Rebbouh, F. Grandjean, *J. Am. Chem. Soc.,* 2005, **127**, 2303.
13. J. C. Peters, J. D. Feldman, T. D. Tilley, *J. Am. Chem. Soc.,* 1999, **121**, 9871.
14. P. J. Schebler, C. G. Riordan, I. A. Guzei, A. L. Rheingold, *Inorg. Chem.,* 1998, **37**, 4754.
15. T. A. Betley, J. C. Peters, *Angew. Chem. Int. Ed.,* 2003, **42**, 2385.
16. T. A. Betley, J. C. Peters, *Inorg. Chem.,* 2002, **41**, 6541.
17. P. J. Bailey, P. P. Pinho, S. Parsons, *Inorg. Chem.,* 2003, **42**, 8872.
18. C. Janiak, L. Braun, F. Girgsdies, *J. Chem. Soc., Dalton Trans.,* 1999, 3133.
19. C. Janiak, *Coord. Chem. Rev.,* 1997, **163**, 107.
20. F. Jackle, K. Polborn, M. Wagner, *Chem. Ber.,* 1996, **129**, 603.
21. S. Bieller, M. Bolte, H. W. Lerner, M. Wagner, *Chem. Eur. J.,* 2006, **12**, 4735.

22. D. Rieger, S. D. Lotz, U. Kernbach, S. Schroeder, W. P. Fehlhammer, *J. Organomet. Chem.,* 1995, **498**, 135.
23. I. Nieto, F. Cervantes-Lee, J. M. Smith, *Chem. Commun.,* 2005, 3811.
24. K. Niedenzu, S. S. Seelig, W. Weber, *Z. Anorg. Allg. Chem.,* 1981, **483**, 51.
25. S. Bieller, M. Bolte, H. W. Lerner, M. Wagner, *Z. Anorg. Allg. Chem.,* 2006, **632**, 319.
26. P. J. Bailey, D. Lorono, C. McCormack, F. Millican, S. Parsons, P. Pinho, R. Pfeifer, F. Rudolphi, A. Sanchez Perucha, *Chem. Eur. J.,* 2006, **12**, 5293.
27. S. Trofimenko, *J. Am. Chem. Soc.,* 1967, **89**, 1967.
28. D. L. Reger, M. E. Tarquini, *Inorg. Chem.,* 1982, **21**, 840.
29. B. Singaram, T. E. Cole, H. C. Brown, *Organometallics,* 1984, **3**, 774.
30. C. A. Dodds, M Garner, J. Reglinski, M. D. Spicer, *Inorg. Chem.,* 2006, **45**, 2733.
31. M. A. Casado, V. Hack, J. A. Camerano, M. A. Ciriano, C. Tejel, L. A. Oro, *Inorg. Chem.,* 2005, **44**, 9122.
32. J. Camerano, M. A. Casado, M. A. Ciriano, L. A. Oro, *Dalton Trans.,* 2006, 5287.
33. a) A. C. Rosenzweig, C. A. Frederick, S. J. Lippard, P. Nordlund, *Nature,* 1990, **345**, 593; b) J. Mrozinski, *Coord. Chem. Rev.,* 2005, **249**, 2534; c) T. C. Harrop, P. K. Mascharak, *Coord. Chem. Rev.,* 2005, **249**. 3007.
34. C. P. Brock, M. K. Das, R. P. Minton, K. Niedenzu, *J. Am. Chem. Soc.,* 1988, **110**, 817.
35. A. H. Ilkhechi, M. Bolte, H-W. Lerner, M. Wagner, *J. Organomet. Chem.,* 2005, **690**, 1971.

CHAPTER II

REACTION OF TRIS(DIMETHYLAMINO)BORANE WITH AZOLE HETEROCYCLES

2.1 INTRODUCTION

In the previous Chapter different procedures for the synthesis of boron-centred ligands using a variety of boron precursors have been reviewed. However, only two of the methodologies discussed have been used for the formation of chiral tripodal pyrazolyl borates. Examples of other chiral azolyl borate ligands are yet to be reported and one of the aims of the present work is to find novel routes for the synthesis of these kinds of ligands and their application in asymmetric processes. Our group has been especially interested in chiral versions of the hydrotris(methimazolyl)borate (Tm) ligand.

Chirality can be introduced into the Tm ligand framework by two different means; either with a chiral group at the boron atom replacing the existing hydrogen thus placing it exactly on the 3-fold axis, or by introducing enantiopure groups at the various unsubstituted positions of the azole heterocycles retaining the overall C_3-symmetry of the resulting ligands. The latter is most readily achieved by replacing the methimazolyl *N*-methyl groups with chiral groups as shown in Figure **2.1**.

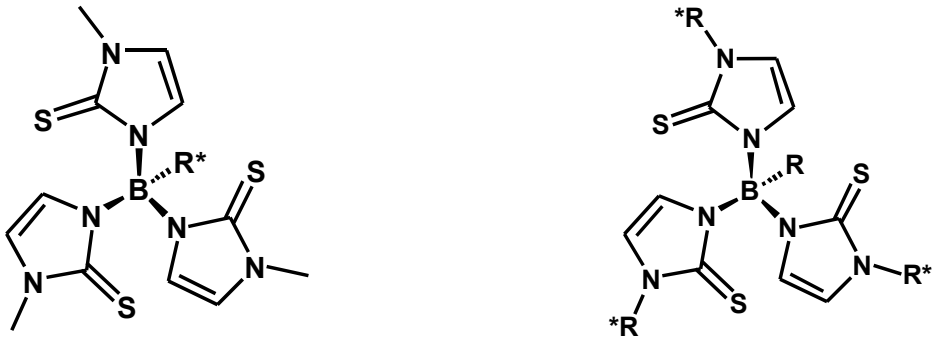

Figure 2.1. *Chiral groups can be introduced at the boron or at the azole heterocycles.*

Considering the approach of attaching a chiral group at the boron atom, there is only one known example of such a ligand, which involves the use of the chiral isopinocampheylborane as starting material as discussed in the previous chapter.[1]

However, this synthetic route was found to be only applicable to the synthesis of pyrazolyl ligands and the same methodology using methimazole only resulted in decomposition products.

The second approach that involves the introduction of chiral bulky groups in positions close to the donor atoms is known to dramatically influence the coordination behaviour of the resulting ligands and the chemical and physical properties and reactivities of their metal complexes.[2] For example, tris(pyrazolyl)borates with bulky groups attached at the 3 positions of the pyrazolyl rings have been extensively studied and gained the denomination of "second generation" of scorpionates. The favourable properties of these bulky tripodal ligands have led to their widespread adoption in inorganic chemistry with applications in fields like C-H activation or bioinorganic chemistry. The first example of a chiral tripodal borate ligand with chiral groups at the 3 position of the heterocycle was already discussed in the Section **1.1**.[3] The chiral ligand coordinates the metal centre through the three pyrazole imine nitrogen atoms, creating a chiral cage that surrounds the metal ion as seen in the Fig. **2.2**.**b**.

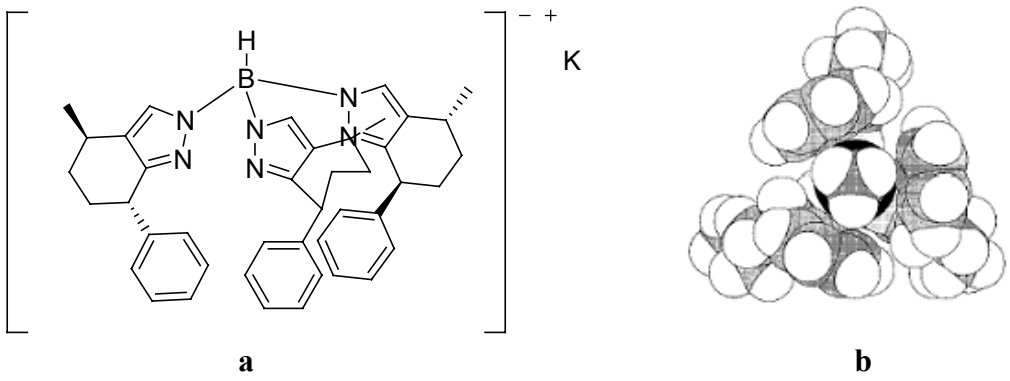

a **b**

Fig. 2.2. *Chiral scorpionate (**a**) and a space-filling model of a Cu complex viewed along its C_3-axis (**b**).*

Since then, only another example of a chiral borate ligand has been reported by Ward and coworkers.[4] One of the possible reasons for this is the sometimes complex and limited applicability of the synthetic methodologies published to date for the formation of such ligands. Another reason is the limited modifications that are possible to the ligand framework once it has been formed. Our interest in the synthesis of chiral tripodal borate ligands for their application in asymmetric processes lead to the design of additional routes to the synthesis of such ligands which are discussed in the following sections.

2.1.1 DERIVATISATION OF THE 4th BORON POSITION

The first approach considered was the derivatisation of the forth position at the borate ligand involving the removal of the hydrogen at this position first, followed by the insertion of the chiral group. There are no examples in the literature regarding the substitution of the B-H hydrogen in tripodal hydrotris(azolyl)borates. The only well defined reactivity is the acid-base reaction with excess heterocycle to yield tetrasubstituted borates at high temperatures. The B-H moiety is also known to form agostic interactions (M···H-B) in several metal complexes to complete the metal coordination sphere. For example, Takats and Marques have reported a samarium complex where two Tp and one Cp are simultaneously coordinated to the metal.[5]

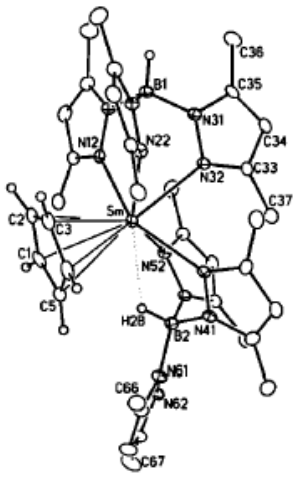

Fig. 2.3. *Samarium complex with two Tp and a Cp ligands coordinated.*

In this complex one Tp coordinates in a $\kappa^3_{[N,N,N]}$ fashion while the Cp is η^5 coordinated to the metal. The other Tp coordinates using only two of the pyrazolyl groups. However, the electronic demand at the metal centre requires the formation of a Sm···H-B agostic interaction. This special coordination behaviour could well be explained due to excessive steric hindrance if both Tp ligands were coordinating through their three pyrazole groups or to the preference for the M···H-B formation instead of the pyrazole coordination. Recently, Jalon and coworkers have reported a series of monohydride Ru(II) complexes of the formula $[Ru(H)(Tp^R)(cod)]$, where the Tp is $\kappa^3_{[N,N,BH]}$-coordinated to the metal showing a similar interaction.[6] Reaction of these complexes with two electron donor ligands like phosphines or cyanides leads to the replacement of one of the pyrazole groups instead of the B-H···Ru agostic interaction, this being a clear example of the strength of the metal-hydrogen interaction. (Scheme **2.1**).

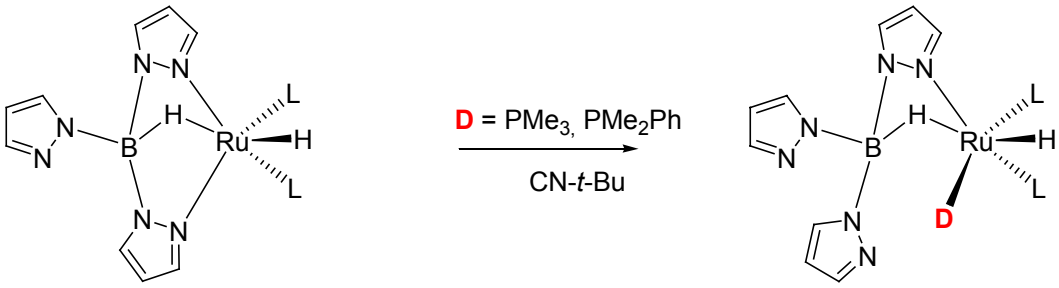

Scheme 2.1. *Agostic M···H-B is preferred to pyrazolyl coordination.*

The B-H moiety of ligands belonging to the Tm family behaves in a different fashion with certain transition metal precursors. Metal-boron dative bonding was first authenticated by the isolation of the metal complexes of the formula $[M(CO)(PPh_3)\{B(Met)_3\}]$ where M = Rh, Ru, Os, Ir, Pt (Scheme **2.2**).[7] These compounds are known as *metallaboratranes* and they are the first example where the metal seems to act as a Lewis base producing a dative bond with the Lewis acidic boron atom.

The difference in reactivity between Tp and Tm ligands can be associated with the size of the chelate ring formed upon metal complexation. Whilst for Tp derivatives six membered rings are formed, for the Tm family, the existence of an additional carbon atom between the nitrogen linked to the boron centre and the sulphur donor, creates more flexible eight-membered rings as discussed in Section **1.1**. This feature allows the labilisation of one of the methimazolyl arms followed by formation of a B-H···M agostic interaction, oxidative addition of the B-H to the metal and ultimate coordination of the pedant methimazolyl group to form the metallaboratrane as shown in the Scheme **2.2**.

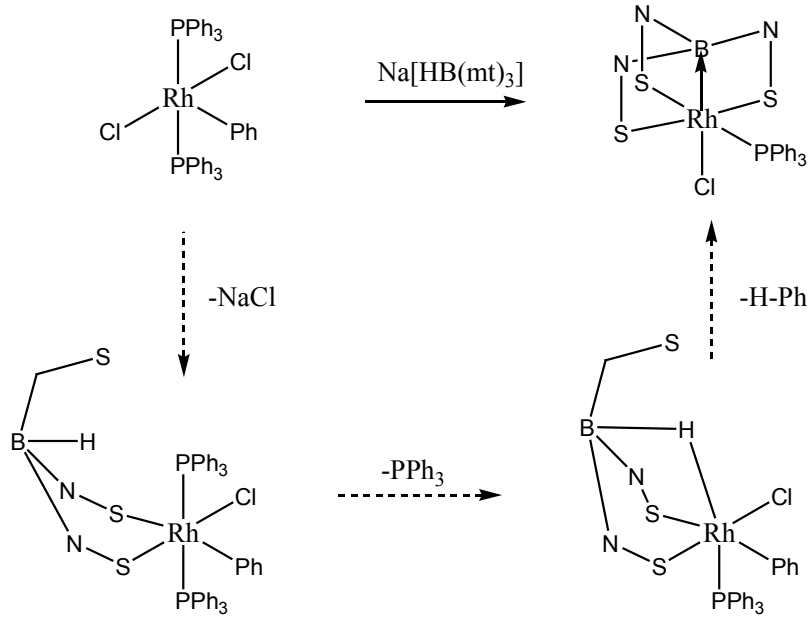

Scheme 2.2. *Formation of a metallaboratrane.*

Very recently, the B-H moiety of a tripodal borate ligand has been activated through a redox process in the synthesis of analogous metallaboratranes.[8] Reaction of a rhodium precursor with the sodium salt of the hydrotris(thioxotriazolyl)borate (NaTt) in the presence of two equivalents of the one-electron oxidant [Ferrocenium]PF_6 led to a double oxidative-deprotonation process with the ultimate formation of the metal-boron bond (Scheme **2.3**). Decoordination of a thioxotriazolyl arm followed by agostic interaction of the B-H bond is again observed. Stepwise double oxidation, due to the presence of the oxidant, polarised the bond from $B\text{-}H^{\delta-}$ to $B\text{-}H^{\delta+}$ thus facilitating proton loss and formation of the B-Rh dative bond.

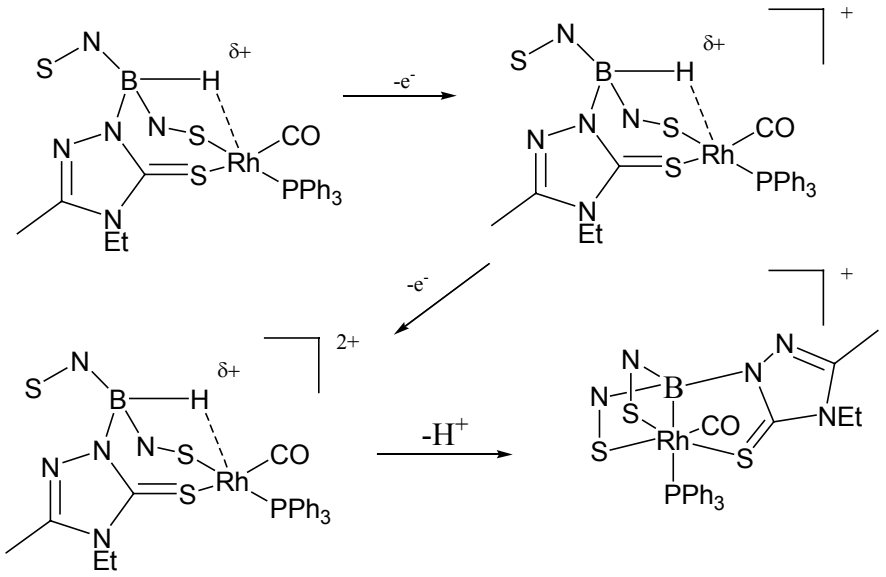

Scheme 2.2. *Redox activation of the B-H bond in the synthesis of a metallaboratrane.*

These examples illustrate that the B-H bond in tripodal borate ligands is rather unreactive. This bond is able to be polarised through a redox process and to form agostic interaction with diverse metals, but its ultimate cleavage must be followed by stabilization of the free *p*-orbital at the boron as shown in the formation of the metallaboratranes.

The B-H moiety seems to be a strong covalent bond that does not show any acidic, and very little hydridic, character. Previous attempts carried out in the lab to cleave the B-H bond with bases to form a stable organoborane were unsuccessful. Diverse bases such as MeLi, BuLi, LDA, NaH or NaOMe did not lead to deprotonation of the ligand. Also considering the possibility of abstracting it as a hydride, trityl chloride or ionic trityl salts were employed, however no reactivity was found.[9]

Due to the limited applicability of the melt reaction between azole heterocycles with borohydride salts and the lack of reactivity of the B-H bond in preformed hydrotris(azolyl)borate systems, the development of more general procedures for the synthesis of tripodal borate centred ligands containing an alternative to H in the 4th position was required to achieve our aim of placing a chiral group in this position.

2.1.2 TRIPODAL BORATE LIGANDS FROM $B(NMe_2)_3$

In 1985 Niedenzu reported the reaction of tris(dimethylamino)borane $B(NMe_2)_3$ with pyrazole to yield the compound (dimethylamido)tris(pyrazolyl)borate **1.41** as discussed in the previous chapter.[10]

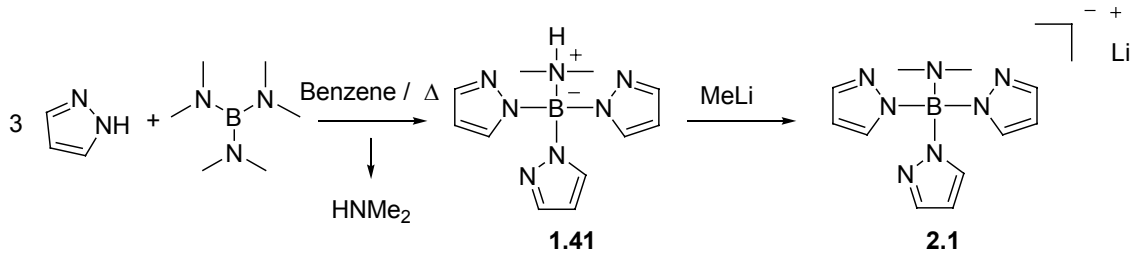

Scheme 2.3. *The first use of $B(NMe_2)_3$ for the synthesis of a scorpionate ligand.*

The mechanism of the reaction involved a transamination process between the borane and the heterocycle releasing dimethylamine gas to yield the ligand where the forth position at the boron was occupied by a dimethylamino group. This compound could be deprotonated with MeLi to form the lithium salt (**2.1**). A molybdenum complex with the formula $LMo(CO)_2(\eta^3\text{–}CH_2CRCH_2)$ was synthesised and it was found that the ligand did not coordinate the metal centre through the three pyrazole rings. Instead, the dimethylamino group was coordinating the metal atom whilst a pyrazolyl ring remained uncoordinated.

This was somewhat surprising since a bicyclo [2,2,1]-cage was formed instead of the presumably more stable [2,2,2]-cage common for the rest of the scorpionate family, but it could be explained considering the basicity of the dimethylamino group which is higher than that of the pyrazole.

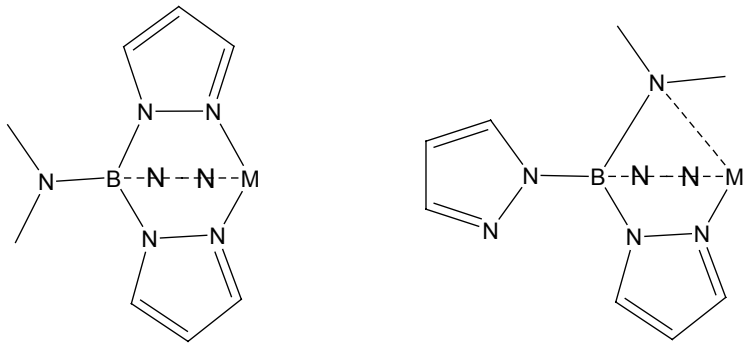

Fig. 2.4. *Possible bicyclo cages formed upon metal complexation of* **2.1**.

The X-ray crystal structure of the potassium salt of **2.1** shows the special coordination mode via two pyrazole groups and the dimethylamino group (Fig. **2.5**).

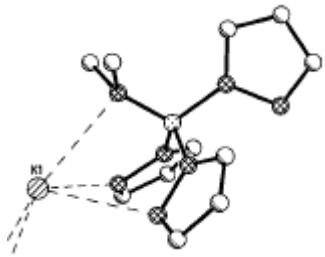

Fig. 2.5. (*Dimethylamido)tris(pyrazolyl)borate* **2.1** *coordinates the K atom in a* κ_3*–[*N_{pyr}*,*N_{pyr}*,*N_{NMe}*] fashion.*

In principle, it was considered that the high basicity and reactivity of the dimethylamino group could make the forth position at the boron more easily derivatised than if it was occupied by a hydrogen atom. Therefore, it was decided to investigate the possibilities of introducing chiral groups at the boron by displacement of the dimethylamino moiety following its conversion to a suitable leaving group.

2.2 RESULTS

The reaction between one equivalent of $B(NMe_2)_3$ with three equivalents of methimazole yielded the tripodal ligand (**2.2**) after two hours under refluxing benzene by precipitation of a colourless solid from the solution in good yield (82%).

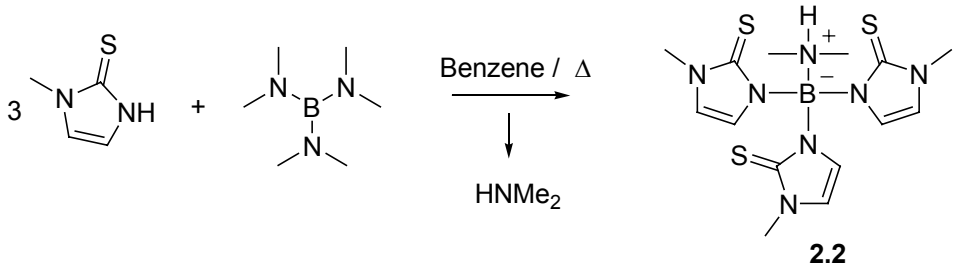

Scheme 2.5. *Reaction of $B(NMe_2)_3$ with methimazole under benzene reflux.*

Spectroscopic Analysis

The ^{1}H-NMR spectrum of this compound does not show complex signals to analyze. The only special feature is that the methyl groups of both the methimazolyl and the dimethylamino groups appear at identical chemical shift with a singlet 3.48 ppm that integrates as 15 hydrogen atoms. The NH group is responsible for a broad singlet at 9.72 ppm which is also confirmed by a broad band at 3100 cm^{-1} in the IR spectrum. In the ^{13}C-NMR the methyl groups now appear at different chemical shifts, 34.7 and 34.9 respectively.

Molecular Structure

Crystals suitable for X-ray diffraction studies were grown by slow cooling of a hot solution of **2.2** in benzene. The comparison of **2.2** with the anionic Tm ligand in the solid state is hampered by the fact that **2.2** is neutral and it is not bound to a metal centre. All the reported structures of Tm ligands are metal complexes. For comparison purposes TmZnCl will be used as a model.

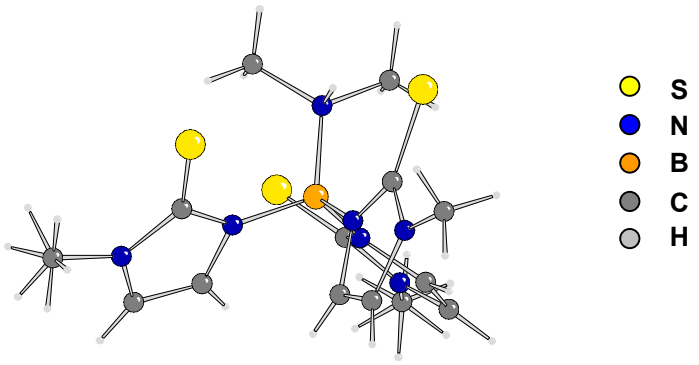

Fig. 2.6. *(Dimethylamido)tris(methymazolyl)borate* **2.2**.

The B-N distances of the methimazole rings in **2.2** lie in the range of 1.542 - 1.560 Å whilst the B-N(7) distance for the amine nitrogen is longer with a value of 1.605 Å. This is consistent with the different hybridisation of the methimazole nitrogen atoms (sp^2) when compared to the amine one (sp^3). The B-N distances in the TmZnCl fall in the same range (mean 1.549 Å). When comparing the C=S distances between the ligand **2.2** and the Zn complex there are obvious differences due to metal coordination in the latter case. The C=S bond lengths in **2.2** are in the range of 1.694-1.700 Å whilst for the metal complex they are significantly longer (1.715-1.723 Å). The steric hindrance at the amine group in **2.2** due to the two methyl groups is reflected in the N-B-N angles. The N_{met}-B-N_{met} angles average between methimazole groups is 106.49º whilst for N_{met}-B-N_{Me2} is 112.50º. In the Fig. **2.6** it is also possible to observe that two of the methimazole rings are placed with their S atoms pointing towards the amine group whilst the third one is pointing away. This is due to the formation of two hydrogen bonds between two sulphur atoms and the amine proton (S-N distance 2.294 Å) whilst the distance S-N of the methimazole ring that does not form a hydrogen bond is much longer (3.153 Å). Selected bond and angles of **2.2** are shown in the Table **2.2**.

Table 2.2. SELECTED BOND LENGTHS (Å) AND ANGLES (°) FOR **2.2**.

B-N(1)	1.542(3)	C(5)-S(2)	1.700(2)
B-N(3)	1.559(3)	N(5)-C(9)	1.370(3)
B-N(5)	1.556(3)	C(9)-N(6)	1.365(3)
B-N(7)	1.605(3)	N(1)-B-N(3)	106.5(17)
N(1)-C(1)	1.373(3)	N(1)-B-N(5)	109.9(18)
C(1)-N(2)	1.356(3)	N(1)-B-N(7)	112.5(18)
C(1)-S(1)	1.694(3)	N(3)-B-N(5)	107.8(18)
N(3)-C(5)	1.359(3)	N(3)-B-N(7)	109.5(18)
C(5)-N(4)	1.358(3)	N(5)-B-N(7)	110.4(17)

Attempts to replace the dimethylamino group bonded to the boron centre were focused on its conversion to a good leaving group followed by substitution with a suitable nucleophile. Deprotonation of the amide in a similar fashion to that reported for the pyrazolyl analogue **1.41** was first considered. The free amine could then be treated with a range of electrophiles to form the leaving group.

However, the treatment of **2.2** with a broad range of bases (MeLi, BuLi, LDA, NaH) and reaction with different electrophiles (MeI, MeCOCl, PhCOCl) failed and resulted only in the isolation of free methimazole or the product of the addition of the electrophile to the methimazolyl anion.

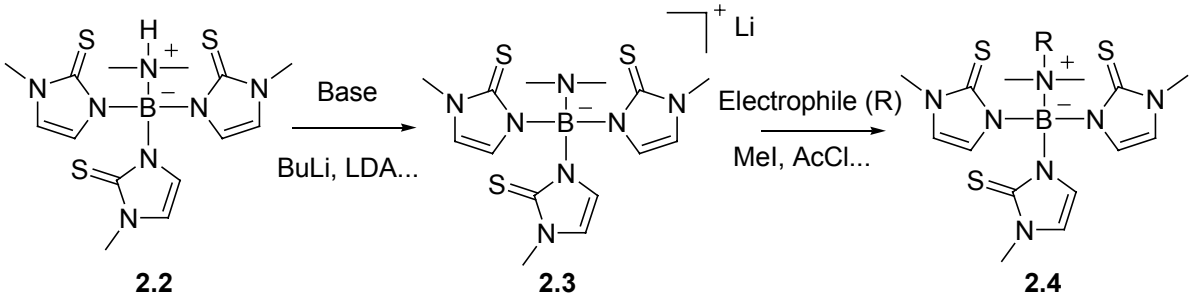

2.2 **2.3** **2.4**

Scheme 2.6. *Designed route to the formation of a good leaving group at the boron centre.*

The decomposition appears to occur at the deprotonation stage which contrasts with the reactivity of $(NHMe_2)B(pyrazolyl)_3$ and is assumed to be due to a weaker coordination of the methimazolyl rings to the boron centre, which is

consistent with the stability of the heterocycle anions as indicated by the acidic pK_a values for pyrazole and methimazole (14 and 12 respectively).

It was therefore decided to study the reactivity between $B(NMe_2)_3$ and an azole heterocycle with an acid pK_a similar to pyrazole. 2-Methylimidazole has an acid pK_a of 15, hence it was expected to form (**2.5**) which was of interest as an intermediate to the proposed new ligand (**2.7**) (Scheme **2.7**).

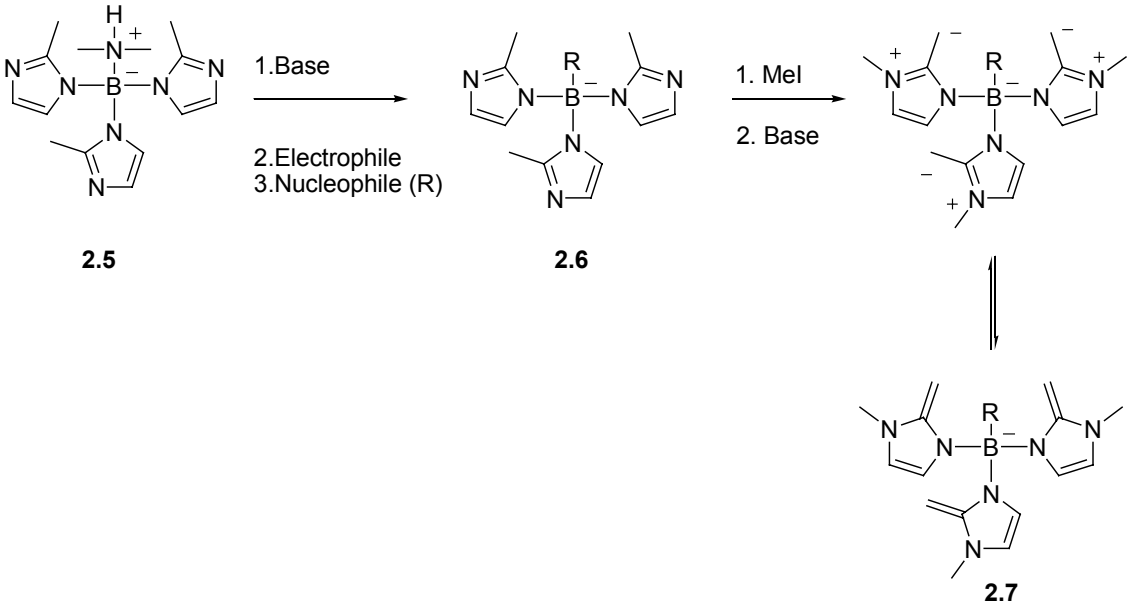

Scheme 2.7. *Synthetic route to target ligand* **2.7**.

A monodentate ligand comparable to **2.7** is the 1,3,4,5-tetramethyl-2-methyleneimidazoline system (**2.8**) (MI) reported by Kuhn and coworkers in 1993.[11]

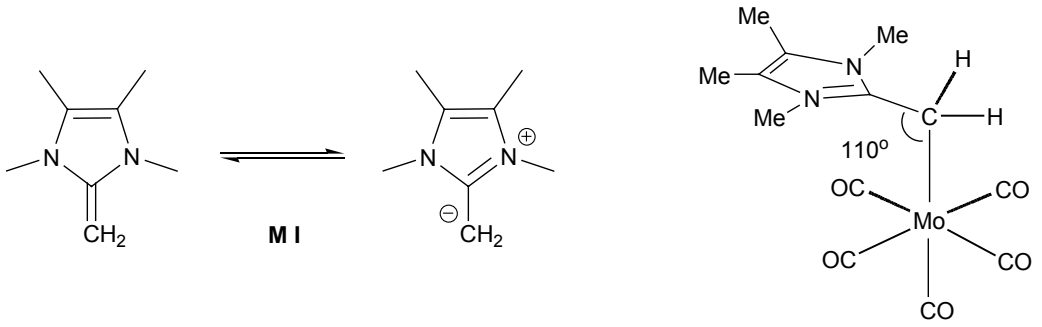

2.8 **2.9**

Fig. 2.6. *Zwitterionic and enamine forms of* **2.8** *and a Mo complex* **2.9**.

This ligand is known to coordinate to metals in its zwitterionic rather than in the enamine form as deduced from the geometry around the coordinated carbon atom in its complexes. In the $Mo(CO)_5$ complex (**2.9**), for example, the C-C-Mo bond angle is 110.4° indicating sp^3 hybridisation, and the C-C bond length is 143 pm consistent with a single bond. The ligand induces a strong *trans influence* as deduced from the crystallographic data reported in which the Mo-CO bond *trans* to the MI ligand is significantly shorter (196.9 pm compared with an average of 205.1 pm for the *cis* CO ligands), while the C-O bond for the *trans* ligand is the longest (115.6 pm compared with a mean of 114.0 ppm for the *cis* ligands). These characteristics resemble the ubiquitous *N*-heterocycle carbenes that are widely used as transition metal ligands due to their strong σ-donor and lack of π-acceptor properties.[12]

Surprisingly, the reaction between 2-methylimidazole and $B(NMe_2)_3$ did not form the expected compound **2.5**. Instead, the homoleptic tetrakis(2-methylimidazolyl)borate (**2.10**), where four heterocycles are now coordinated to the boron atom, was the only product of the reaction.

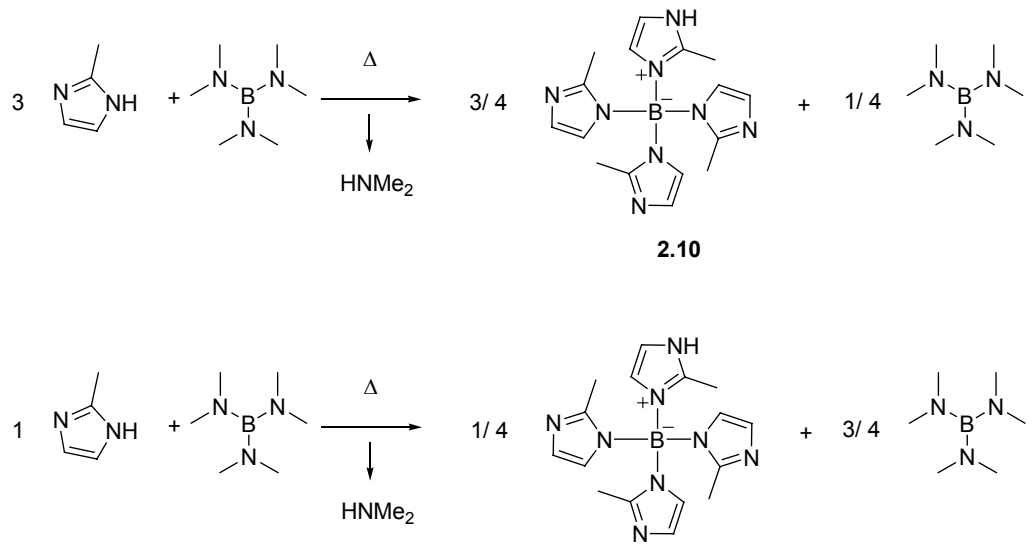

Scheme 2.8. *2-methylimidazole forms the tetrasubstituted borate* **2.10** *upon reaction with $B(NMe_2)_3$.*

No traces of the trisubstituted ligand were detected in the reaction mixture, and curiously, the same tetraimidazolyl borate compound was formed even if only one equivalent of the heterocycle was used. An explanation of the outcome of this reaction follows.

2.2.1 MECHANISM OF THE REACTION

This reaction pattern must involve an alternative mechanism to the simple transamination reaction between the NH of the heterocycle and the NMe_2 groups of the borane as observed in the reactions with pyrazole and methimazole. Comparing the heterocycles it is possible to recognise that, whilst the acid pK_a values for the three are quite similar (Table **2.1**), methimazole and pyrazole are both considerably less basic (basic pK_a values -1.05 and 2.79 respectively) than 2-methylimidazole (basic pK_a 7.85) which can be considered as a relatively strong Lewis base. The basic pK_a´s of the heterocycles therefore seem to play a directing role in the outcome of these reactions.

$B(NMe_2)_3$ is a planar molecule where the vacant *p*-orbital at the boron is stabilized by the lone pairs of the three nitrogen atoms providing significant B-N p-π bonding. The basicity of the dimethylamino groups is reduced and thus the molecule does not react with relatively acidic substances like methimazole at room temperature. Comparing $B(NMe_2)_3$ with the group 15 analogues $E(NMe_2)_3$ (E = P, As, Sb, Bi) the electronic saturation at the central atom is responsible for the pyramidal geometry of these molecules. Since the lone pairs of the nitrogen atoms in these species are readily available, these molecules can act as strong bases. For example, in the reaction of $Sb(NMe_2)_3$ with primary amines, a double metallation occurs, in stark contrast to the reactivity of $B(NMe_2)_3$.[13]

The transamination reaction of $B(NMe_2)_3$ with the azole heterocycles can be accelerated if the heterocycle is basic enough to coordinate to the boron *p*-orbital. The p-π B-N bonding also has the effect of substantially reducing the Lewis acidity of $B(NMe_2)_3$. Thus, a strongly basic heterocycle is required to coordinate to the boron. Although NMR spectroscopy indicates that coordination of the 2-methylimidazole does not occur at room temperature, it can be forced under reflux conditions. This leads to a change in the hybridization of the borane from sp^2 to sp^3 forming a tetrahedral intermediate (**2.11**) where the dimethylamino group nitrogen lone pairs are no longer stabilizing the boron orbital. The reactivity of such species may therefore be expected to be similar to the group 15 $E(NMe_2)_3$ systems. The [(Azole)$B(NMe_2)_3$] system is therefore strongly basic and readily reacts with three more equivalents of the heterocycle to yield the observed tetra(azolyl) system (Scheme **2.9**).

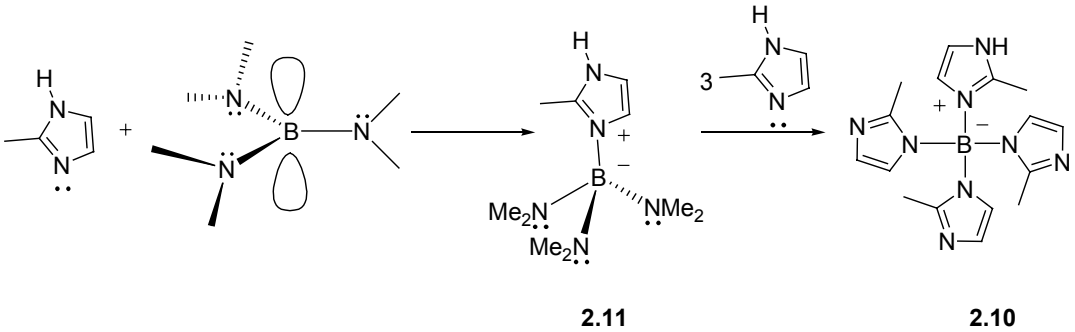

2.11 **2.10**

Scheme 2.9. *Mechanism proposed for the synthesis of* **2.10**.

This mechanism is also consistent with the experiment where both reactants are mixed in a 1:1 ratio yielding the same homoleptic compound and unreacted borane. If both reagents are mixed under the same stoichiometry for each boron atom four heterocycles are required for the synthesis of **2.10**, therefore free borane would be in excess under these stoichiometric conditions. We were interested in delimiting the basic pKa range for this reaction, so a range of imidazoles were synthesised and their reactivity towards $B(NMe_2)_3$ studied. The results are summarized in Table **2.1**.

	BASIC pKa	ACID pKa	PRODUCT
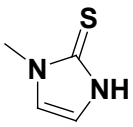	-1.0	12.0	**3:1**
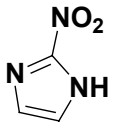	-0.8	7.5	**3:1**
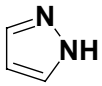	2.8	14.0	**3:1**
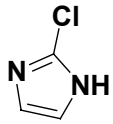	3.5	10.5	**4:1**
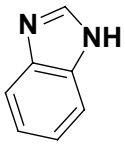	5.7	13.2	**4:1**
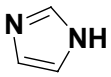	7.0	14.9	**4:1**
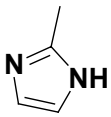	7.8	14.1	**4:1**

Table 2.1. *Imidazole heterocycles react with $B(NMe_2)_3$ to yield different compounds. (3:1) = trisubstituted ligand; (4:1) = tetrasubstituted ligand.*

Imidazole and benzimidazole, both commercially available and with a basic pK_a of 7 and 5.7 respectively, react with the borane to yield the homoleptic tetrasubstituted compounds (**2.12**) and (**2.13**). Both have already been reported in the literature as the potassium salts, synthesised through the melt reaction between KBH_4 and the heterocycle.[13] This is the first synthesis of such systems as the free acids. The ^{1}H-NMR spectra of both compounds show that all heterocycle groups are equivalent and the ^{11}B-NMR confirms the tetrahedral geometry at the boron atom which shows singlet peaks at 6.45 and 5.78 ppm respectively.

Crystals of **2.13** suitable for X-ray diffraction were grown by slow diffusion of pentane into a solution of **2.13** in MeOH. The structure is shown in Fig. **2.7**.**b**

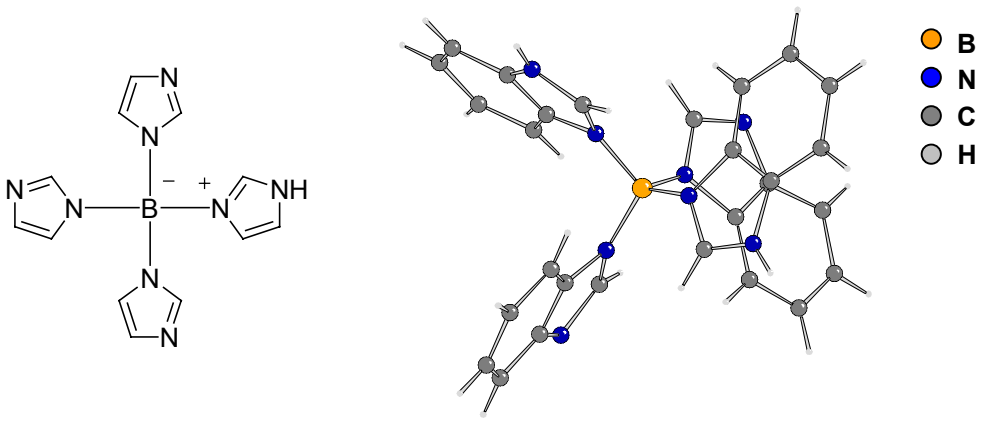

Fig 2.7. a) *Tetra(imidazolyl)borate* **2.12**; **b)** *X-ray structure of tetra(benzimidazolyl)borate* **2.13**.

It is possible to observe the tetrahedral coordination at the boron atom in **2.13**. The position of the proton to balance the charge on the borate anion **2.13** was not evident from the data and it was split equally between nitrogen N31 and N32 since it resulted in unfavourable interaction when assigned to the other two nitrogen atoms. The B-N distances of these two heterocycles are slightly longer when compared to the other two, making this assumption reasonable.

The structure does not show more remarkable features, being quite symmetrical with the N-B-N angles deviating only slightly from the ideal. Selected bond distances and angles are provided in Table **2.3**.

Table 2.3. SELECTED BOND LENGHTS (Å) AND ANGLES (°) FOR **2.13**.

B-N(11)	1.547(6)	C(23)-N(33)	1.388(5)
B-N(12)	1.524(6)	N(14)-C(24)	1.354(5)
B-N(13)	1.527(6)	C(24)-N(34)	1.360(6)
B-N(14)	1.536(6)	N(11)-B-N(12)	110.9(3)
N(11)-C(21)	1.357(4)	N(11)-B-N(13)	110.4(3)
C(21)-N(31)	1.313(4)	N(11)-B-N(14)	105.6(3)
N(12)-C(22)	1.362(5)	N(12)-B-N(13)	109.9(3)
C(22)-N(32)	1.302(5)	N(12)-B-N(14)	111.2(4)
N(13)-C(23)	1.384(5)	N(13)-B-N(14)	108.8(3)

To reduce the basicity of the imine nitrogen atom, electron withdrawing groups were introduced at the 2-position in the imidazole ring. 2-Chloroimidazole (**2.14**) was synthesised by a modified procedure reported by Kirk and coworkers.[15] Protection of the imidazole NH with ethylorthoformate was followed by deprotonation at the 2-position with BuLi (Scheme **2.10**). The resulting 2-lithio derivative was quenched with hexachloroethane and upon deprotection, 2-chloroimidazole was obtained in a better yield (67%) than previously reported, where *N*-chlorosuccinimide was used as the chlorine source. The chloro group in this position leads to a reduction in the basic pK_a by 2.2 units, compared to unsubstituted imidazole, due to its electron withdrawing character.

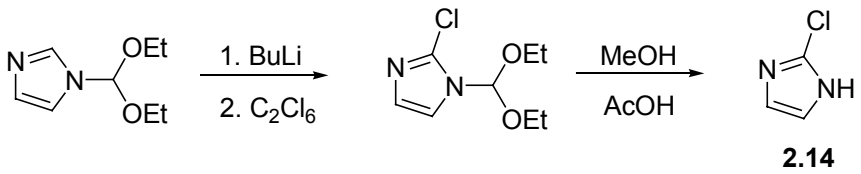

2.14

Scheme 2.10. *Synthesis of 2-chloroimidazole* **2.14**.

Reaction of three equivalents of 2-chloroimidazole with $B(NMe_2)_3$ yielded the homoleptic tetrasubstituted species tetra(2-chloroimidazolyl)borate (**2.15**) indicating that the chloroimidazole is basic enough to coordinate to the borane following the mechanism previously discussed. It is necessary to introduce the more electron withdrawing *nitro* group to reduce the basicity of the imidazole to a value similar to methimazole (2-nitroimidazole basic pK_a = -0.8), so that the trisubstituted compound (dimethylamido)tris(2-nitroimidazolyl)borate (**2.16**) was formed when four equivalents of 2-nitroimidazole were reacted with the borane. No traces of the 4:1 system was found by taking small aliquots from the reaction mixture and analyzing them by mass spectrometry.

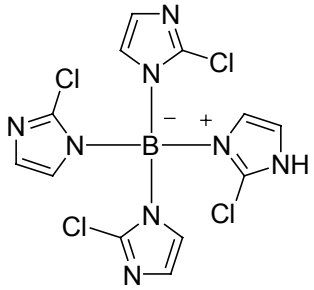

2.15

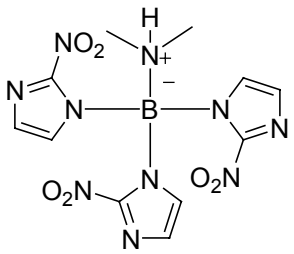

2.16

Fig. 2.8. *2-chloro- and 2-nitroimidazole lead to* **2.15** *and* **2.16** *respectively.*

It is possible to postulate at this stage that the mechanism of the reaction between $B(NMe_2)_3$ and the azole heterocycles depends on the basic pK_a of the latter and that heterocycles with a basic pK_a higher than 3.5 will be able to coordinate to the $B(NMe_2)_3$ before reacting through the acid-base transamination reaction with the dimethylamino groups. For those heterocycles with a basic pK_a lower that 3.5, this coordination is not possible and the transamination reaction with $B(NMe_2)_3$ takes place directly to give the (dimethylamido)tris(azolyl)borate system.

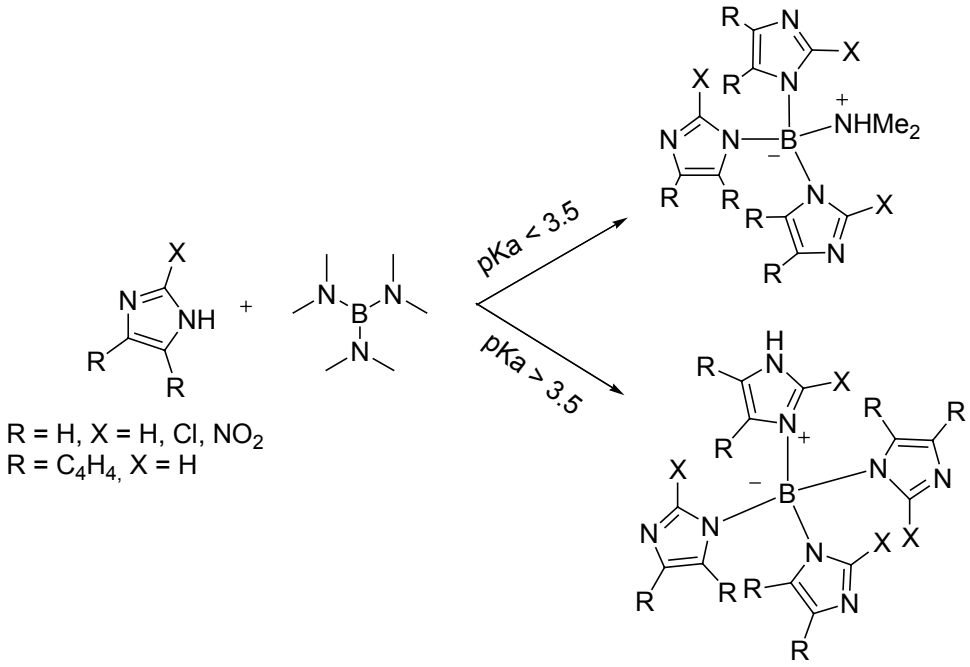

Scheme 2.11. *The outcome of the reaction depends on the basic pK_a of the heterocycles.*

To further establish this mechanism, a one-pot reaction was undertaken in which one equivalent of *N*-methylimidazole, one equivalent of $B(NMe_2)_3$ and three equivalents of methimazole were heated together in toluene under reflux. Since the *N*-methylimidazole does not present any acidic proton that could result in a transamination reaction with the borane, and has a basic pK_a of 7.8, it was expected to coordinate to the free *p*-orbital of the borane. Use of *N*-methylimidazole in this way is therefore serving to "activate" the $B(NMe_2)_3$ by increasing the basicity of the dimethylamino groups to reaction with methimazole to yield a tripodal species where the forth position at the boron is now occupied by the *N*-methylimidazole. After two hours heating at reflux in toluene, a colourless solid precipitated from the solution which was isolated and washed with dry hexane to yield the ligand (*N*-methylimidazole)B(methimazolyl)$_3$ (**2.17**) in excellent yield (88%).

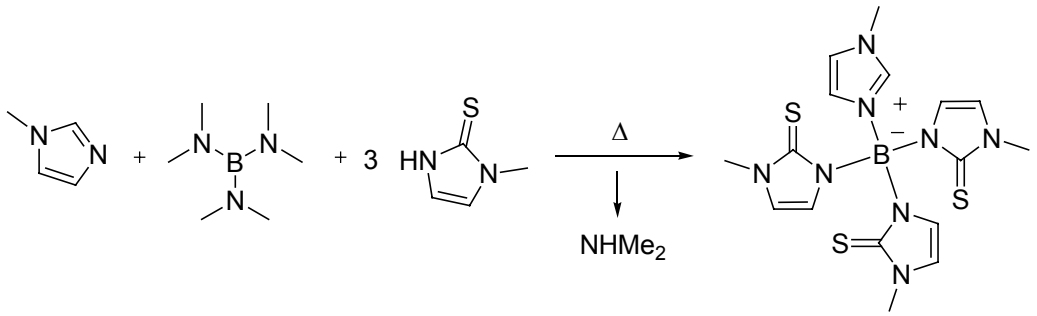

2.17

Scheme 2.12. *One pot synthesis of* **2.17**.

The ^{1}H-NMR of **2.17** shows a singlet peak for the H in the 2-position of the *N*-methylimidazole at 8.97 ppm and two broad singlets at 7.19 and 6.95 ppm corresponding to the other protons of this group. The methimazolyl protons appear at 6.92 and 6.84 ppm as two doublets with a coupling constant of 2.35 Hz. These signals integrate as three protons each. The methyl group at the 3-positions of the methymazolyl rings appears as a singlet at 3.49 ppm (9H) whilst the one corresponding to the *N*-methylimidazole group appears at 3.81 ppm (3H). The ^{11}B-NMR shows a single peak at 8.05 ppm characteristic for tetrahedral coordinated boron compounds.

Examples of this kind of ligand with groups other than H attached to the boron are scarce in the literature as discussed in the previous Chapter, and this synthetic protocol may have the potential to provide a large number of ligands featuring different groups at the boron-forth position.

2.2.2 SCOPE OF ACTIVATORS OF THE BORANE

To determine the scope of this synthetic methodology a range of different Lewis bases were investigated as activators for $B(NMe_2)_3$ in this reaction. It was noticed that the use of strongly Lewis basic activators resulted in reduced reaction times under refluxing toluene reaction conditions. The use of 4-methoxypyridine, with a basic pK_a of 7.1 yields the ligand (**2.18**) in eight hours; 4-dimethylaminopyridine (DMAP, pK_a = 9.7) yielded (**2.19**) in six hours; and finally 1,8-diazabicyclo[5.4.0]undec-7-ene (DBU) (pK_a = 14) formed the tripodal ligand (**2.20**) in less than one hour.

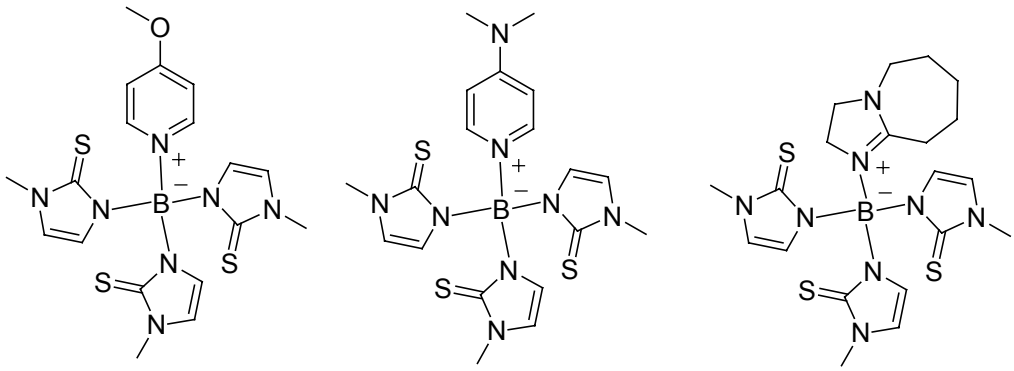

2.18 **2.19** **2.20**

Fig. 2.8. *Neutral Tm analogous ligands with different groups at the 4th position.*

As presented in the previous section, heterocycles with a basic pK_a higher than 3.5 can coordinate to the free *p*-orbital of the borane activating the dimethylamino groups to the transamination reaction with methimazole. Although the basic pK_a is crucial in the reaction outcome, *steric requirements* must also be taken into account. For example, triethylamine, with a basic pK_a of 12.1 was expected, not only to coordinate to the borane, but also to yield the tripodal ligand (triethylamino)B(methimazolyl)$_3$ in about four hours following the tendency of the other Lewis bases studied before. However, the only product of the reaction was the known 3:1 reaction product, (dimethylamido)tris(methymazolyl) borate **2.2** leaving the triethylamine in solution.

We therefore assume that steric effects of the ethyl groups are playing an important role preventing the coordination of this base to the borane.

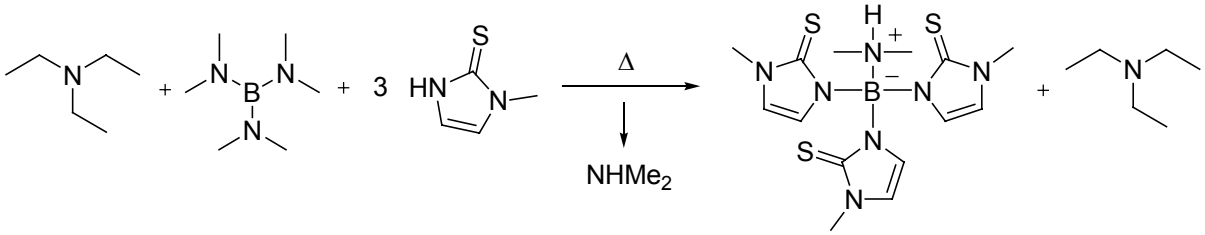

2.2

Scheme 2.13. *Steric issues prevent the coordination of Et_3N to the borane.*

2.2.3 SCOPE OF THE AZOLE HETEROCYCLES

The next step was to determine which azole heterocycles other than methimazole were able to be used to the synthesis of analogous tripodal ligands. As explained before, the traditional melt reaction is not generally applicable since it depends on the acid pK_a and the melting point of the heterocycles. The new route reported should not be so dramatically influenced by these two factors.

Three equivalents of pyrazole were reacted with one equivalent of *N*-methylimidazole and one equivalent of $B(NMe_2)_3$ to yield the tripodal ligand (*N*-methylimidazole)B(pyrazolyl)$_3$ (**2.21**) in excellent yield (92%). Ligand **2.21** did not precipitate from the reaction mixture, so the solvent was removed under vacuum to yield a colourless solid that did not require further purification. This compound can be regarded as a new *third generation* scorpionate following the nomenclature introduced by Trofimenko for tris(pyrazolyl)borates with groups at the boron forth position other than H. Metal complexes with third generation scorpionate ligands have recently been reported to be excellent magnetic materials[16] and it has been found that the substituents at the 4th position are responsible for the special characteristics and properties of such metal complexes.[17]

The ^{1}H-NMR spectrum of this ligand shows three signals for the pyrazolyl rings as expected for equivalent groups and the ^{11}B-NMR spectrum shows a sharp singlet at 3.76 ppm confirming the tetrahedral coordination at boron.

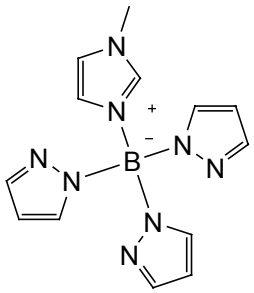

2.21

Fig. 2. 11. *Third generation Scorpionate using pyrazole as starting heterocycle.*

Analogous anionic hydrotris(azolyl)borate salts (azolyl = pyrazole, methimazole) may be prepared using the conventional melt reaction. It was therefore decided to investigate whether heterocycles which are known to be unreactive to the melting procedure with borohydride salts were reactive in the new tris(dimethylamino)borane route. For a long time our group has been interested in the synthesis of Tm analogous with different donor groups other that sulphur. For this reason 1-R-4-imidazolin-2-one (R = Ph, Et), the oxygen analogues of methimazole, were synthesised but found to be completely inert when reacted with borohydride salts under melt reaction conditions. The reaction between three equivalents of the imidazolin-2-one, one equivalent of *N*-methylimidazole and one equivalent of $B(NMe_2)_3$ was undertaken to form the new ligands (**2.22**) and (**2.23**) in excellent yields (85% and 89% respectively).

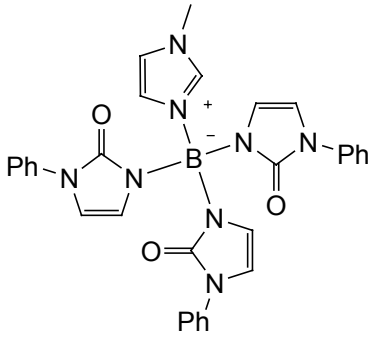

2.22

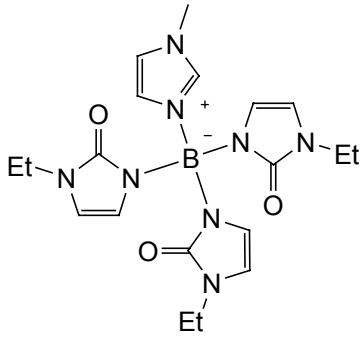

2.23

Fig. 2. 12. *Oxygen donor ligands of the $E(L_2D)_3$ type synthesised by this route.*

Ligand **2.23** was synthesised in two hours but did not precipitate from the reaction mixture. The solvent was half removed and the ligand precipitated by addition of ether. This ligand was found to be extremely hygroscopic, presumably due to effective hydrogen bonding to water through the oxygen donors. The ^{1}H-NMR spectrum shows the proton at the 2 position of the *N*-methylimidazole as a low-field singlet at 9.14 ppm. The other two protons of this ring appear as doublets at 7.77 and 6.76 ppm respectively, with a coupling constant of 1.69 Hz. The protons for the methimazole rings appear at 6.13 and 5.69 ppm as doublets with a coupling constant of 2.86 Hz. The carbonyl group is responsible for a quaternary signal at 156.21 ppm in the ^{13}C-NMR spectrum which is also confirmed by IR as an intense band at 1688 cm^{-1}. The ^{11}B-NMR spectrum shows a singlet peak at 3.65 ppm confirming the tetrahedral coordination of the boron centre.

Ligand **2.22** with phenyl groups at the 3 positions is, on the other hand, very stable and could be handled under atmospheric conditions. This may be due to the electron withdrawing character of the phenyl groups reducing the basicity of the oxygen atoms. Surprisingly, this ligand is highly insoluble in all common solvents and its characterization was carried out by elemental analysis and FAB-nominal mass spectrometry. We assume that there must be a special crystal packing in the solid state that results in its low solubility.

To further investigate the reactivity of 3-phenylimidazolin-2-one with $B(NMe_2)_3$ the reaction between the two in the absence of an activating Lewis base was undertaken in refluxing toluene. This reaction was expected to yield a tripodal ligand similar to **1.41** and **2.2** where the forth position at the boron is occupied by a dimethylamino group. After two hours a colourless solid precipitated from the solution. Upon filtration the solid was found to be highly soluble in chlorinated solvents but its characterization lead to some unexpected results. The compound isolated was not the (dimethylamino)tris(3-phenyl-imidazolyl-2-one)borate expected. It was found to be the dimer (**2.24**) where two azole heterocycles are bridging two boron atoms which are bonded to two more heterocycles.(Scheme **2.12**).

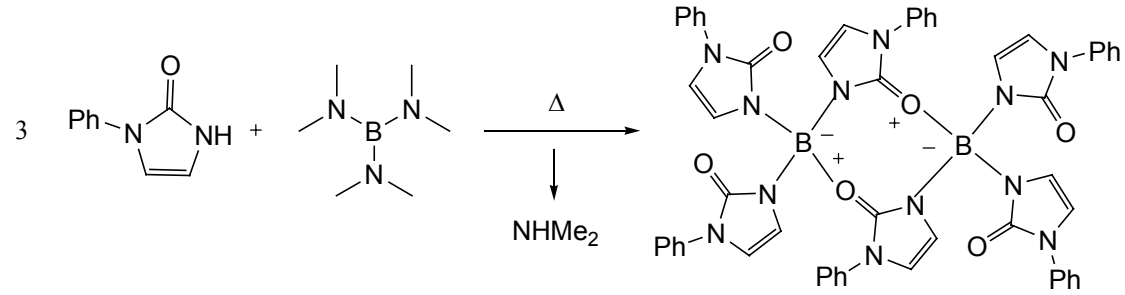

2.24

Scheme 2.12. *Unexpected imidazabole formation.*

Such dimeric compounds are also known in the literature for pyrazole and are defined as pyrazaboles.[18] These compounds have been extensively studied by the group of Chujo who has applied them as polymeric materials.[19] Therefore the nomenclature *imidazabole* for **2.24** seems appropriate. Niedenzu reported that the thermolysis of (dimethylamido)B(pyrazolyl)$_3$ **1.41** provides the pyrazabole (**2.25**), by displacement of the dimethylamino groups and pyrazolyl coordination to form the dimer (Scheme **2.13**).

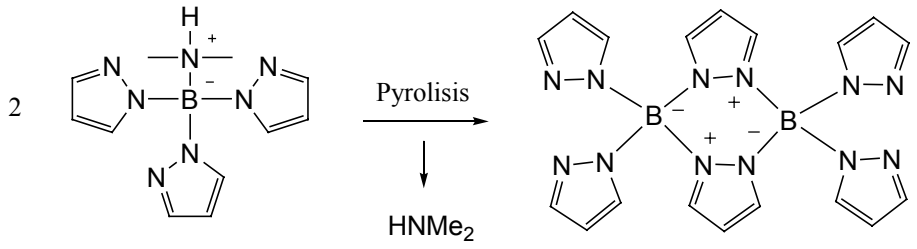

1.41 **2.25**

Scheme 2.13. *Pyrazabole formation by pyrolisis of* **1.41**.

We assume that in the reaction between the $B(NMe_2)_3$ and the phenyl-imidazoline, refluxing in toluene is able to induce a similar reactivity. For the *imidazabole* to be formed, the heterocycle must present a good bridging group like the imine nitrogen in the case of pyrazole (B-N is isoelectronic with C-C) or the oxygen atom in the other case (boron being highly oxophilic) since otherwise the dimer would be unstable. All our attempts to form a similar dimeric compound from (dimethylamido)B(methymazolyl)$_3$ **2.2** were therefore unsuccessful. The sulphur atoms are not able to bridge two boron centres and only decomposition products and free methimazole were isolated after pyrolisis of **2.2**.

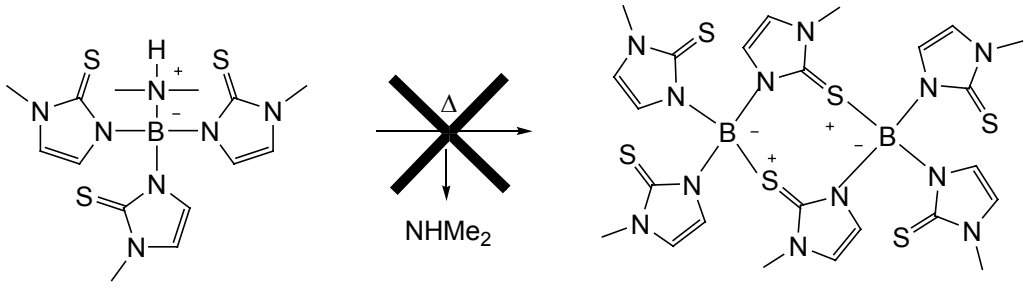

2.2 **2.26**

Scheme 2. 14. *Attempted synthesis of a methimazabole* **2.26**.

Since high temperatures are responsible for the formation of the dimer **2.24**, the reaction between $B(NMe_2)_3$ and the phenyl-imidazoline-2-one was carried out in toluene at 70^0C. After two hours no traces of starting heterocycle were detected by TLC.

Heating was discontinued and the remaining yellowish solution was concentrated to half volume. Dry ether was added and the flask stored in the fridge overnight. Small crystals were formed, isolated and characterised as (**2.27**) in good yield (78%).

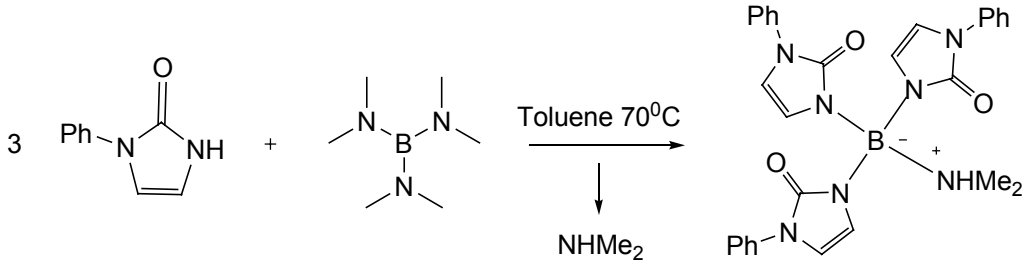

2.27

Scheme 2.15. *Lower temperatures yield the tripodal ligand* **2.27**.

The ^{1}H-NMR confirms the synthesis of **2.27**. The methyl groups of the amino group appear at 2.89 ppm and the NH is responsible for a broad band at 8.62 ppm. The heterocycle protons appear as doublets at 6.41 and 6.69 ppm with a coupling constant of 2.97 Hz. The aromatic protons appear at 7.25, 7.45 and 7.69 ppm respectively. The ^{13}C-NMR spectrum shows eight peaks, with the C=O at 156.15 ppm being the most down-field shifted signal. The presence of the NMe_2 group is confirmed by a signal at 41.09 ppm. Mass spectrometry of the solid reveals a molecular ion at 533.97 due to the protonated ligand **2.27** and IR confirms the C=O group with an intense band at 1678 $cm^{-1.}$

2.3 CONCLUSIONS

This chapter has dealt with the development of a novel synthetic route to borate ligands using $B(NMe_2)_3$ as the boron source. The reactivity of this borane with diverse imidazole heterocycles has been studied and found to yield tetra or tri-substituted borate systems depending on the basic pK_a of the heterocycles. For heterocycles with a basic pK_a higher than 3.5 the tetrasubstituted compounds were always obtained.

For those heterocycles which are not basic enough a transamination reation takes place to yield the trisubstituted ligands where the 4^{th} position at the boron is occupied by a dimethylamino group. A mechanism for the reaction has been proposed and found to be reasonable by additional experiments. This new protocol is a high yielding and versatile procedure that allows the easy modification of the ligands by means of using diverse activators or azole heterocycles as starting materials. Only the pK_a of the Lewis bases, and in certain cases steric factors, can play a limiting role in its applicability, however, many common nitrogen bases present a basic pK_a higher than 3.5, so the scope, in this regard, can be considered quite broad.

Interestingly, this methodology allows the synthesis of previously elusive tripodal ligands like [(*N*-methylimidazole)B(2-R-imidazoline-2-one)] **2.22** since the melting point and acid pK_a of the heterocycles are no longer limiting. Imidazaboles, dimeric structures which have not been reported previously were synthesised by reaction of $B(NMe_2)_3$ with 3-phenylimidazolin-2-one.

2.4 REFERENCES CHAPTER II

1. P. J. Bailey, P. P. Pinho, S. Parsons, *Inorg. Chem.,* 2003**, 42**, 8872.
2. C. Bergquist, H. Storrie, L. Koutcher, B.M. Bridgewater, R.A. Friesner, and G. Parkin*, J. Am. Chem. Soc.,* 2000, **122**, 12651.
3. M. C. Keyes, B. M. Chamberlain, S. A. Caltagirone, J. A. Halfen, W. B. Tolman, *Organometallics*, 1998, **17**, 1984.
4. G. R. Motson, O. Mamula, J. C. Jeffery, J. A. McCleverty, M. D. Ward, A. von Zelewsky, *J. Chem. Soc., Dalton Trans.,* 2001, 1389.
5. I. Lopes, G. Y. Lin, A. Domingos, R. McDonald, N. Marques, J. Takats, *J. Am. Chem. Soc.,* 1999, **121**, 8110.
6. A. Caballero, F. Gomez, F. A. Jalon, B. Manzano, A. M. Rodriguez, S. Trofimenko, M. Sigalas, *Dalton Trans.,* 2001, 427.
7. A. F. Hill, G. R. Owen, A. J. P. White, D. J. Williams, *Angew. Chem. Int. Ed.,* 1999, **38**, 2756.
8. R. J. Blagg, J. P. H. Charmant, N. G. Conelly, M. F. Haddow, A. G. Orpen, *Chem. Commun.,* 2006, 2350.
9. P.P. Pinho, P. J. Bailey, *unpublished results.*
10. K. Niedenzu, S. Trofimenko, *Inorg. Chem.,* 1985, **24**, 4222.
11. N. Kuhn, H. Bohnen, J. Kreutzberg, D. Blaeser, R. Boese, *J. Chem. Soc., Chem. Commun.*, 1993, 1136.
12. W. A. Herrmann, *Angew. Chem. Int. Ed.,* 2001, **40**, 1291.
13. A. D. Hopkins, A. J. Wood, D. S. Wright, *Coord. Chem. Rev.,* 2001, **216-217**, 155.
14. T. A. Khan, M. A. Khan, Z. Khan, M. M. Haq, *Synth. React. Inorg. Met,-Org. Chem.,* 2003, **33**, 297.
15. K, Kirk, *J. Org. Chem.,* 1978, **43**, 4381.
16. D. L. Reger, J. R. Gardinier, W. R. Gemill, M. D. Smith, A. M. Shahin, G. J. Long, L. Rebbouh, F. Grandjean, *J. Am. Chem. Soc.,* 2005, **127**, 2303.
17. D. L. Reger, J. R. Gardinier, M. D. Smith, A. M. Shanin, G. J. Long, L. Rebbouh, F. Grandjean, *Inorg. Chem.,* 2005, **44**, 1852.

18. K. Niedenzu, S. S. Seelig, W. Z. Weber, *Z. Anorg. Allg. Chem.,* 1981, **483**, 51.

19. F. Matsumoto, Y. Chujo, *Macromolecules,* 2003, **36**, 5516.

CHAPTER III

COORDINATION STUDIES

3.1 INTRODUCTION

Due to our interest in applying the tripodal borate ligands introduced in the previous chapter in reactions catalysed by octahedral metals, coordination studies were undertaken. The chosen metal precursors were $[Ru(p\text{-cymene})Cl_2]_2$ and $[Mn(CO)_3(MeCN)_3]PF_6$ for the zwitterionic analogues of the Tm and Tp ligands (ZTm and ZTp from now onwards), and metal halides ($FeCl_3$, $ZnCl_2$, $AlCl_3$) for the new oxygen donor imidazoline-2-one ligands. Certain complexes of ruthenium(II) are known to catalyse the transfer-hydrogenation of prochiral ketones, the reaction on which we have focused our efforts and which will be covered in detail in the next chapter. The tricarbonylmanganese(I) precursor was chosen due to the possibility to determine the electron-releasing or withdrawing nature of the ligands by analyzing the carbonyl stretches by IR spectroscopy. Carbonyl infrared data have long been used as an indicator of the retrodative capacity of transition metal centres.[1,2]

3.2. COORDINATION MODES OF TRIPODAL BORATE LIGANDS

3.2.1 Hydrotris(pyrazolyl)borate ligands (Tp)

The Tp ligand is an anionic, six-electron, relatively hard σ-donor ligand. In six coordinate environments it enforces nearly facial octahedral coordination to the metal with N-M-N bite angles close to the ideal 90º value.

However, as Parkin and coworkers have demonstrated bulky subtituents like ^{t}Bu or Ph groups in the 3-positions of the pyrazole rings enforces 4-coordination as exemplified by monomeric alkylmagnesium and alkylzinc species using these ligands.[3] The most common coordination mode for poly(pyrazolyl)borates is the κ^3-mode, where the three pyrazolyl rings bind the metal centre in a facial tripodal fashion, although unusual coordination modes for pyrazolyl borates, from "κ^0" to κ^5 are also known and will be discussed next.

Carmona and coworkers have reported the interconversion of κ^3-*N,N,N*, κ^2-*N,N*-, κ^1-*N*- and "κ^0"-$Tp^{Me}{}_2$ rhodium complexes where $Tp^{Me}{}_2$ is the hydrotris(3,5-dimethylpyrazolyl)borate ligand.[4] The reaction of the rhodium complex (**3.1**) with excess PMe_3 yields the complex (**3.4**) quantitatively under mild conditions (room temperature, 1h) as shown in Schemes **3.1** and **3.2**.

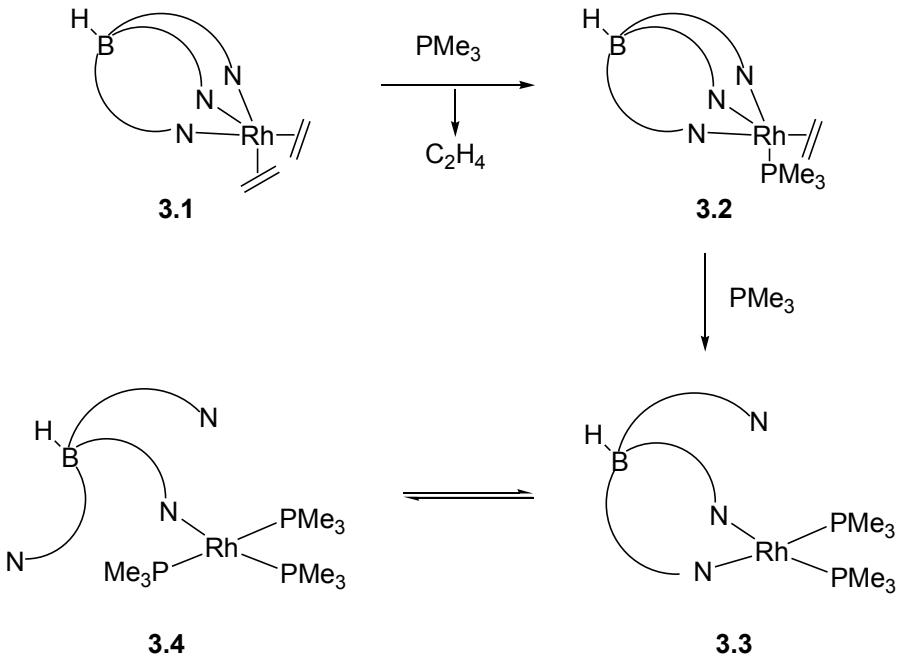

Scheme 3.1. *Variation of the coordination modes of Tp´Rh complexes.*

Complete displacement of the coordinated $Tp^{Me}{}_2$ ligand is also possible but forcing conditions are necessary (120ºC, 6h).

The ligand acting as "κ^0" coordinated was isolated using the $TpRh(H)_2$ (**3.5**) as the metal precursor. Reaction with PMe_3 at room temperature affords the ionic pair (**3.7**).

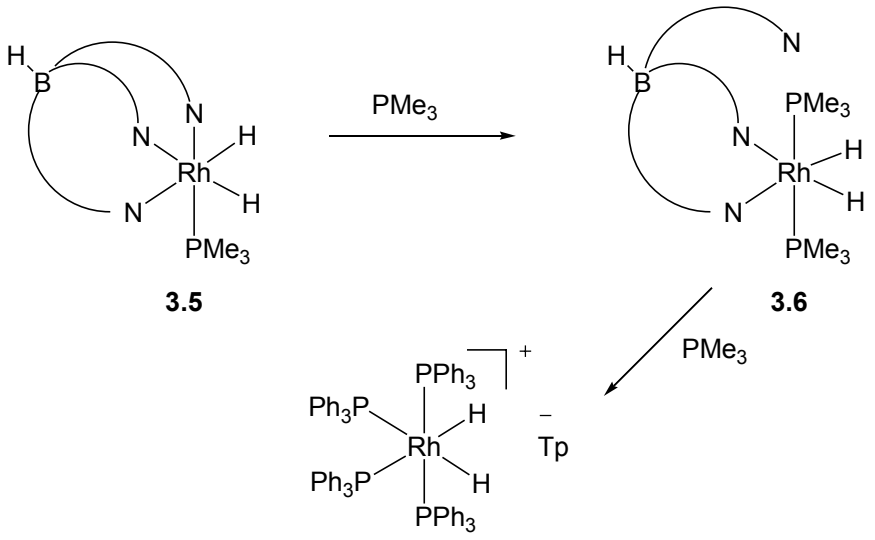

Scheme 3.2. *"κ^0" coordination mode for $[Tp][Rh(H)_2(PMe_3)_4]^+$.*

There is no bonding interaction between the Rh centre and the Tp ligand, the shortest Rh···N distance being 4.627 Å. This is the first example of a stepwise change in the denticity of Tp ligands from κ^3 to "κ^0" where the Tp ends up acting as an uncoordinated counter-anion. The same group has also reported higher modes of coordination for substituted Tp ligands.[5] The reaction between Tp^{Ph} and $[IrCl(coe)_2]_2$ (coe = cyclooctene) in the presence of ethene leads to (**3.8**) where the ligand is κ^4-coordinated to the metal centre. The C-H bond activation process is considered to be favoured by the close proximity of the phenyl groups to the metal centre since the same reaction with Tp^{Me} ligand leads to the formation of the κ^3-coordinated $Tp^{Me}Ir(\eta_2\text{-}C_2H_4)_2$. Upon heating (**3.9**) in benzene a second C-H bond activation process occurs where the ligand κ^5-coordinates to the metal centre, and although X-ray analysis shows a considerable distortion of the pentadentate ligand, the preferred octahedral environment at the coordinated metal prevails.

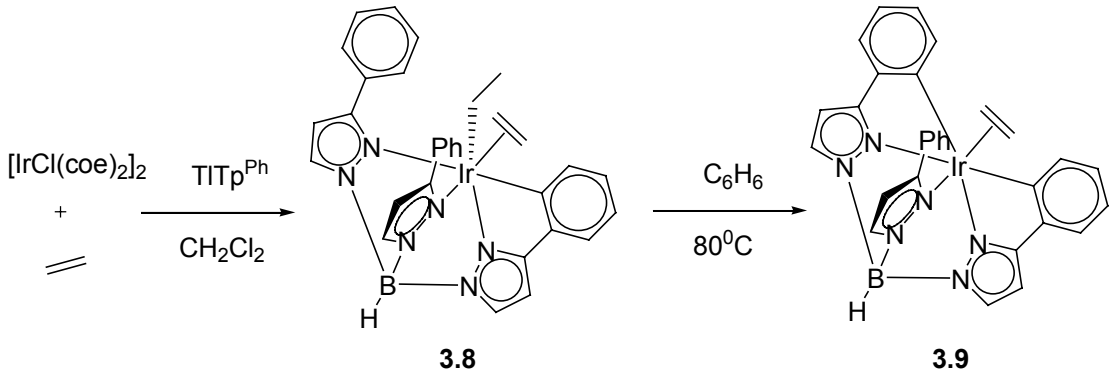

Scheme 3.3. *First example of* κ^5*-coordination mode for Tp ligands.*

3.2.2 Hydrotris(methimazolyl)borate ligand (Tm)

The Tm ligand is also known to favour a facial tridentate κ^3-*S,S,S*-coordination mode upon metal complexation where the conformation of the eight-membered chelate rings formed is responsible for the C_3-symmetric geometry of the complexes as shown in Section **1.2**. Tm ligand derivatives are also known to coordinate in a κ^1- or κ^2-mode in cases where the steric bulk of the ligand prevents the coordination to the metal centre, and even a κ^4-coordination mode in the case of the metallaboratranes discussed in Chapter II. Higher modes have not been reported to date and an example of a Tm ligand acting as a non-coordinating "κ^0" counter-anion has yet to be characterised.

3.3 MANGANESE COMPLEXES

The complexes of poly(pyrazolyl)borates with the metals of group 7 have become recently interesting due to their potential application in the preparation of radiopharmaceuticals incorporating ^{99m}Tc or $^{186/188}$Re isotopes.[6] Extending these studies to the lightest member of the group has been used as a valid approach given the availability of manganese precursors and simplified synthetic methodologies. The first characterization of a poly(pyrazolyl)borate manganese complex was reported by Trofimenko in 1968.[7]

The reaction between NaTp and $Mn(CO)_5Br$ proceeded readily to yield the compound $TpMn(CO)_3$ with high yields. IR studies of this compound in hexanes revealed two carbonyl stretches at 2041 and 1941 cm^{-1} for the three CO ligands present in the complex. This situation is due to the symmetry of the ligand that forms a C_{3v}-symmetric complex in solution and therefore only two carbonyl stretches are expected for the A and E modes respectively. Comparison of these values with the ones obtained for $CpMn(CO)_3$ (2028, 1947 cm^{-1} in hexanes) indicates that the electron donor ability of Tp differs somewhat from Cp, appearing to provide less electron density to the metal. The neutral analogue of the Tp ligand where three pyrazole groups are attached to a carbon atom (known as Tpm ligand) was first synthesised by Huckel and coworkers in 1937.[8] Reger and coworkers have reported the manganese complex $[Tpm(Mn)(CO)_3]$ OTf which shows two carbonyl stretches at 2051 and 1956 cm^{-1}.[9] This indicates that the Tp ligand has better donor properties than its neutral counterpart.

A few years ago the first manganese complex of the Tm ligand $[TmMn(CO)_3]$ was reported by our group.[10] It was synthesised from the reaction between $[Mn(CO)_3(MeCN)_3]$ PF_6 and NaTm in refluxing ethanol. Two carbonyl stretches at 2003 and 1905 cm^{-1} were recorded for the complex in toluene solution. The κ^3-*S,S,S*-coordination by the tripodal Tm ligand and the three CO ligands provides C_3 molecular symmetry to the resulting complex and therefore it exists as a racemic mixture. For this symmetry the same number of carbony stretches are predicted (A + E modes). The infrared spectra recorded in KBr pellets showed four carbonyl stretches of similar intensity due to the presence of two independent molecules in the asymmetric unit. It is worth noting now that the infrared spectrum of this complex indicates that the Tm ligand is a better donor than both Tp and Cp ligands. The additional electron density at the metal centre in the $TmMn(CO)_3$ is responsible for an increased degree of backbonding to the CO groups and the observed shift to lower energies for the CO stretches. The donor ability of these ligands will be discussed further in Section **3.6**.

3.4 RUTHENIUM COMPLEXES

The chemistry of poly(azolyl)borate ruthenium complexes has also attracted interest recently due to their application in processes that involve C-H bond activation, ligand exchange reactions, or charge-transfer processes amongst others.[11] The scorpionates usually coordinate to ruthenium in a κ^3 or κ^2-coordination mode that can, in some cases, be controlled. In 1997, Tocher and coworkers reported a synthetic protocol for the synthesis of ruthenium(II) arene complexes with poly(pyrazolyl)borate and -methane ligands and this work will serve as a reference for comparison purposes.[12] The zwitterionic ligands introduced in the previous chapter are formally neutral, where the central boron atom has a negative charge that is balanced by the positively charged quaternary nitrogen coordinated to it. It is interesting to determine whether the behaviour of these ligands is closer to the anionic poly(azolyl)borates or more similar to the neutral poly(azolyl)methanes.

The synthetic methodology introduced by Tocher starts with a ruthenium(II) arene dimer of the generic formula $[\{Ru(\eta^6\text{-arene})(\mu\text{-}Cl_2)\}_2]$, where the arene may be mesitylene, *p*-xylene or hexamethylbenzene, and where two chlorides are bridging both metal centres. These dimers can be cleaved in the presence of a donor solvent like acetonitrile or methanol. Dichloromethane, on the other hand, does not promote the cleavage of the Ru-chloride bonds. The solvent, the temperature and the extent of dissolution of the ruthenium precursor have been reported to direct the hapticity of the resulting scorpionate complexes; either in the κ^2- or κ^3-coordination modes. The Scheme **3.4** shows the synthetic protocol for the synthesis of such compounds.

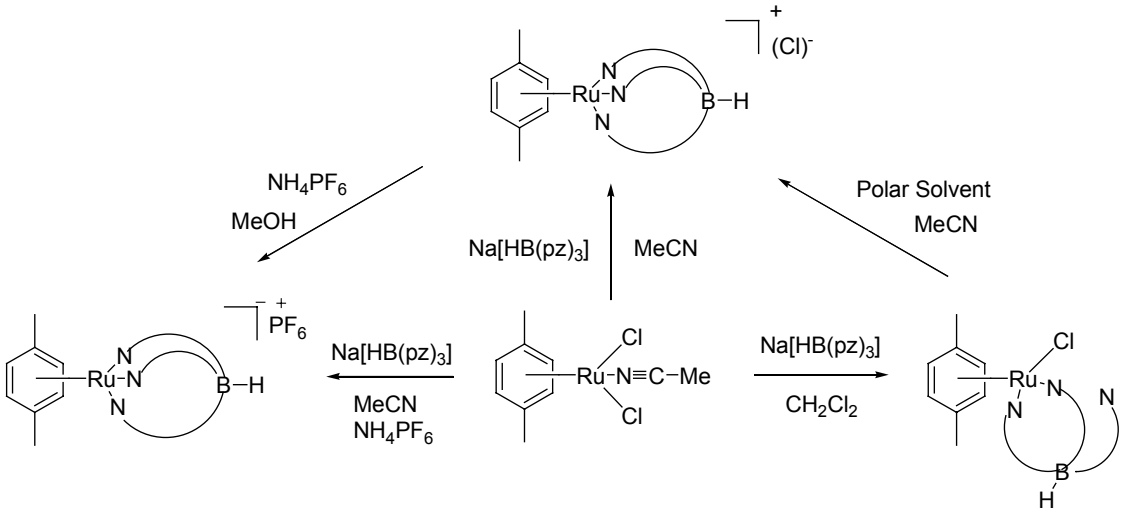

Scheme 3.4. *Methodology for the synthesis of Ru(arene)(scorpionate) complexes.*

The ruthenium dimer is dissolved in MeCN and stirred prior to the addition of the borate ligand. The stirring period of the metal precursor in MeCN affects the coordination behaviour of the scorpionate ligands since the acetonitrile displaces sequentially each chloro ligand from the ruthenium centre to form, in the first instance, $[Ru(arene)(MeCN)Cl_2]$, where the dimer has been opened, followed by $[Ru(arene)(MeCN)_2Cl]^+$, where two molecules of solvent are now coordinated to the ruthenium atom, and finally $[Ru(arene)(MeCN)_3]^{2+}$, where both chloro ligands have been displaced. Coordination of the tripodal ligand to the latter species induces the replacement of the three acetonitrile molecules, the ligand finally being coordinated in the κ^3-mode.

When the complex $[Ru(arene)(MeCN)_2Cl]^+$ is treated with the tripodal ligand in a solvent that does not promote Ru-Cl bond cleavage, dichloromethane for instance, the ligand does not coordinate in a κ^3-mode since a chloro ligand is still linked to the metal. However, it is possible to force tridentate coordination by dissolving and heating the κ^2-species in a polar solvent. Ultimately, treatment of the κ^3-species with a methanolic solution of NH_4PF_6 provokes salt metathesis where the chloro ligands are substituted by two of PF_6^- anions that generally makes the whole complex insoluble, thus facilitating its separation.

It is worth noting that the κ^3-coordination mode of the ligand is irreversible and that for tris(pyrazolyl)methanes similar reactivities have been observed.

Ruthenium complexes of the Tm ligand have also been reported.[10] In Chapter II the metallaboratranes were first introduced where the reaction between the Tm ligand and $[Rh(Ph)(PPh_3)_2(Cl)_2]$ yielded the first example of a complex where the metal had formed a dative bond with the boron centre. Metallaboratranes of ruthenium have also been reported upon the reaction between Tm ligand and $[Ru(CH{=}CH_2)(CO)(PPh_3)_3Cl]$. However this is a special example since reaction of Tm with different ruthenium precursors like $Ru(DMSO)_4Cl_2$, [{Ru(*p*-cymene)Cl_2}] or $[CpRu(MeCN)_3]PF_6$ did not form similar metallaboratranes.[10] In all cases the Tm coordinated in the κ^3-mode retaining the B-H moiety intact.

3.5 RESULTS

3.5.1 [ZTmRu(*p*-cymene)](Cl_2) (3.10)

$[Ru(p\text{-cymene})Cl_2]_2$ was dissolved in dry MeCN and the mixture stirred for one hour to yield a reddish coloured solution. Ligand **2.17** [(*N*-methylimidazole)B(methimazolyl)$_3$], was then added in small portions and the mixture stirred at room temperature. A colour change to deep red indicated complexation which took place in one hour. Upon concentration of the solvent the ruthenium complex (**3.10**) was precipitated in 82% yield by addition of Et_2O.

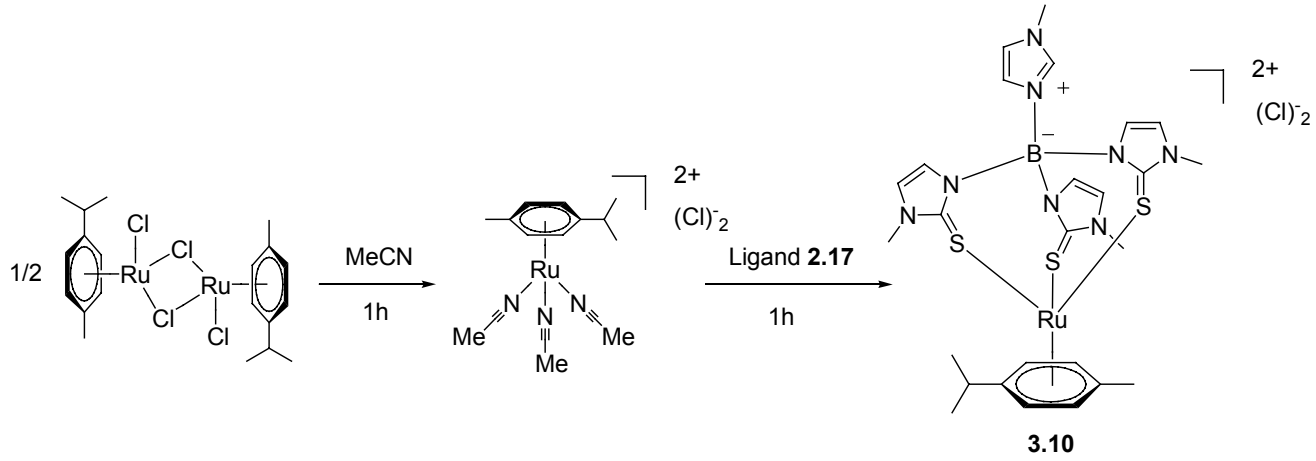

3.10

Scheme 3.5. *Synthesis of the ruthenium(II) complex* **3.10**.

Spectroscopic Analysis

The ^{1}H and ^{13}C-NMR spectra obtained for **3.10** are consistent with the structure found in the solid state; the protons of the methimazolyl groups are equivalent indicating that the ligand is coordinated in the κ^3-mode. The methimazolyl signals have undergone an average downfield shift of + 0.91 ppm with respect to the free ligand environment in ZTm. This is a similar, but slightly higher shift than for [TmRu(*p*-cymene)]Cl (mean + 0.43 ppm).[10] An interesting feature of this spectrum is the appearance of the signals due to the arene CH protons of the *p*-cymene ligand. The Ru(II)(*p*-cymene) fragment is found in many complexes and these protons usually appear as a clear $(AB)_2$ system in their NMR spectra. However, in the spectrum of **3.10** a complex multiplet appears between 5.94 and 5.84 ppm. This can be attributed to the diastereotopic nature of these protons in the chiral environment provided by the coordination of the ZTm ligand as has been observed for the [TmRu(p-cymene)]Cl.[10] The molecular ion (M^+/2= 334) was the only peak observed by mass spectrometry.

.

Molecular Structure

Single crystals of **3.10** suitable for X-ray diffraction studies were obtained by slow diffusion of hexane into a dichloromethane solution of **3.10**. The structure shows that the ZTm ligand adopts a facially capping arrangement with the η^6-*p*-cymene ligand completing the ruthenium coordination sphere (Fig. **3.2**). The asymmetric unit contains two independent pair of complexes displaying $\delta\delta\delta$ and $\lambda\lambda\lambda$-stereochemistry for the three ligand arms. There are only minor diferences in the metric parameters between the two enantiomers and only those for the $\delta\delta\delta$ enantiomer will be discussed below. The chiral twist that the Tm ligands forms upon metal complexation has led to the introduction of a unified set of parameters to denote this special kind of torsion (Fig. **3.1**).[13]

The first parameter, θ^m, defined by the mean N-B-M-S torsional angle for each methimazolyl buttress, have values of 49.8° and -49.5° for the two enantiomers of **3.10**. The other torsional parameter ω^m, which is defined as the mean angle made by the normal to the methimazole ring with the B-M vector, has values that fall in the range observed for Tm complexes of other octahedral metals (mean 57.75° and –56.28°).

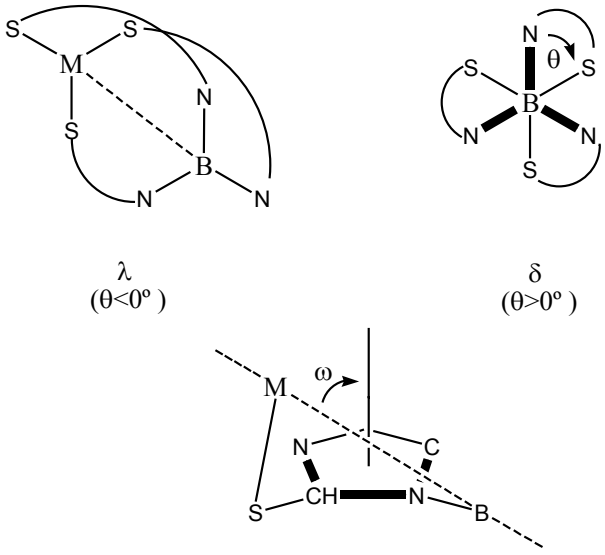

Fig. 3.1. *Parameters "θ and ω" introduced by Hill to determine the torsional behaviour of Tm ligands.*

The B-N(14) distance for the coordinated *N*-methylimidazole ring is slightly longer (1.567 Å) than the B-N distance for the methimazolyl rings (mean 1.549 Å) due to the covalent character of these latter bonds when compared to the coordinated *N*-methylimidazole ring. The C-S and S-Ru bond lenghts (1.730 Å and 2.426 Å respectively) do not differ significantly from those found in the corresponding complex containing the Tm ligand (mean 1.723 Å and 2.411 Å).[10] The three S-Ru-S angles are all close to 90º [89.11º-91.80º] and they fall in the same range found in [RuTm(*p*-cymene)]Cl. These results indicate that the binding of ligand **3.10** to the ruthenium centre is similar to that for the anionic Tm. Selected bond distances and angles are provided in Table **3.1**.

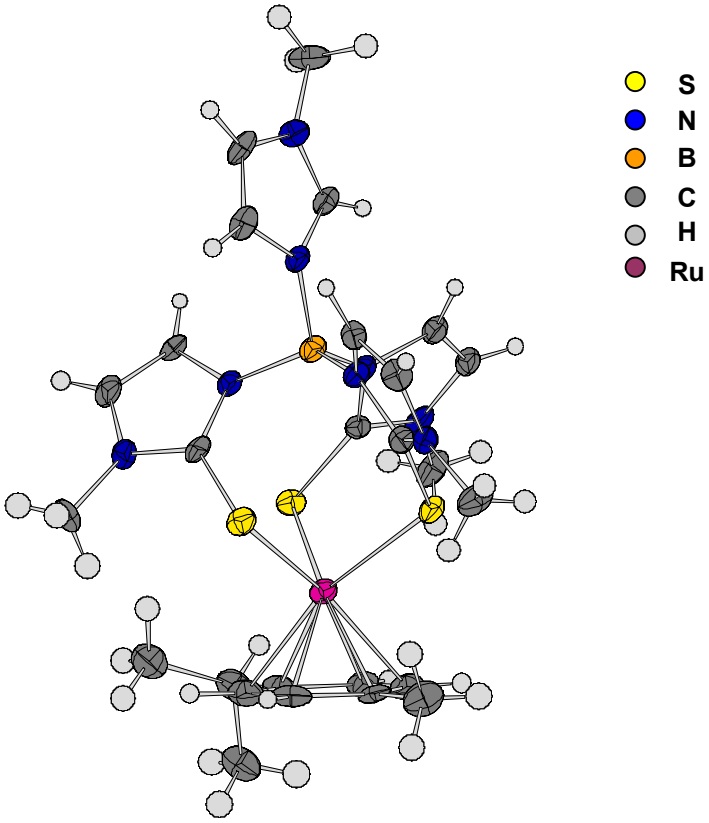

Fig. 3.2. *X-ray structure of the Ru complex* **3.10**. *Only one enantiomer is shown and the two Cl counterions have been omitted for clarity.*

Table 3.1. SELECTED BOND LENGTHS (Å) AND ANGLES (°) FOR **3.10**.

B-N(14)	1.567(2)	Ru-C(45)	2.207(8)
B-N(11)	1.559(2)	Ru-C(55)	2.198(9)
B-N(12)	1.538(2)	Ru-C(65)	2.185(8)
B-N(13)	1.551(2)	Ru-C_{centr}	1.445(8)
C(21)-S(21)	1.721(9)	N(11)-B-N(12)	113.3(7)
C(22)-S(22)	1.734(8)	N(11)-B-N(13)	111.3(7)
C(23)-S(23)	1.735(8)	N(11)-B-N(14)	105.0(7)
S(21)-Ru	2.441(2)	N(12)-B-N(13)	110.0(7)
S(22)-Ru	2.428(2)	N(12)-B-N(14)	105.2(7)
S(23)-Ru	2.409(2)	N(13)-B-N(14)	111.9(7)
Ru-C(15)	2.218(9)	S(21)-Ru-S(22)	91.41(8)
Ru-C(25)	2.188(9)	S(21)-Ru-S(23)	89.11(7)
Ru-C(35)	2.218(8)	S(22)-Ru-S(23)	91.80(8)

3.5.2 [ZTmMn(CO)$_3$](PF$_6$) (3.11)

To a solution of [Mn(CO)$_3$(MeCN)$_3$]PF$_6$ in acetonitrile, ligand **2.17** [(*N*-methylimidazole)B(methimazolyl)$_3$] was added in small portions and the resulting mixture heated to reflux for 2h. A yellowish solid precipitated from the solution which was isolated in 75% yield.

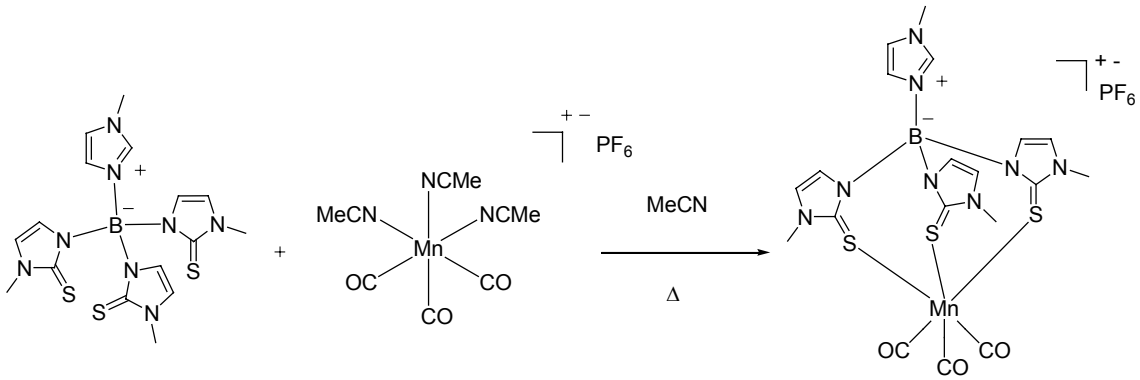

2.17 **3.11**

Scheme 3.6. *Synthesis of the manganese(I) complex* **3.11**.

Spectroscopic Analysis

Two $\nu_{C\text{-}O}$ signals are observed in the IR spectrum of an acetonitrile solution of complex (**3.11**), these consist of two medium intensity bands at 2007 and 1914 cm^{-1}. This is consistent with the known structure; given the *pseudo*-C_3-symmetry conferred on the complex by the twisted conformation of the [TmMn] unit, two bands are predicted for the C-O stretching modes. The presence of the *N*-methylimidazole in the axial boron site prevents overall C_3-symmetry for complexes of this ligand. In the solid state spectrum (KBr disc) of **3.11** four absorptions of approximately equal intensity due to C-O stretching are observed at 1999, 1988, 1898 and 1889 cm^{-1} which are attributable to the presence of the two enantiomeric molecules in the unit cell of the complex. Interestingly all IR stretches of complex **3.11**, both in solution and in the solid state, are very similar to [$TmMn(CO)_3$] (2003, 1905 cm^{-1} in solution, 1994, 1984, 1896, 1884 cm^{-1}) meaning that the donor properties of the two ligands are very similar. The bands in **3.11** are somewhat shifted toward higher energy in accord with the existence of a formal positive charge on the metal centre. As mentioned before, the metal complex $CpMn(CO)_3$ showed two carbonyl stretches at 2028 and 1947 cm^{-1} so the ν(CO) value can be seen to move to lower frequency along the series Cp $\rightarrow$ ZTm $\rightarrow$ Tm indicative of a progressive increase in donor properties of the facial ligands. Cp is able to act as a π-acceptor and competes with the CO groups for electron density resulting in a higher ν(CO) value for the Cp complex. The ZTm and Tm have lower values suggesting progressively greater electron density at the metal. The lone pairs of the sulphur donors of ZTm and Tm will overlap efficiently with the metal orbitals resulting in a strong π-donation. The ^{1}H-NMR and ^{13}C-NMR spectra are also consistent with the X-ray crystal structure of **3.11**. The protons of the three methimazolyl groups are equivalent which suggests a symmetrical mononuclear structure in solution. The molecular ion peak (M^+ = 571.9) is the base peak observed by mass spectrometry.

Molecular Structure

Single crystals suitable for X-ray diffraction studies were obtained by slow diffusion of ether into a dichloromethane solution of **3.11**. The S-coordination by the tripodal ZTm and the three CO ligands provide the expected *pseudo*-C_3 molecular symmetry and therefore there are two enantiomeric molecules in the unit cell. Discussion will again be restricted to the $\delta\delta\delta$ enantiomer only (Fig. **3.3**). The B-N distance for the coordinated *N*-methylimidazole ring is slightly longer (1.591 Å) than the average B-N distance for the methimazolyl rings (1.541 Å) due to the covalent character of these bonds. The manganese atom adopts a slightly distorted octahedral geometry and there are only minor deviations from 90º in the angles around Mn, with the average S-Mn-S angles being 92.62º, C-Mn-C 90.80º and S-Mn-C 89.63º. The Mn-S average distance is 2.429 Å and the Mn-C distance is 1.795 Å. In comparison with the analogous Tm complex these are only slightly different (mean Mn-S 2.401 Å, and Mn-C 1.802 Å).[10] The torsional parameter, θ^{m} has values of 49.3° and -49.5°, for the two enantiomers, almost identical to those found for [ZTmRu(*p*-cymene)]Cl_2. The other torsional parameter, ω^{m}, has values that fall in the range observed for Tm and ZTm complexes of other octahedral metals (mean 56.99 and –56.79°) meaning that the ligand adopts a similar propeller twist in both metal complexes. Selected bond distances and angles are provided in Table **3.2.**

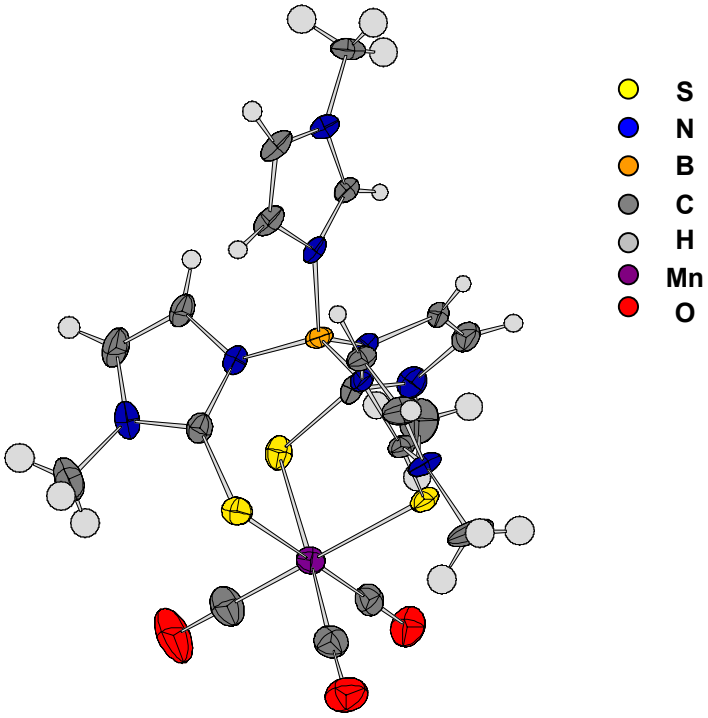

Fig. 3.3. *X-ray structure of the manganese complex* **3.11**. *Only the δδδ enantiomer is shown and the counterion PF_6 is also omitted.*

Table 3.2. SELECTED BOND LENGTHS (Å) AND ANGLES (°) FOR **3.11.**

B-N(14)	1.591(7)	N(11)-B-N(12)	115.0(4)
B-N(11)	1.535(8)	N(11)-B-N(13)	113.0(4)
B-N(12)	1.542(7)	N(11)-B-N(14)	103.0(4)
B-N(13)	1.548(7)	N(12)-B-N(13)	108.0(4)
C(21)-S(21)	1.714(6)	N(12)-B-N(14)	108.5(4)
C(22)-S(22)	1.724(6)	N(13)-B-N(14)	111.9(7)
C(23)-S(23)	1.723(5)	S(11)-Mn-S(12)	91.11(5)
S(21)-Mn	2.432(1)	S(11)-Mn-S(13)	93.53(5)
S(22)-Mn	2.413(1)	S(12)-Mn-S(13)	93.22(5)
S(23)-Mn	2.460(1)	C(15)-Mn-C(16)	92.20(3)
Mn-C(15)	1.798(7)	C(15)-Mn-C(17)	89.70(3)
Mn-C(25)	1.794(7)	C(16)-Mn-C(17)	90.40(3)
Mn-C(35)	1.794(7)		

3.5.3 [ZTpRu(*p*-cymene)](PF$_6$)$_2$ (3.12)

[Ru(*p*-cymene)Cl$_2$]$_2$ was dissolved in dry MeCN and the mixture was stirred for 60 min to yield a reddish coloured solution. Ligand **2.21** [(*N*-methylimidazole)B(pyrazolyl)$_3$] was then added and the mixture was stirred at room temperature for three hours. A colour change from red to orange was detected after this time. The solvent was removed under vacuum and the solid was redissolved in MeOH. Excess NH_4PF_6 was added at once and the mixture was vigorously stirred. No solid precipitated, therefore the solvent was removed and the resulting solid was extracted with 10 ml of acetone. The organic phase was separated from the excess of NH_4PF_6 by filtration and the solvent was removed to give [ZTpRu(*p*-cymene)](PF$_6$)$_2$ (**3.12**) as a yellowish solid in 93% yield.

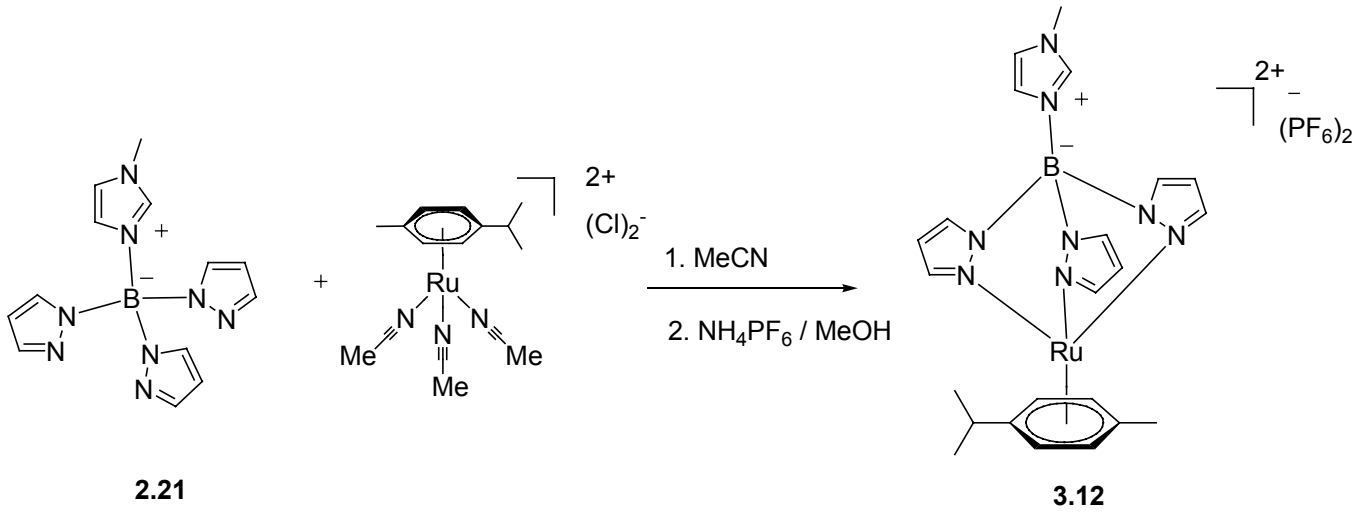

2.21 **3.12**

Scheme 3.7. *Synthesis of the ruthenium(II) complex* **3.12**.

Spectroscopic Analysis

The ^{1}H and ^{13}C-NMR spectra obtained for **3.12** are consistent with a κ^3-coordinated ligand and therefore only one set of pyrazolyl resonances is present. The pyrazolyl signals have undergone an average downfield shift of +0.63 ppm with respect to the free ligand environment. The largest of these shifts is observed for H^3 (+0.87 ppm), consistent with the proton in the 3 position being structurally *endo* to

the metal fragment and hence most likely to experience the greatest change in chemical environment. The arene CH protons of the *p*-cymene ligand from the Ru(II)(*p*-cymene) fragment appear as a clear $(AB)_2$ system as two doublets with a coupling constant of 6.31 Hz similar to previously reported analogous Ru arene complexes.[12] This observation, which contrasts with the Tm and ZTm complexes, is explained by the *pseudo*-C_{3v}-symmetry that the complex presents since six-membered chelate rings are now formed upon complexation in contrast to the eight membered rings founded for the Tm and ZTm ligands. By mass spectrometry the molecular base peak corresponds to the $M^+/2$ (265.01).

Molecular Structure

The formulation of **3.12** was unequivocally confirmed by carrying out an X-ray crystal structure determination. Crystals of **3.12** suitable for crystallography were grown by slow diffusion of ether into a concentrated solution of **3.12** in acetone. Only one molecule is present in the asymmetric unit contrasting with the racemic pair found for **3.10** and **3.11**. The compound **3.12** exists as a half sandwich complex where the *p*-cymene moiety occupies three of the six coordination sites and the scorpionate the other three. The ruthenium atom is η^6-bonded to the arene ligand with an average Ru-C distance of 2.216 Å and a separation between the arene plane and the Ru of 1.462 Å, very similar to that observed in related arene ruthenium complexes.[12] The boron atom is tetrahedral (average N-B-N angle of 109.45º). Curiously, the B-N distance for the coordinated *N*-methylimidazole group (1.529 Å) is the shortest when compared with the three covalently bonded pyrazolyl rings which show a B-N average bond length of 1.538 Å. This is in striking contrast to the B-N bond lengths found in [ZTmRu(*p*-cymene)]$(PF_6)_2$. The three *endo*-cyclic nitrogen atoms show an average N-Ru distance of 2.104 Å. This value is lower than the one found in [TpRu(p-cymene)]PF_6 and [TpmRu(*p*-cymene)]$(PF_6)_2$ (mean 2.112 Å in both cases). It seems that for the ligand to accommodate a tripodal coordination, the three B-N bonds must be stretched resulting in a shortening of the N-Ru average bond length.

.

The bite-angle of the chelate ligand is 83.85º similar to those reported for analogous trischelated complexes like TpRu(*p*-cymene) (84.86º) or TpRuCp (83.84º). A molecule of acetone is present in the unit cell forming short H contacts with the *p*-cymene moiety. The two PF_6^- anions are located surrounding the *N*-methylimidazole group forming short contact interactions with the ring. This part of the complex is less sterically hindered therefore the preferred positions for the location of the counteranions. Other PF_6^- anions from neighbouring molecules are forming short contacts with the pyrazole rings and are located parallel to the ruthenium atom as observed in the crystal lattice. Selected bond lengths and angles are provided in Table **3.3**.

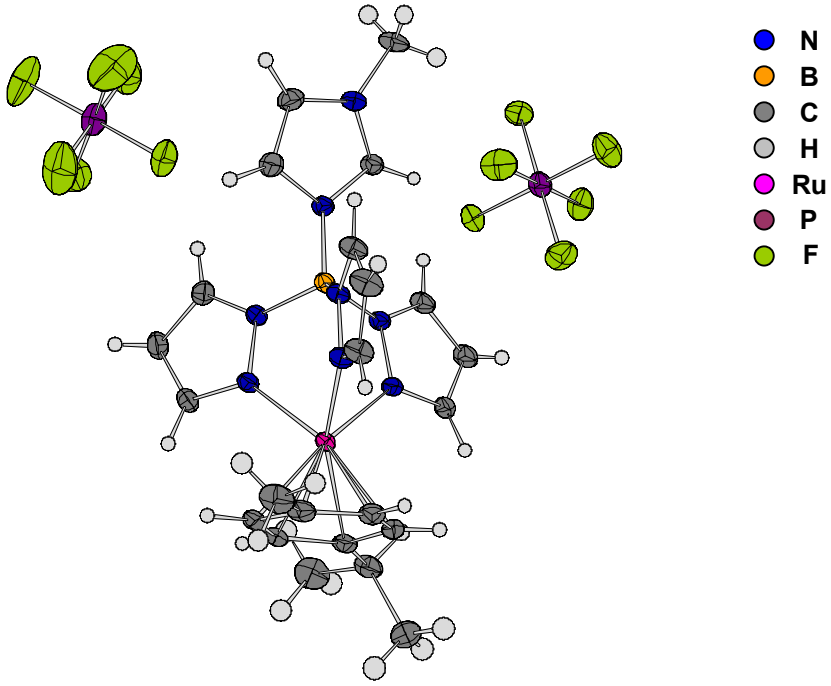

Fig. 3.4. *X-ray structure of [ZTpRu(p-cymene)]$(PF_6)_2$* **3.12**.

Table 3.3. SELECTED BOND LENGHTS (Å) AND ANGLES (°) FOR **3.12**.

B-N(14)	1.529(3)	Ru-C(35)	2.195(7)
B-N(11)	1.535(3)	Ru-C(35)	2.247(7)
B-N(12)	1.539(3)	N(21)-Ru-N(22)	81.16(7)
B-N(13)	1.540(3)	N(21)-Ru-N(23)	85.23(6)
N(21)-Ru	2.113(1)	N(22)-Ru-N(23)	85.17(7)
N(22)-Ru	2.078(1)	N(11)-B-N(12)	111.0(2)
N(23)-Ru	2.118(1)	N(11)-B-N(13)	115.1(2)
Ru-C(15)	2.185(2)	N(11)-B-N(14)	106.6(2)
Ru-C(25)	2.260(2)	N(12)-B-N(13)	106.3(2)
Ru-C(35)	2.210(2)	N(12)-B-N(14)	109.0(2)
Ru-C(35)	2.202(2)	N(13)-B-N(14)	108.6(2)
Ru-C_{centr}	1.462		

3.5.4 [ZTpMn(CO)$_3$](PF$_6$) (3.13)

To a solution of [Mn(CO)$_3$(MeCN)$_3$]PF$_6$ in acetonitrile, ligand **2.21** [(*N*-methylimidazole)B(pyrazolyl)$_3$] was added and the resulting mixture stirred overnight and heated to 50ºC for 1 hour. The solvent was reduced in volume and the compound [ZTpMn(CO)$_3$](PF$_6$) (**3.13**) precipitated as a yellow solid by addition of Et$_2$O in 76% yield.

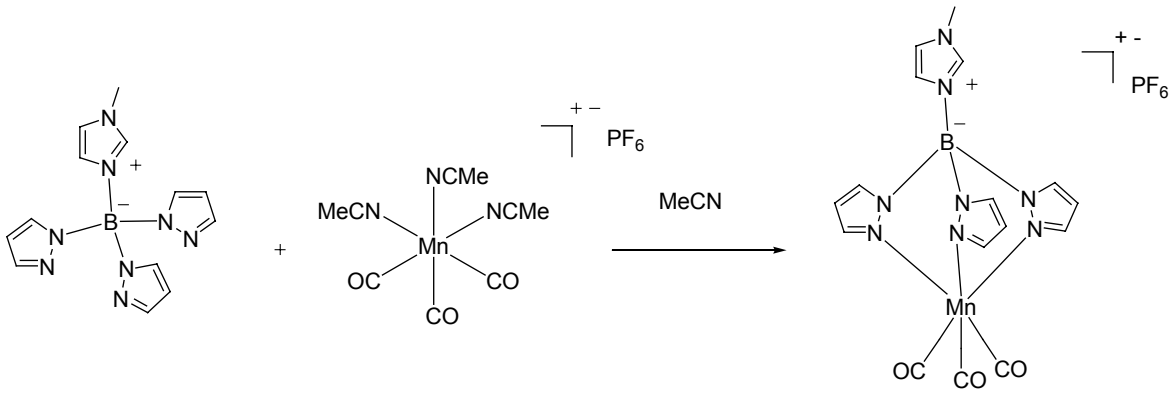

2.21 **3.13**

Scheme 3.8. *Synthesis of the manganese(I) complex* **3.13**.

Spectroscopic Analysis

The solution IR spectrum in hexanes of the complex shows two $\nu_{C\text{-}O}$ signals as two medium intensity bands at 2041 and 1941 cm^{-1}. This is consistent with the carbonyl stretches found in the IR of the analogous $TpMn(CO)_3$ where the $\nu_{C\text{-}O}$ bands appear at exactly the same energy. This suggests that the steric and electronic effects of the replacement of the H^- by *N*-methylimidazole at the boron are negligible. Compared with the anionic Cp and Tp ligands, the ZTp seems to show similar σ-donor properties with also little or inexistent π-interaction from the heterocycle π-system. However, when compared to the neutral carbon centred Tpm ligand, it is also possible to afirm that the ZTp ligand shows stronger donor properties. The complex $[TpmMn(CO)_3]OTf$ presents two carbonyl signals in the IR spectrum at 2051 and 1956 cm^{-1}.[9] The different donor ability of these neutral ligands could be ascribed to the zwitterionic nature of the ZTp ligand which presents a formal negative charge at the boron centre. The ^{1}H-NMR and ^{13}C-NMR spectra are also consistent with a tripodal coordination of the ligand in **3.13**. The protons of the three pyrazolyl rings are equivalent and the signals have again undergone an average downfield shift of +0.70 ppm with respect to the free ligand environment. The largest of these shifts is observed for H^3, +1.21 ppm, consistent with the proton in the 3 position, closer to the manganese metal centre. The molecular ion peak ($M^+ = 433$) is the only one observed by mass spectrometry.

Molecular Structure

Crystals of **3.13** were obtained by slow diffusion of ether into a solution of **3.13** in acetone. The structure had two positions of disorder. Part of the *N*-methylimidazole ring was disordered over two sites. The methyl carbon and one other carbon are shared by the two orientations of the ring. The PF_6^- counter-ion was also disordered. The two axial flourine atoms were correctly placed but the four equatorial ones were badly disordered so they had to be modelled as a ring of electron density instead of four discrete atoms.

Never-the-less, the structure is acceptable for analysis, the final R-factor being just under 10%. The boron atom is tetrahedrally coordinated with an average B-N distance of 1.542 Å for the pyrazole rings. The B-N bond length for the coordinated *N*-methylimidazole ring is 1.544 Å, slightly longer as expected. The N-B-N angles are close to the ideal (mean 108.26º). There are only minor deviations from 90º in the angles around Mn, with the average N-Mn-N angles being 85.48º, C-Mn-C 90.68º and N-Mn-C 91.61º. The Mn-N average distance is 2.046 Å, and the mean Mn-CO distance is 1.810 Å. Compared to $TpMn(CO)_3$ the complex shows only minor differences (mean Mn-S 2.038 Å, and Mn-C 1.825 Å). Selected bond distances and angles are provided in Table **3.4**.

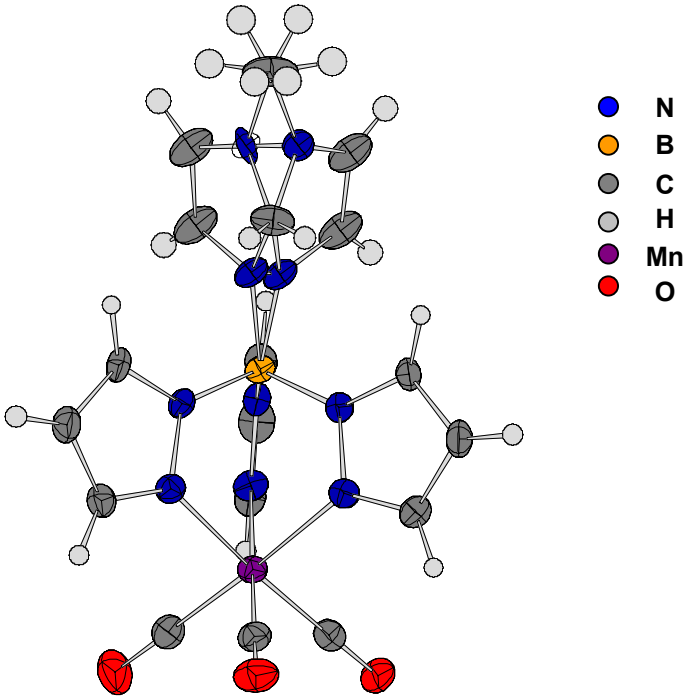

Fig. 3.5. *X-ray structure of the manganse complex* **3.13**. *The PF_6 counteranion is omitted. The disorder at the N-methylimidazole ring is shown.*

Table 3.4. SELECTED BOND LENGHTS (Å) AND ANGLES (°) FOR **3.13**.

B-N(14)	1.544(6)	C(15)-Mn-C(16)	90.78(2)
B-N(11)	1.538(6)	C(15)-Mn-C(17)	89.74(2)
B-N(12)	1.543(6)	C(16)-Mn-C(17)	91.62(2)
B-N(13)	1.542(6)	N(21)-Mn-N(22)	85.97(2)
N(21)-Mn	2.053(4)	N(21)-Mn-N(23)	84.77(2)
N(22)-Mn	2.051(4)	N(22)-Mn-N(23)	85.71(2)
N(23)-Mn	2.048(4)	N(11)-B-N(12)	108.0(3)
Mn-C(15)	1.810(5)	N(11)-B-N(13)	108.2(3)
Mn-C(25)	1.804(5)	N(11)-B-N(14)	116.4(4)
Mn-C(35)	1.816(5)	N(12)-B-N(13)	108.9(4)
C(15)-O(25)	1.154(6)	N(12)-B-N(14)	110.6(4)
C(16)-O(26)	1.143(6)	N(13)-B-N(14)	104.4(4)
C(17)-O(27)	1.141(6)		

3.5.5 [(DBUTm)Ru(*p*-cymene)]$(PF_6)_2$ (3.14)

[Ru(*p*-cymene)Cl_2]$_2$ was dissolved in dry MeOH and the mixture stirred for 30 minutes to yield a reddish coloured solution. Ligand **2.20** [{1,8-diazabicyclo (5.4.0)undec-7-ene}B(methimazolyl)$_3$] was then added in small portions and the mixture stirred for 3 hours at room temperature. The solvent was then reduced to half its volume and excess NH_4PF_6 was added causing immediate precipitation of (**3.14**) as an orange solid that was isolated in 85% yield.

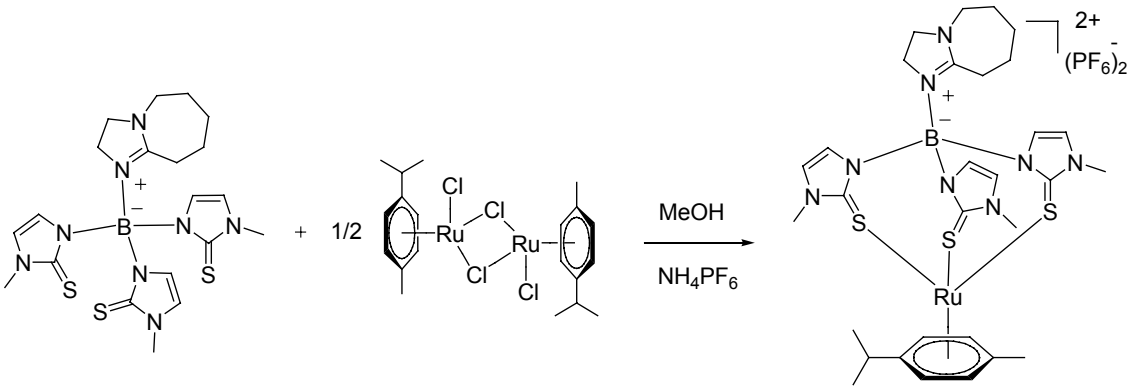

2.20 **3.14**

Scheme 3.9. *Ruthenium coordination of the ligand* **3.14**.

Spectroscopic Analysis

The ^{1}H and ^{13}C-NMR spectra obtained for **3.14** are consistent with the structure found in the solid-state where the tripodal ligand is κ^3-coordinated to the metal and therefore only one set of methimazole resonances is recorded. These signals have undergone an average downfield shift of +0.53 ppm with respect to the free ligand environment following the same tendency as for the examples **3.10** and **3.11**. The signals due to the arene CH protons of the *p*-cymene ligand appear this time as two overlapped quartets with a coupling constant of 6.52 Hz. This is again attributed to the diastereotopic nature of these protons in the chiral environment provided by the coordination of the DBUTm ligand as has been observed for the [ZTmRu(p-cymene)]Cl_2. The molecular ion peak ($M^+/2$= 369.2) was the only peak observed by mass spectrometry.

Molecular Structure

The structure of **3.14** was confirmed by X-ray diffraction studies (Fig. **3.6**). A single crystal of **3.14** was obtained from a concentrated acetonitrile solution of the complex by slow diffusion of ether. As found for **3.10**, the unit cell contains a pair of enantiomeric complexes displaying $\delta\delta\delta$ and $\lambda\lambda\lambda$-stereochemistry for the three ligand arms. There are only minor differences in the metric parameters between the two enantiomers and only those for the $\delta\delta\delta$ enantiomer will be discussed below. The B-N distances for the coordinated DBU is slightly longer (1.583 Å) than the B-N distance for the methimazolyl rings (1.562 Å) due to the covalent character of these latter bonds as found for **3.10**. The C-S and S-Ru average bond lengths (1.724 Å and 2.426 Å respectively) do not differ significantly from those found in the corresponding complex containing the ZTm ligand (1.720 Å and 2.425 Å). The three S-Ru-S angles are all close to 90º [86.84º-95.06º] in the same range as found for [ZTmRu(*p*-cymene)]Cl_2. The torsional parameter θ^{m} has a value of 49.17° and -49.17°, respectively, almost identical to that observed for [ZTmRu(*p*-cymene)Cl_2].

The other torsional parameter, ω^m, has values that fall in the range observed for Tm and ZTm complexes of octahedral metals (mean 57.51 and –57.51°).

These results indicate that the binding of ligand **2.20** to the ruthenium centre is similar to that for ZTm and Tm. **3.14** crystallises with one molecule of water in the unit cell. This is most likely due to the fact that the solvents used for crystallisation were not previously dried and the procedure was carried out in the presence of air and moisture. Selected bond distances and angles are provided in Table **3.5**.

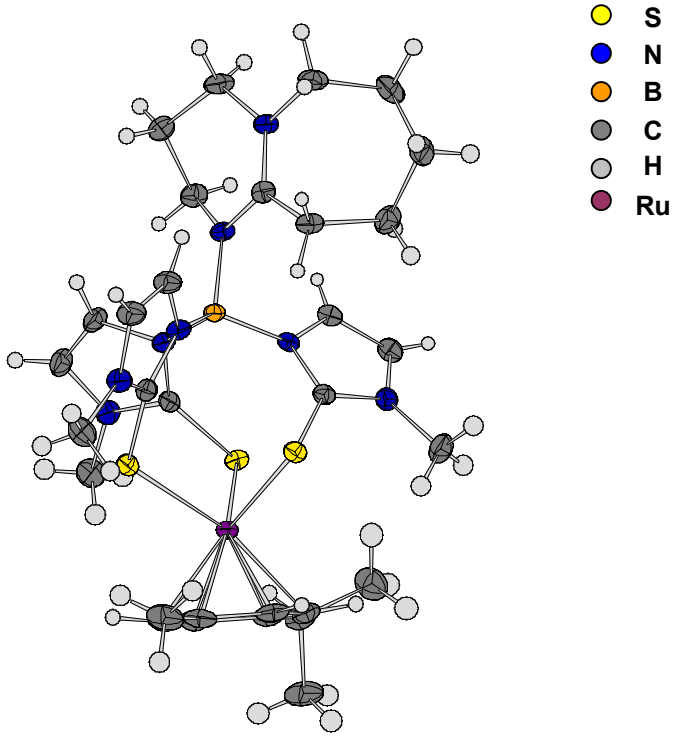

Fig. 3.6. *Ruthenium(II) complex of the DBUTm ligand. Only one enantiomer is shown. Two PF_6 and H_2O molecules are ommited for clarity.*

Table 3.5. SELECTED BOND LENGHTS (Å) AND ANGLES (°) FOR **3.14**.

B-N(14)	1.583(4)	Ru-C(45)	2.200(4)
B-N(11)	1.554(5)	Ru-C(55)	2.243(4)
B-N(12)	1.570(5)	Ru-C(65)	2.221(4)
B-N(13)	1.553(5)	Ru-C_{centr}	1.453
C(21)-S(21)	1.731(4)	N(11)-B-N(12)	110.2(3)
C(22)-S(22)	1.719(4)	N(11)-B-N(13)	117.4(3)
C(23)-S(23)	1.731(4)	N(11)-B-N(14)	110.4(3)
S(21)-Ru	2.395(9)	N(12)-B-N(13)	110.6(3)
S(22)-Ru	2.423(9)	N(12)-B-N(14)	103.8(3)
S(23)-Ru	2.460(9)	N(13)-B-N(14)	110.2(3)
Ru-C(15)	2.189(4)	S(21)-Ru-S(22)	90.94(3)
Ru-C(25)	2.219(4)	S(21)-Ru-S(23)	86.84(3)
Ru-C(35)	2.178(4)	S(22)-Ru-S(23)	95.06(3)

3.5.6 COORDINATION STUDIES OF THE IMIDAZOLINONE LIGANDS

The coordination chemistry of the oxygen donor ligand **2.22** was studied through its reactivity with the metal halides $ZnCl_2$, $FeCl_3$ and $AlCl_3$. Hard metal centres are necessary due to the harder character of this oxygen donor ligand. No reactivity with manganse or ruthenium metal precursors was found. The ligand [(*N*-methylimidazole)B(3-ethylimidazoline-2-one)$_3$ **2.22** was dissolved in dry CH_2Cl_2 and this solution treated with a solution of the metal halide in CH_2Cl_2. Reactions were carried out at room temperature and small aliquots were taken from the reaction mixtures every hour to follow the reactions. It was found that in all cases deboronation of the tripodal ligand occurred and free heterocycle could be isolated from the reaction mixtures.

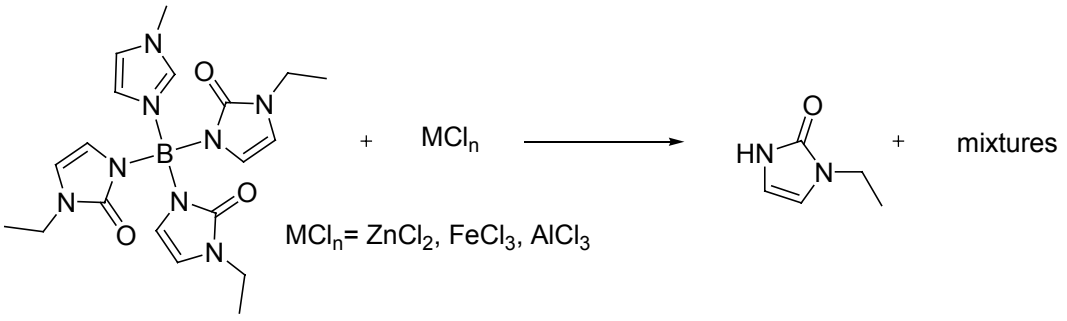

2.22

Scheme 3.10. *Deboronation of the ligand* **2.22** *upon reaction with metal halides.*

Decomposition of scorpionates upon reaction with metal halides is a phenomenon that has received attention recently.[14] Lerner and coworkers have reported the decomposition of scorpionates in the presence of MX_2 transition metal halide salts to give complexes of transition metal and pyrazole derivatives. It was found that scorpionates with bulky groups either at the boron centre or at the pyrazole rings decompose more readily in the presence of metal halides. The substitution of the H atom in the Tp ligand with a bulky electron donating group increases the electron richness at the boron centre thus lengthening the B-N bond distances, rendering it more sensitive to attack at the B-N bond. The difference in the Lewis acidity between the metal and the boron centre would be the ultimate cause for the deboronation since the stronger Lewis acid will preferentially bind with the pyrazolide anion. This feature has been observed for compound [ZTpRu(*p*-cymene)]$(PF_6)_2$ **3.12** where the B-N_{pyr} bond lenghts are longer than for the monocationic [TpRu(*p*-cymene)](PF_6) due to the *N*-methylimidazole ring occupying the forth position at the boron atom as previously discussed.

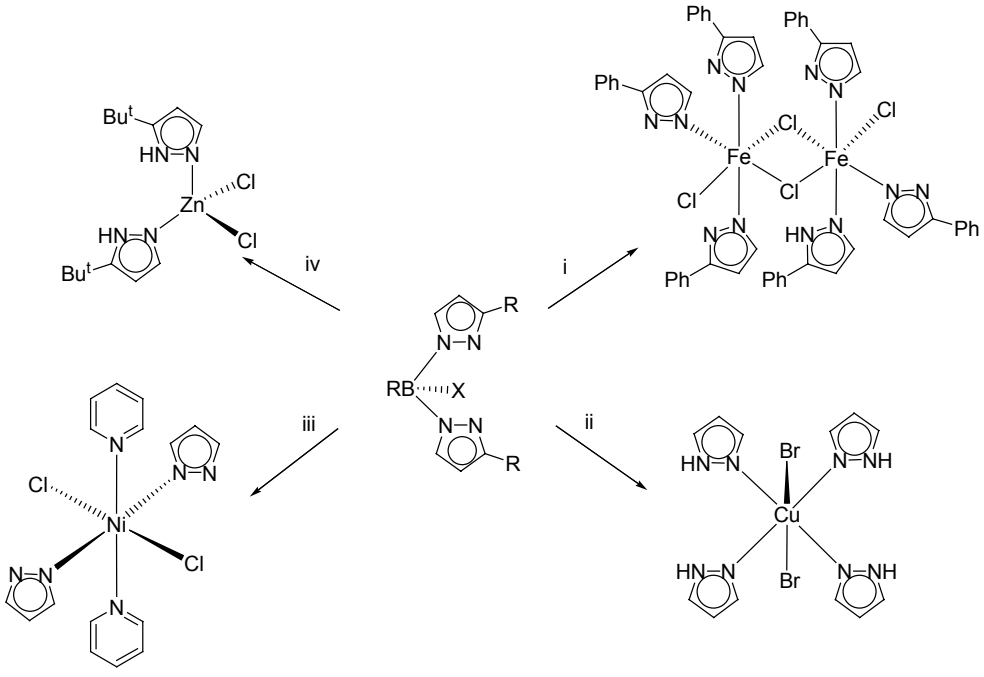

Scheme 3.11. *Deboronation of scorpionates upon complexation to metal dihalides. i) R=tBu; X= tBupz; $FeCl_2$. ii) R=H; X= pz; $CuBr_2$. iii) R=H; X=pz; $Ni(py)_2Cl_2$. iv) R=tBu; X=tBupz; $ZnCl_2$.*

3.6 CONCLUSIONS

The coordination chemistry of the most representative ligands introduced in the previous chapter has been studied by their complexation to manganse(I) and ruthenium(II). The aim of this study was to address two issues; whether the donor ability of the zwitterionic ligands is closer to the anionic poly(azolyl)borates or whether they are more similar to their neutral counterparts; and if bulky groups at the forth position can affect the coordination behaviour of the ligands. Coordination of the novel oxygen ligands introduced in the Chapter II was also attempted, but they undergo a deboronation process upon reaction with the metal precursor in a similar manner to that reported for pyrazolyl borates. By analysis of the IR stretches of the manganse triscarbonyl complexes in hexanes solution, both ZTp and ZTm appear to present similar donor abilities to their anionic analogues. Remarkably the carbonyl stretches of the complex **3.13** $[ZTpMn(CO)_3]PF_6$ ligand, have the same energy as the neutral $TpMn(CO)_3$ (2041 and 1941 cm^{-1}). For $ZTmMn(CO)_3$ the values are only slightly higher than for the $TmMn(CO)_3$. Both ligands seem to be slightly weaker donors than their anionic counterparts this being consistent with the difference in their electronic structure due to the existence of a formal positive charge at the metal centre. The ν(CO) values can be seen in Table **3.6** to move to lower frequency along the series Tpm $\rightarrow$ ZTp $\approx$ Cp $\approx$ Tp $\rightarrow$ ZTm $\rightarrow$ Tm indicative of a progressive change in donor properties of the ligands. As previously discussed, the Cp ligand is able to act as a π-acceptor competing with the CO for electron density, hence the high energy values recorded for the $CpMn(CO)_3$ complexes when compared to the Tm analogues. ZTp and Tp have equal values, suggesting similar electron donation to the metal centre. This is commensurate with these ligands acting as strong σ-donor but unable to act as π-acceptors. For ZTm and Tm, the lone pairs of the sulphur donors overlap very effectively with the metal orbitals giving a strong π-donation and they are the stronger donor ligands in these series. The difference between them could be ascribed to their different electronic structure since ZTm is neutral and Tm is anionic and complexation to the metal will be stronger in the latter case.

Table 3.6. IR data for mononuclear manganese (I) tricarbonyl complexes.

COMPLEX	ν_{CO}/cm^{-1}	*Medium*	*Ref*
{HB(3,5-$(CF_3)_2$pz)$_3$} Mn(CO)$_3$	2065, 1975	KBr	*15*
[{HC(pz)$_3$} Mn(CO)$_3$]OTf	2051, 1956	DCM	*9*
[{HC(3,5-Me_2pz)$_3$} Mn(CO)$_3$]OTf	2044, 1949	DCM	*9*
{HB(pz)$_3$} Mn(CO)$_3$	2041, 1941	Hex	*8*
(ZTp)Mn(CO)$_3$ PF$_6$	**2041, 1941**	**Hex**	
{pzB(pz)$_3$} Mn(CO)$_3$	2039, 1936	MeCN	*8*
(Tt)Mn(CO)$_3$	2039, 1958, 1928	KBr	*16*
CpMn(CO)$_3$	2028, 1947	Hex	*17*
{(Ipc)B(PZ)$_3$} Mn(CO)$_3$	2031, 1927	Toluen	*18*
{HB(3,5-Me_2pz)$_3$} Mn(CO)$_3$	2023, 1912	KBr	*19*
(ZTm^{Me})Mn(CO)$_3$PF$_6$	**2007, 1914**	**Hex**	
(ZTm^{Me})Mn(CO)$_3$PF$_6$	**1999, 1988, 1898, 1889**	**KBr**	
(Tm^{Me}) Mn(CO)$_3$	2003, 1905	Toluene	*10*
(Tm^{Me}) Mn(CO)$_3$	1994, 1984, 1896, 1884	KBr	*10*

In the Table **3.6** the values of different substituted Tm and TpMn(CO)$_3$ are classified in decreasing order by their IR energy bands. The solvent medium used for the study is different in some cases and this slightly affects the band energies. It is possible to observe that ZTp and ZTm occupy positions close to their anionic counterparts as previously discussed, their σ–π donor properties being apparently rather similar.

The structural discussion for the STm (S stands for substituted, either *N*-methylimidazole or DBU) derivatives reveals that the ligands bind in a similar facial fashion to the metal centre occupying three coordination positions. The resulting complex undergoes a twist to relieve angle strain that gives C_3-symmetry to the metal complexes. The more flexible hybridization offered by the sulphur easily accommodates this folding. The torsion parameters for the substituted STm ligands are similar to those found for the Tm ligand, and the narrow ranges observed might suggest a substantial degree of rigidity for these ligands. The ligands tend to coordinate in a κ^3–mode, and only in the case of complexation to ruthenium(II) could the ZTp be isolated in the κ^2-mode where a chloro ligand is still coordinated to the metal centre. The chloro ligand can be displaced forcing tripodal coordination of the ligand when treated on polar solvents that promote Ru-Cl bond cleavage. In both the ZTm and ZTp examples, the forth position at the boron is occupied by a heterocycle group (*N*-methylimidazole, DBU) does not affect the coordination behaviour of the ligands. The similarity of the spectroscopic (IR, NMR) and crystallographic data for the complexes studied suggest that the electronic and steric effects of the group at the boron forth position are negligible. Complexation of the oxygen ligand **2.22** to metal halides leads to deboronation of the ligand in all cases. Scorpionates with bulky groups at the boron forth position and at the pyrazolyl rings are known to be more likely to suffer decomposition due to the lengthening of the B-N bond that makes the ligands more sensitive to attack at this position.

3.7 REFERENCES CHAPTER III

1. C. A. Tolman, *Chem. Rev.,* 1977, **77**, 313.
2. A. R. Chianese, X. Li, M. C. Janzen, J. W. Faller, R. H. Crabtree, *Organometallics,* 2003, **22**, 1663.
3. G. Parkin, *Handbook of Grignard Reagents*, G. S. Silverman, P. E. Rakita. (Eds.), Dekker, Inc., 1996.
4. M. Paneque, S. Sirol, M. Trujillo, E. Gutierrez, M. A. Monge, E. Carmona, *Angew. Chem. Int. Ed.,* 2000, **39**, 218.
5. C. Slugovc, K. Mereiter, S. Trofimenko, E. Carmona, *Chem. Commun.,* 2000, 121.
6. S. Santos, N. Marques, *New. J. Chem.,* 1995, **19**, 551.
7. S. Trofimenko, *J. Am. Chem. Soc.,* 1969, **91**, 588.
8. W. Huckel, H. Bretschneider, *Berichte der Deutschen Chemischen Gesellschaft [Abteilung] B*: *Abhandlungen*, 1937, **70B**, 2024.
9. D. L. Reger, T. C. Grattan, K. J. Brown, C. A. Little, J. J. Lamba, A. L. Rheingold, R. D. Sommer, *J. Organomet. Chem.,* 2000, **607**, 120.
10. P. J. Bailey, D. Lorono, C. McCormack, S. Parsons, M. Price, *Inorg. Chim. Acta,* 2003, **354**, 61.
11. S. Trofimenko, *Chem. Rev.,* 1993, **93**, 943.
12. S. Bhambri, D. A. Tocher, *J. Chem. Soc. Dalton Trans.,* 1997, 3367.
13. M. R. Foreman, A. F. Hill, A. J. White, D. J. Williams, *Organometallics,* 2003, **22**, 3831.
14. S. Bieller, A. Haghiri, M. Bolte, J. W. Bats, M. Wagner, H.-W. Lerner, *Inorg. Chim. Acta,* 2006, **359**, 1559.
15. H. V. R. Dias, H, -J. Kim, H, -L. Lu, K. Rajeshwar, N. R. de Tacconi, A. Derecskei-Kovacs, D. S. Marynick, *Organometallics*, 1996, **15**, 2994.
16. P. J. Bailey, M. Lanfranchi, L. Marchio, S. Parsons, *Inorg. Chem.,* 2001, **40**, 5030.
17. D. V. Tellers, S. J. Skoog, R. Bergman, T. B. Gunnoe, W. D. Harman, *Organometallics*, 2000, **19**, 2428.
18. P. J. Bailey, P. P. Pinho, S. Parsons, *Inorg. Chem.*, 2003, **42**, 8872.

19. J. E. Joachim, C. Apostolidis, B. Kanellakopulos, R. Maier, N. Marques, D. Meyer, J. Müller, A. Pires de Matos, B. Nuber, J. Rebizant, M. l. Ziegler, *J. Organomet. Chem.,* 1993, **448**, 119.

CHAPTER IV

CHIRAL TRIPODAL BORATE LIGANDS

PART I

4.1 INTRODUCTION

Asymmetric metal complex catalysis is a powerful method for the synthesis of enantiopure chiral compounds and the design of such catalysts has become a major research area in the past few years.[1] The catalysts are formed by a metal, responsible for the reactivity of the system, and a ligand that controls the steric and electronic properties of the catalyst. Introducing elements of rotational symmetry within the ligand backbone can serve the very important function of reducing the number of possible diastereomeric transition states. Rotational axes, C_n, are the only symmetry elements compatible with chirality. Catalysts where the ligand has a two-fold rotational axis have been extensively studied and employed in asymmetric synthesis, specially in reactions catalysed by square-planar metal complexes.[2]

By definition, C_2-symmetry is characterised by the fact that the rotation of the complex 180º about the C_2-axis leads to an identical situation. Therefore, for a square-planar complex containing a bidentate C_2-symmetric ligand, the symmetry of the ligand makes the two vacant coordination sites equivalent or homotopic.

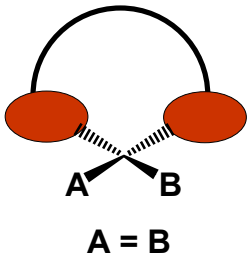

Fig. 4.1. *Bidentate ligand coordinated to a square planar metal.*

If the same approach is considered for systems with an octahedral metal centre, it is possible to observe (Fig **4.2**) that the bidentate ligand is not able to induce homotopic properties to the four remaining coordination sites.

Now there exists a pair-wise inequivalency that can lead to an increase of the number of diastereomeric transition states, thus lowering the stereoselectivity of any catalytic process occurring at the metal. The design of catalysts with C_3-symmetry should be advantageous in two aspects. First, the presence of additional donor atoms chelating the metal centre would form a more stable complex through the reaction conditions, and second, three rather than two stereocentres in the ligand would increase the stereochemical density around the metal that is known to lead to a better asymmetric induction.[3]

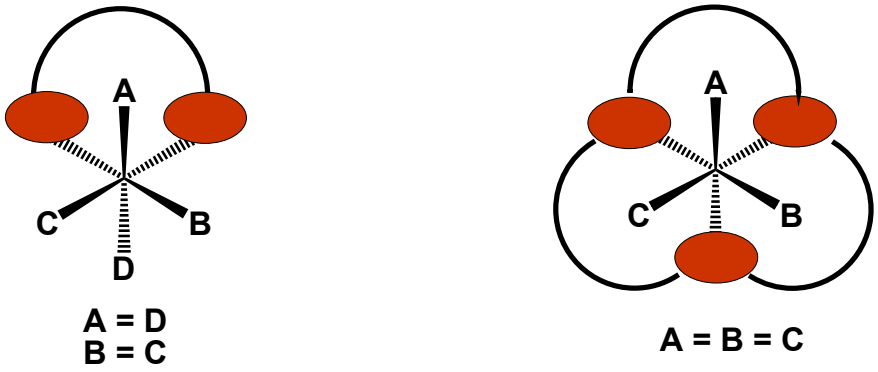

Fig. 4.2. *Bidentate and tridentate ligands in octahedral metals.*

Examples of successful C_2-symmetric ligands are BINAP and BINOL (**4.1**) both formed by two linked naphthalene moieties that provide chirality to the ligand due to hindered rotation (*atropisomerism*) about the single bond located perpendicular to the 2-fold rotational axis. An analogous situation for C_3-symmetric ligands is also possible but the restricted rotation will be then with respect a 3-fold axis. Ligands of this type, although rather uncommon, are also known. For example certain types of tripodal ligands with the generic structure $E(L_2D)_3$ (E = central tripod atom, L = linking atom, D = donor atom) have been reported to coordinate a metal atom forming C_3-symmetric complexes.(Fig. **4.3**).

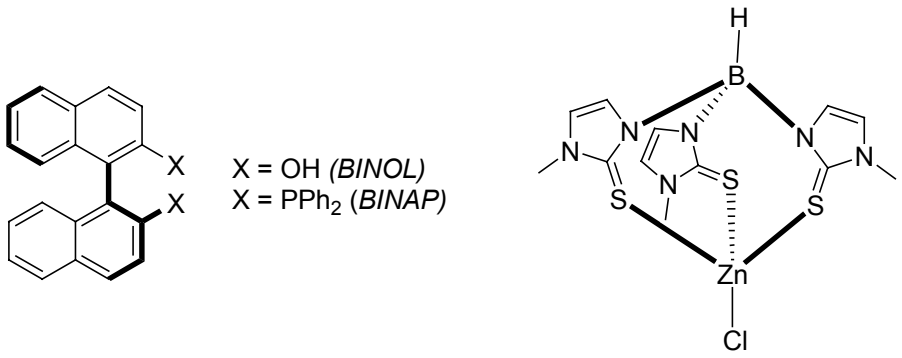

4.1 **4.2**

Fig. 4.3. *C_2-symmetric ligands* **4.1** *and C_3-symmetric complex TmZnCl* **4.2**.

The formation of such C_3-symmetric structures is directed by the size of the chelate rings formed on complexation to a metal. The eight-membered rings formed upon complexation, undergo a twisting due to angle strain, that confers this special symmetry to the resulting complex. These complexes show *helical chirality*, where the molecules are shaped as a right- or left-handed spiral like a screw or spiral stairs. The configurations are designed Δ (clockwise) or Λ (anticlockwise) according to the helical direction.

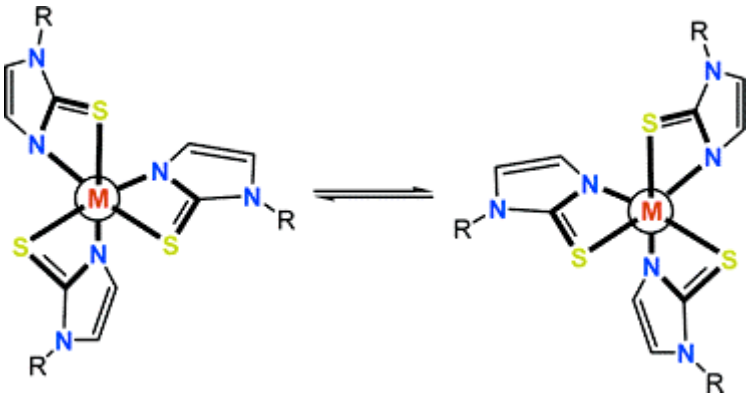

Fig. 4.4. *Two enantiomers are formed upon complexation of the $E(L_2D)_3$ ligands.*

One of the best studied examples of such ligands is hydrotris(methimazolyl)borate (Tm) introduced in Chapter I. This ligand forms C_3-symmetric complexes when coordinated a metal centre as discussed in Chapter I.[4]

Due to this resulting geometry, a chiral cage is formed that leads to two possible enantiomers. Both enantiomers, Λ and Δ, are shown viewed down their C_3 axis in the Fig **4.4**.

We have been exploring the use of these kinds of chiral complexes in asymmetric catalysis. However, there are two issues which need to be addressed before they may successfully be applied in this field. One is the tendency of these complexes to racemise, and previous work in the group has been concentrated on determining the energy barriers and the mechanisms of this racemisation. The second issue is the development of synthetic routes to ligands containing chiral groups to enable the formation of single diastereomer complexes. This present Chapter will deal with this topic, however a brief introduction to the first issue follows.

4.2 MECHANISM OF RACEMISATION

There are two possible mechanisms for the racemisation of these chiral complexes; dissociative and non-dissociative. In the dissociative mechanism, one arm of the ligand decoordinates from the metal centre allowing the low energy inversion of the remaining 8-membered metallocycle, and this is followed by the re-coordination of the pedant arm to form the second enantiomer. The lability of the metal-donor bond on the one hand, and the donor properties of the solvent on the other, are known to dramatically influence the energy of this process.

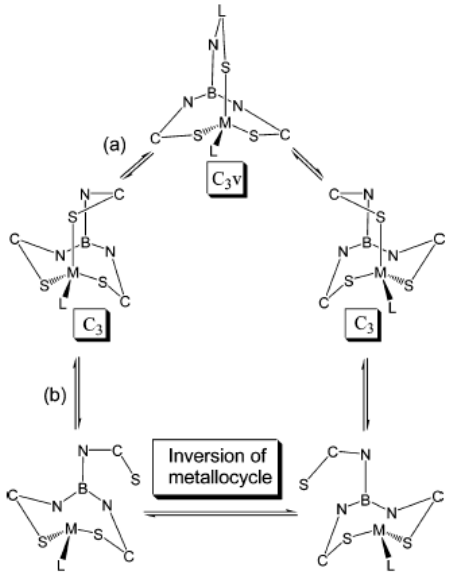

Fig 4.5. *Interconversion of chiral atropisomeric metal-Tm complexes.* a) *through a nondissociative mechanism;* b) *through a dissociative process.*

The non-dissociative mechanism involves the racemisation of the enantiomer by rotation of the bicyclic metal-ligand cage via a strained C_{3v}-symmetric transition state. The energy of this process will depend on the angle strain present in the molecule at this stage. Previous studies undertaken within the group showed that the energy difference between the ground state C_3-symmetric structure and the C_{3v}-symmetric transition state were 121 and 160 kJmol^{-1}, for model tetrahedral Zn(II) and octahedral Mn(I) metals respectively, as estimated by DFT calculations.[5] On the other hand, it was found experimentally that for tetrahedral complexes of the metals Zn(II), Cd(II), Hg(II), Cu(I) and Ag(I), the energy of racemisation was typically 70 kJmol^{-1}, and that donor solvents like acetonitrile or dimethylsulfoxide could reduce this energy. These observations lead to the conclusion that a dissociative mechanism was responsible for the racemisation of such tetrahedral complexes. In the case of octahedral metals Ru(II) and Mn(I), experimental evidence of racemisation was not found meaning that the energy of the process must be higher than 90 kJmol^{-1} , which is the limit of the method of NMR line-shape analysis used.[6]

Whether the racemisation in the octahedral complexes studied occurs via the non-dissociative or dissociative mechanism is still unknown and a full kinetic analysis is required once single diasteromer complexes have been isolated. The fact that the energy of this process is close to 100 $kJmol^{-1}$ means that separation of the enantiomers is theoretically possible, but it has not yet been achieved.

4.3 SINGLE DIASTEREOMER SYNTHESIS

Using the methodology presented in Chapter II it should be possible to synthesise chiral tripodal borate ligands by using chiral activators or chiral azole heterocycles in the multicomponent reaction starting from $B(NMe_2)_3$ discussed in Section **2.4.2**. Chiral Lewis bases with a basic pK_a higher than 3.5 are available commercially (tetramisole hydrochloride) or are straightforward to synthesise from chiral aminoacids (oxazolines, imidazolines). The chiral groups in these compounds are usually located in adjacent positions to the imine donor atom this being the reason for their high stereoinductive properties when applied in catalysis.[7] These chiral groups are expected to influence and *even direct* the helical twist of the metal-ligand cage formed upon coordination to metal centres, and thus form selectively one of the two possible diastereomers. The alternative diastereomer will have a higher energy as a result of unfavourable interactions between the chiral group(s) at the ligand and the C_3-symmetric cage. For example, considering a ligand with a chiral group with *S*-configuration either at the boron (*R**) eventually it could form two diastereomers upon complexation to a metal centre; *S*-Δ (**4.3**) or *S*- Λ (**4.4**). Chiral groups at the azole heterocycle would induce similar effects.

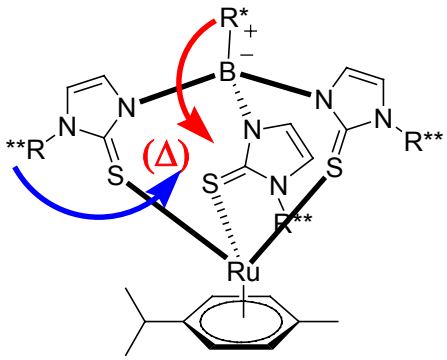

(*S*, Δ)

4.3

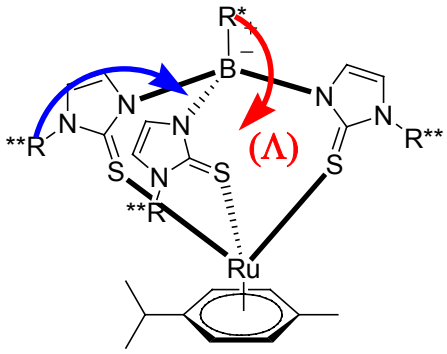

(*S*, Λ)

4.4

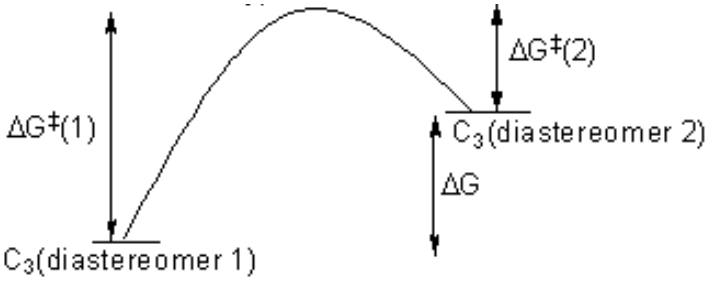

Fig 4.6. *Interaction between the chiral centres (R* or R**) and the chiral bicyclo cage (Λ, Δ) might lead to diastereomers of different energy.*

The two possible diastereomers would have different energies and if the difference between them is high enough, only the most stable diastereomer would be formed on complexation of the chiral ligand to a metal. The racemisation to the other diastereomer would not take place since this process would lead to a higher energy structure.

4.3.1. CHIRAL ACTIVATORS

4.3.1.1 Chiral Oxazolines

The first choice was the use of chiral oxazolines since these systems have a chiral centre next to the imine nitrogen atom that will coordinate to the borane and would therefore be expected to influence the chiral bicyclo-cage formed upon metal complexation. Moreover, they are easily synthesised from commercially available enantiopure aminoalcohols by reaction with DMF-DMA in refluxing toluene, thus allowing the synthesis of diverse oxazolines with different chiral groups.[8] The basic pK_a of oxazolines lies between 5 and 6 which is within the pK_a range of Lewis bases known to be effective activators of $B(NMe_2)_3$ to reaction with azoles in the synthetic route to ZTm ligands. The oxazolines are formed in excellent yields as oily compounds and, although water sensitive, they can be stored under nitrogen for long periods of time.

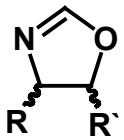

4.5

Fig. 4.7. *Structure of chiral oxazolines (R =Me, Ph…; R' =H, Ph...).*

In addition, examples of oxazolines coordinated to boranes are known in the literature. An oxazoline-borabenzene adduct has been reported by Fu and coworkers where for the first time a chiral oxazoline coordinates the free *p*-orbital of a borane (Fig. **4.8**).[9]

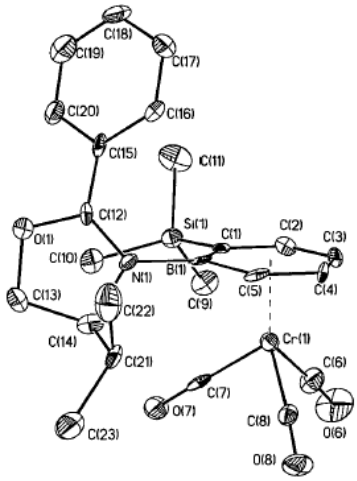

4.6

Fig. 4.8. *Oxazoline-borobenzene adduct reported by Fu.*

4.3.1.2 Chiral Imidazolines

Imidazolines are stronger Lewis bases but synthetically more challenging compounds than oxazolines. Chiral imidazolines can be synthesised through different methods, usually involving expensive enantiopure 1,2-diamines.[10] Using chiral aminoalcohols as starting materials, Casey and co-workers have reported a versatile and high yielding route to imidazolines that allows functionalization of the ring at different positions (Scheme **4.1**).[11] Depending on the functionalization it is possible to control their basicity, nucleophilicity and donor properties. The basic pK_a values of these imidazolines range from 7 to 11 and their basicity is therefore ideal to coordinate to the $B(NMe_2)_3$.

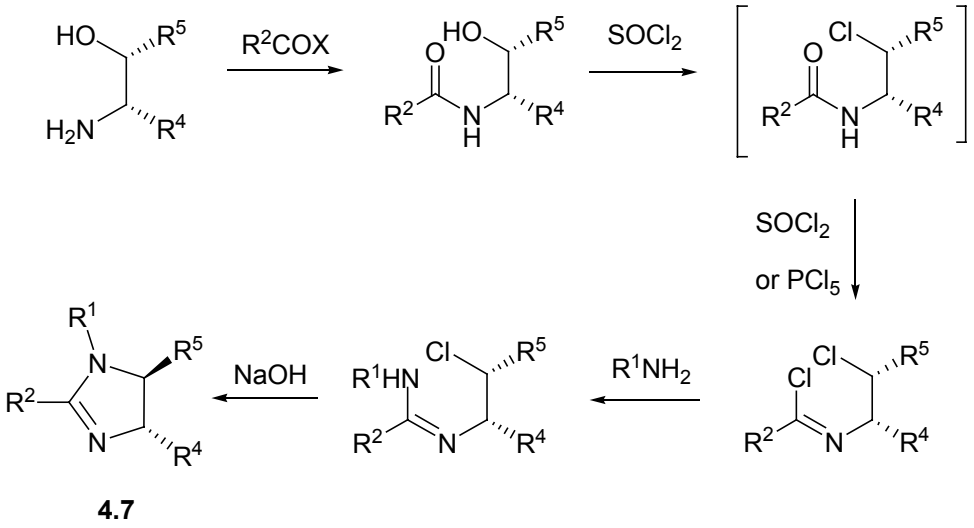

4.7

Scheme 4.1. *Casey´s route to substituted imidazolines.*

4.3.1.3 Commercially Available Lewis Bases

(-) Tetramisole hydrochloride (**4.8**) is a commercially available product widely used as an anthelmintic in the treatment of many nematodes particularly in veterinary applications. Very recently it has been used as an efficient organocatalyst.[12] It has a basic pK_a of 9.9 ideal to act as an activator of the aminoborane. There is a phenyl ring at the 6-position that it is expected to interact with the methimazole rings in the resulting ZTm ligand to direct the helical cage formed upon coordination to a metal centre. In the literature, there is only one chiral borate ligand bearing a chiral group at the boron centre as discussed in the introductory Chapter. The chirality at this position, although far from the metal centre, is known to interact with the azole rings; therefore tetramisole was considered as a potential chiral activator for the $B(NMe_2)_3$. The tetramisole is sold as the hydrochloride salt, so liberation of the free base prior to reaction with $B(NMe_2)_3$ must be performed.

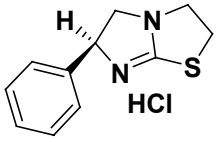

4.8

Fig 4.9: *(-) Tetramisole hydrochloride.*

4.3.2. CHIRAL HETEROCYCLES

4.3.2.1 Chiral Methimazole

The second approach to the synthesis of chiral tripodal borates involves the use of chiral azole heterocycles to form a C_3-symmetric ligand. For a long time, we have been interested in studying whether chiral groups at the methimazole heterocycles can direct the orientation of the helical bicyclic-cage formed upon metal coordination. Therefore the chiral methimazole (**4.9**) was synthesised from the commercially available chiral α-methylbenzyl amine as reported by Jones and coworkers.[13] Surprisingly this heterocycle did not react with borohydride salts to form the borate salt (**4.10**), apparently due to steric reasons, since its acid pK_a and melting point are within the range established by Reglinski and coworkers for the reaction to occur (Scheme **4.2**).[14]

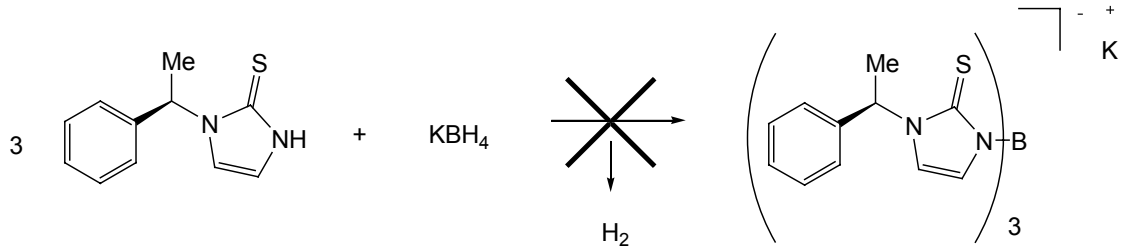

4.9 **4.10**

Scheme 4.2. *Chiral heterocycle is unreactive in the melt reaction with KBH_4.*

However, this chiral heterocycle is expected to react with the dimethylamino groups of $B(NMe_2)_3$ upon activation with a Lewis base such as *N*-methylimidazole following the mechanism reported in Chapter II.

4.3.2.2 Oxazolidinethiones

Other interesting azole heterocycles are oxazolidinethiones, which have been used as chiral auxiliaries in different types of organic transformations.[15] These heterocycles can be synthesised from chiral aminoalcohols by refluxing with CS_2 in aqueous $NaHCO_3$ as reported by Ortiz and coworkers (Fig. **4.10**).[16] The chirality in this heterocycle is located at the C_4 and C_5 so it is expected to be very close to the chiral cage formed upon metal complexation and therefore able to significantly influence it. The fact that these heterocycles are straightforwardly synthesised opens the possibility of a readily available library of tripodal oxazolidinethione borate ligands.

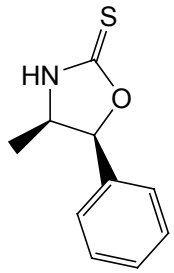

4.11

Fig. 4.10. *Oxazolidinethione derivered from norephedrine.*

4.3.3 CHIRAL COUNTERANIONS

A third way of introducing chirality into the system is the use of a chiral counter-anion. As shown in Chapter III both ruthenium and manganese complexes are cationic and they are usually paired with PF_6^- anions.

The possibility of exchanging them with chiral anions was also considered to determine whether this would allow the separation of the resulting diastereomeric salts. Chiral anions like tartrate (**4.13**) or TRISPHAT (**4.12**), have been widely used for enantiomeric resolutions.

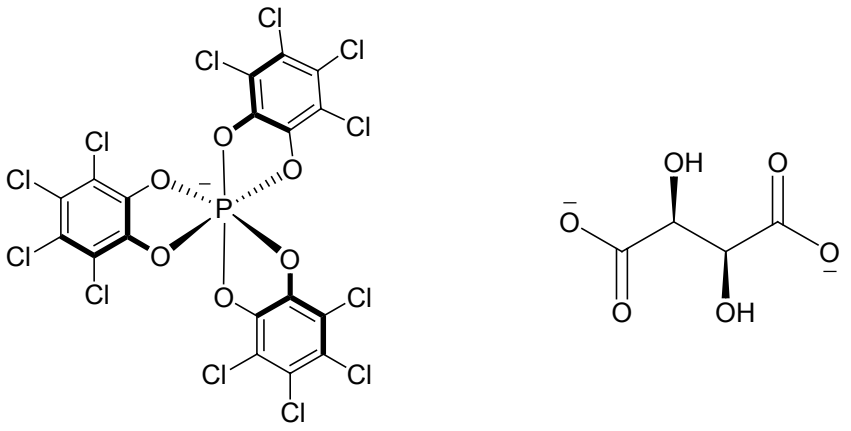

4.12 **4.13**

Fig 4.11. *TRISPHAT and tartrate chiral anions.*

The formation of tightly associated ionic pairs between chiral cations and chiral anions can lead to diastereomeric salts that present large chemical and physical differences between them. A high level of asymmetric recognition between the chiral cations and anions can be achieved as has been reported by the group of Lacour and coworkers.[17] The TRISPHAT anion was chosen due to its properties; it is a D_3-symmetric anion known to be configurationally stable in solution and to interact with organometallic cations. Both enantiomers can easily be prepared in enantiopure form. The Λ-TRISPHAT (**4.15**) is synthesised as the tri-*n*-butyl ammonium salt and is highly soluble in chlorinated solvents, whilst the Δ-TRISPHAT (**4.14**), prepared as the chinchonidinium salt, requires more polar mixtures (acetone or DMSO) for its solubilization. TRISPHAT has been applied as a resolving agent for chiral cations, as an NMR chiral shift reagent and as an asymmetric inducing reagent and some special features are discussed next.

4.3.3.1 TRISPHAT as an NMR chiral shift reagent

Enantiomers cannot be distinguished by ^{1}H-NMR since all protons are surrounded by equal environments as has been observed for the complexes **3.10** and **3.11**, where both enantiomers Δ and Λ provide the same ^{1}H-NMR spectra. Upon addition of a chiral substance, close interactions between the two chiral centres can lead to diastereotopic protons that are distinguishable by ^{1}H-NMR. One of the most widely used group compounds as NMR shift reagents are chiral lanthanide reagents, which have been applied, for example, in the determination of the absolute configuration of amino acids. However, due to their paramagnetic properties, they cause broadening of the resonances making the analysis less precise. It is also known that these compounds do not interact with cationic species. On the other hand, anionic chiral systems like TRISPHAT are ideal to be used as ^{1}H-NMR chiral shift reagents for chiral cations. The separation of the ^{1}H-NMR signals is directly related to the *interaction between* the anion and the cation, since well separated ionic pairs lead to weaker chiral interaction and poor diastereoselectivity. Therefore, solvent polarity influences the quality of the separation, apolar solvents being preferred in these experiments.

Effective resolution protocols involving configurationally stable Ru(II) complexes, in particular $[Ru(4,4'\text{-}Me_2bpy)_3]^{2+}$ have been developed using the TRISPHAT anion. It was found experimentally that protons of the complex cations sited along the C_3-axis were more strongly perturbed upon the addition of TRISPHAT. Lacour also reported the use of TRISPHAT-F_3 and TRISPHAT-F_4, two fluorine-containing enantiopure hexacoordinated phosphate anions to determine the exact approach direction between the chiral anions and cations.[18] Whilst TRISPHAT is ^{1}H-NMR inactive or "silent", TRISPHAT-F_x contains fluoro groups that can be used to study the interaction with chiral cations by ^{19}F-NMR. The fluorine atoms positioned at the C3 and C4 of the phosphate ought to be sensitive to approaches along the C_3 and the C_2 axis of the anion respectively.

It was confirmed that the TRISPHAT anion approaches along the C_3 axis of the Ru(II) complex cation since the fluorine group at C3 was strongly perturbed when compared to the one on C4.

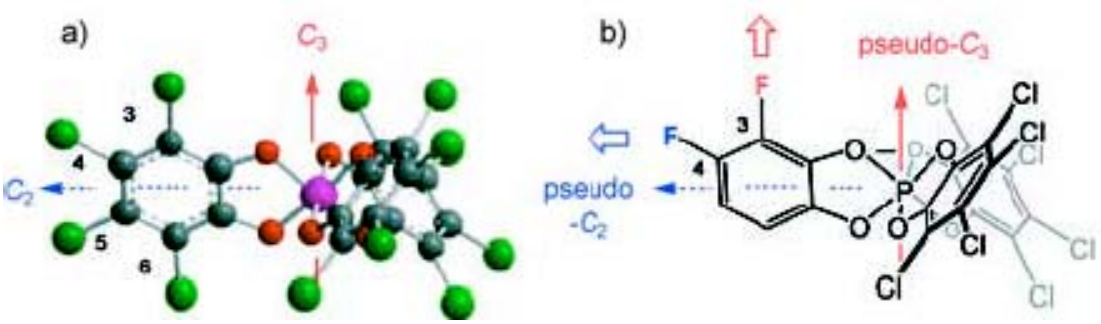

Fig 4.12. *Fluorine groups are located in the pseudo C_3 and C_2 TRISPHAT axes.*

Another important characteristic is that TRISPHAT anions have a stronger influence on homochiral cationic moieties versus heterochiral ones. In this way, homochiral diastereomeric ionic pairs (ΔΔ) have been found to be preferentially formed versus heterochiral ones (ΔΛ).

4.3.3.2 TRISPHAT as a resolver of chiral cations

The most common way to resolve a racemic mixture is by converting the racemate into a pair of diastereomers by treating them with a chiral substance. TRISPHAT has been found to be an excellent resolving agent of chiral organometallic cations. Once the diastereomers are formed, their separation can be performed by one of three different means; selective crystallisation, selective extraction or chromatographic separation. The principles involved in these different methods are discussed next.

In the synthesis of the enantiopure Δ or Λ-TRISPHAT anion there is a *selective crystallization* step where the racemic phosphate anion, which is paired with the tributylammonium cation, is resolved with the chiral chinchonidinium chloride. The Δ-TRISPHAT precipitates selectively as the chinchonidinium salt, the Λ form remaining in solution paired to the tributylammonium cation.

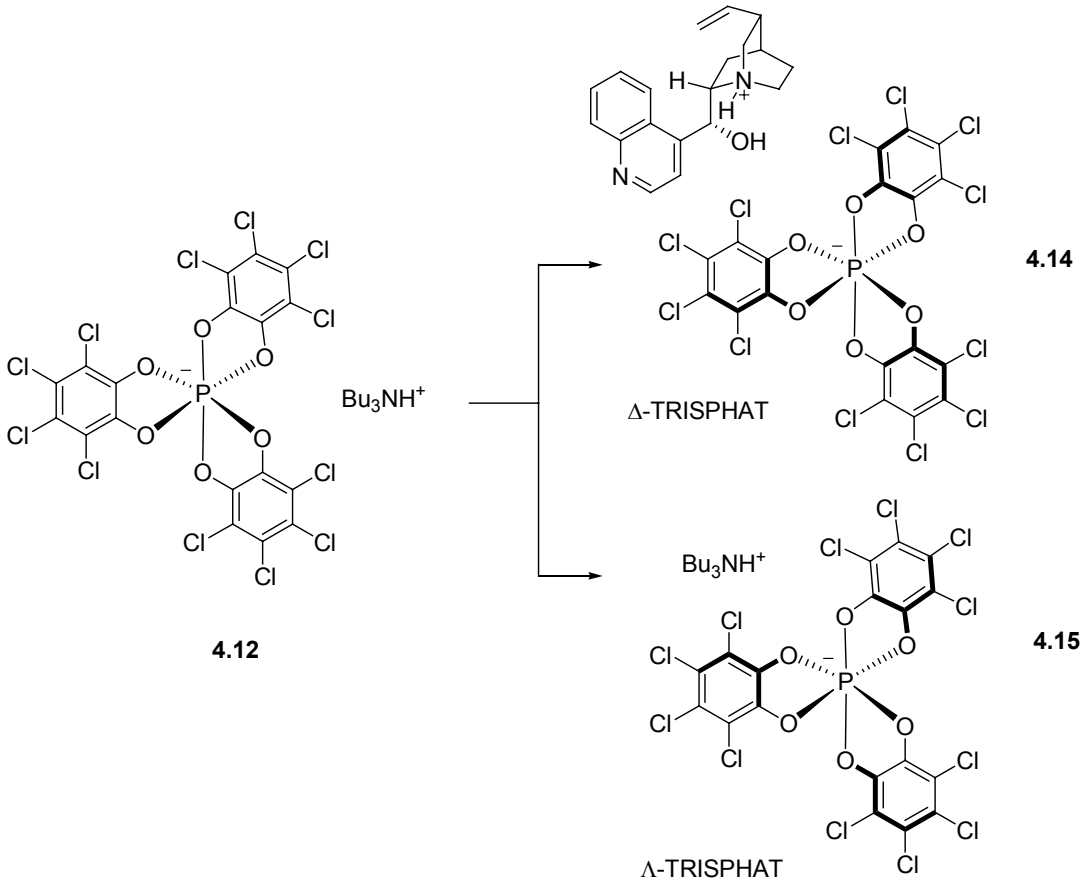

Scheme 4.3. *Synthesis of* Δ *and* Λ*–TRISPHAT.*

Asymmetric extraction involves the preferential separation of one enantiomeric cation, for example Λ–$[Ru(4,4'\text{-}Me_2bpy)_3]^{2+}$, by means of selective diastereomeric interactions with the homochiral TRISPHAT anion through a solvent extraction process. $[\Lambda\text{-TRISPHAT}]^{-+}[(nBu)_3NH]$ is very soluble in chlorinated solvents and highly hydrophobic due to the tributylammonium cation. Since homotopic interactions are preferred, upon mixing a solution of the racemic cation $[Ru(4,4'\text{-}Me_2bpy)_3]^{2+}$ in water with a solution of $[\Lambda\text{-TRISPHAT}]^{-+}[(nBu)_3NH]$ in chloroform, only the Λ-cationic enantiomer of $[Ru(4,4'\text{-}Me_2bpy)_3]^{2+}$ is extracted into the organic phase, the other enantiomer remaining in the aqueous solution.

Diastereoselectivities up to 45% d.e. have been reported in the selective extraction of Λ-$[Ru(Me_2bpy)_3]^{2+}$ with Λ-TRISPHAT demonstrating the efficiency of this resolution procedure.[19]

The last method of enantiomer separation is via *chromatographic resolution* that relies on the different interactions of the diastereomeric ionic pairs with the chromatographic stationary phase. Diastereomers can possess dramatic differences in their retardation factors as has been observed for the resolution of $[Ru(bpy)_3]^{2+}$ with Δ-TRISPHAT by column chromatography over silica gel with dichloromethane as eluent.[20] The TRISPHAT diastereomeric mixtures are poorly retained on silica or alumina and complete diastereomeric separation can be achieved by flash or preparative chromatography.

It was expected that TRISPHAT would form diastereomeric salts with the ruthenium or manganese chiral complexes **3.10** and **3.11** reported in Chapter III. As commented before, homochiral interactions (ΔΔ) have been reported to occur preferentially to heterochiral ones (ΔΛ), therefore it should be possible to form and isolate selectively one diastereomer over the other depending on the chiral anion used. Regarding the interaction of the chiral anion with the complexes, it should also be possible to determine the position where the TRISPHAT anions are located since the protons of the cation sited closer to the anion will be more perturbed. The ruthenium complex **3.10**, for instance, is dicationic where the PF_6^- anions are located close to the *N*-methylimidazole ring. Short contacts between the PF_6^- and the *N*-methylimidazolyl ring were found in the solid state of **3.10** as discussed in Chapter **3.12**. The two TRISPHAT anions are expected to be located in similar positions close to the boron atom, since this part of the complex is the less sterically hindered; there also exists the possibility of similar short contacts to stabilise the ion pairs, and more importantly, these are the positions closer to the C_3-axis of the cations.

However, Amouri and coworkers have recently reported a lithium complex where the TRISPHAT interacts with the arene moiety by π–π stacking, so a similar situation could also be possible for the diastereomeric ion pairs with the ruthenium complex **3.10** due to the *p*-cymene moiety.[21]

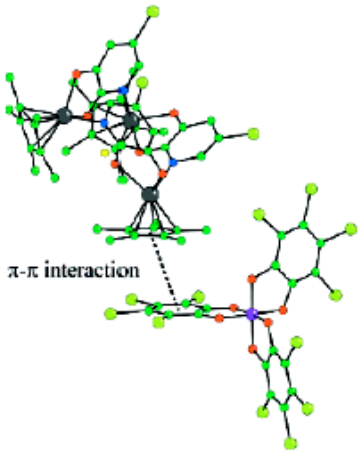

Fig. 4.13. *TRISPHAT π–π stacking with an arene moiety in the solid state.*

4.4. RESULTS

4.4.1 CHIRAL ACTIVATORS

4.4.1.1 Chiral Oxazolines

The first oxazoline synthesised was (4*R*,5*R*)-4-methyl-5-phenyl-2-oxazoline (**4.17**) from the commercially available aminoalcohol norephedrine. One equivalent of the oxazoline, one equivalent of $B(NMe_2)_3$ and three equivalents of methimazole were heated to reflux in 10 ml of dry toluene. After eight hours a colourless solid precipitated from the solution. Analysis of the solid by mass spectrometry (M^+= 443) suggested the presence of the oxazoline coordinated to the borane which also contains two methimazole rings and, surprisingly, an unreacted NMe_2 group.

Further ^{1}H-NMR spectroscopic studies showed that the oxazoline also underwent ring opening, presumably due to nucleophilic attack of the methimazole sulphur atom (Scheme **4.4**). The proton at the 2-position of the oxazoline appears now at 8.59 ppm, in the region characteristic for formamide protons, showing a dramatically low field shift of 1.6 ppm compared to the free oxazoline (7.01 ppm). In addition, the proton at the 5-position where the ring-opening takes place, shows a significant downfield shift of 0.7 ppm. The formation of the formamide group was also supported by IR spectroscopy, where an intense band at 1675 cm^{-1} due to the carbonyl group appears.

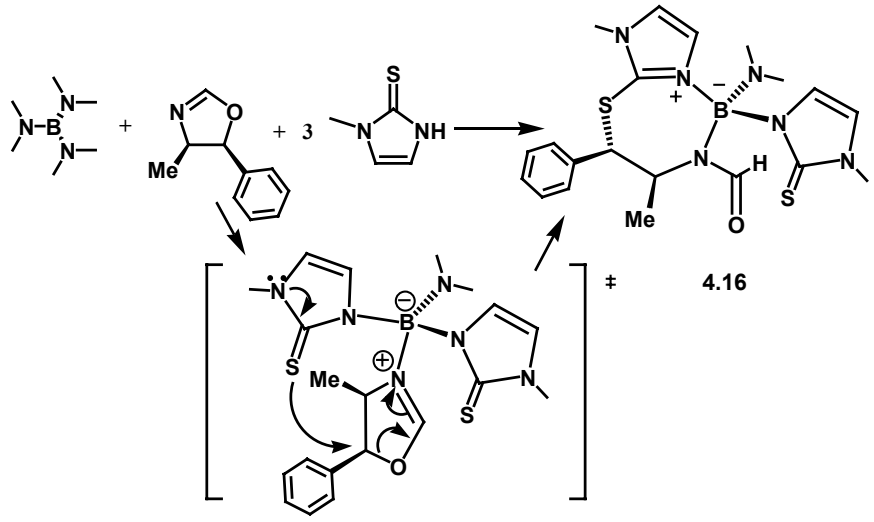

Scheme 4.4. *Oxazoline ring opening process.*

Both the oxazoline and the methimazole have to be coordinated to the borane for the intramolecular ring opening to occur. This is the first example of an oxazoline opened by a thione, although many other nucleophilic ring openings of oxazolines are known.[22] Presumably this particular oxazoline is susceptible to ring opening due to stabilization of the α-carbocation formed upon the opening by the phenyl group at the 5-position. Therefore, four other oxazolines lacking the phenyl ring in this position were synthesised (Fig. **4.13**) and used as activators, and in the examples (**4.20**) and (**4.21**) methyl groups were introduced in an attempt to hinder the nucleophilic attack.

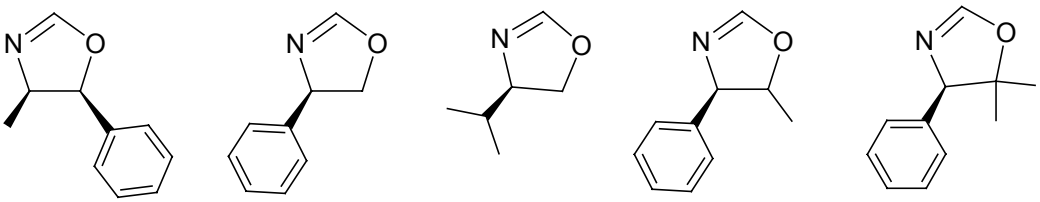

4.17 **4.18** **4.19** **4.20** **4.21**

Fig 4.14. *Oxazolines used in the study.*

Under similar experimental conditions, even the 4,4-dimethyloxazoline **4.21**, with two methyl groups at the 5-position does undergo ring-opening; in all cases the formamide group was evident by ^{1}H-NMR and IR spectroscopies. To further confirm that the nucleophilicity of the methimazole sulphur is responsible for this process, pyrazole was used as the heterocycle. Under the same reaction conditions, **4.22** was formed, the oxazoline remaining intact. The ^{11}B-NMR spectrum confirms the tetrahedral geometry at the boron atom with a singlet at 7.40 ppm. The proton at the oxazoline 2-position now appears at 7.81 ppm in the ^{1}H-NMR spectrum, shifted almost one ppm downfield due to the coordination, whereas the rest of the oxazoline protons are only slightly shifted compared with the free heterocycle. Moreover, the IR of the compound does not show any carbonyl band. There is however an unreacted NMe_2 group remaining on the boron atom responsible for two broad singlets at 3.10 and 3.05 ppm. We have to attribute this to effective shielding of this remaining NMe_2 by the oxazoline substituent at the 5-position. Further reaction with excess pyrazole, or more acidic heterocycles (triazole or methimazole) did not cause any changes in **4.22**. This is somewhat surprising since the dimethylamino group must present a high basicity as discussed in the Chapter II.

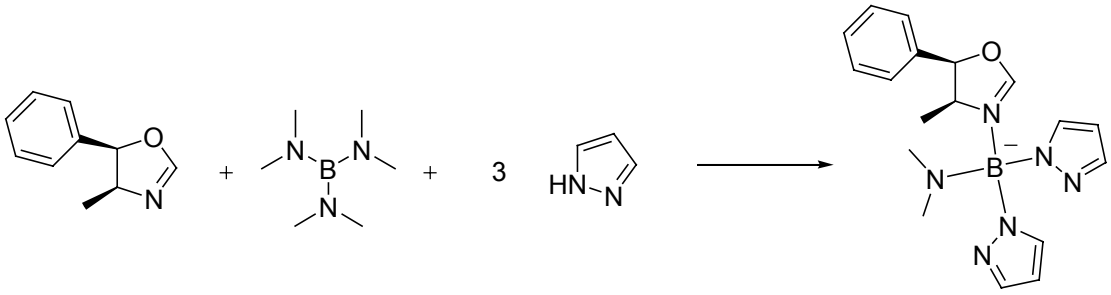

4.22

Scheme 4.5. *Pyrazole does not ring open the oxazoline.*

4.4.1.2 Chiral Imidazolines

Imidazolines are expected to be stable to the ring opening process. The synthetic protocol reported by Casey involves only five steps, but the yields of the resulting imidazolines were found to be quite variable. Only for those where a phenyl group is occupying the 2-position satisfactory yields were obtained. The imidazoline (**4.23**) was synthesised from norephedrine following the reported procedure.[11]

One equivalent of the imidazoline **4.23**, one equivalent of $B(NMe_2)_3$ and three equivalents of methimazole were heated to reflux in toluene. After 2 hours a colourless solid precipitated from the reaction mixture. Analysis of the solid showed that it was the (dimethylamido)tris(methimazolyl)borate **2.2**. The imidazoline remained unreacted in the solution.

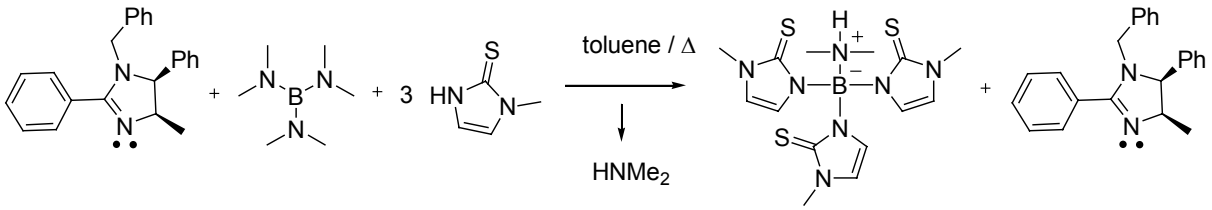

4.23 **2.2** **4.23**

Scheme 4.6. *Imidazoline activation does not take place.*

The imidazoline has therefore not coordinated to the $B(NMe_2)_3$ in the reaction. Since basicity limitations cannot be the case (the basic pK_a´s of imidazolines are in the range 6-11), steric ones are likely to direct the outcome of this reaction. Molecular models of the imidazoline **4.23** show that the lone pair of the nitrogen is partially shielded by the phenyl group at the 2-position. It is assumed that this is the main reason for the imidazoline to remain in solution not activating the borane to reaction with methimazole.

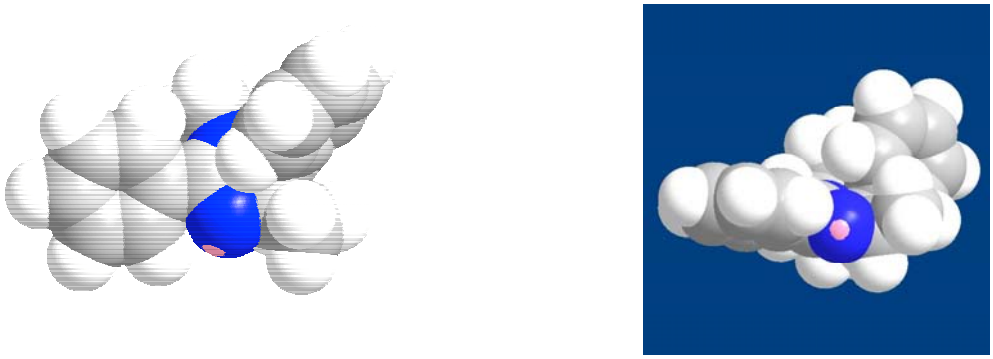

Fig 4.15. *The shielding of the lone pair of the imidazoline prevents coordination.*

Imidazolines with only hydrogen in the 2 positions have been described in the literature but their synthesis is not straightforward involving more than ten low-yielding synthetic steps. Moreover, the experimental observation with analogous oxazolines where one of the positions at the boron is still coordinated by a NMe_2 group made the use of these kinds of compounds not suitable for our purposes and this route was therefore not explored.

4.4.1.3 Chiral Tetramisole

(-) Tetramisole is sold as the crystalline hydrochloride **4.8**. To use it as activator for the borane, the imine nitrogen must be deprotonated. The free base was obtained by dissolving the hydrochloride salt in 1M NaOH, followed by extractive workup. The colourless oil obtained was analysed by ^{1}H-NMR and confirmed as pure tetramisole.

The proton at the 6-position appears at 5.5 ppm as a triplet, which will serve as a reference for further discussions. The tetramisole must be stored under argon and away from the light to avoid decomposition.

Treatment of one equivalent of tetramisole with one equivalent of $B(NMe_2)_3$ and three equivalents of methimazole yields (**4.24**) in 4h under refluxing toluene by precipitation of a colourless solid from the reaction mixture in 83% yield.

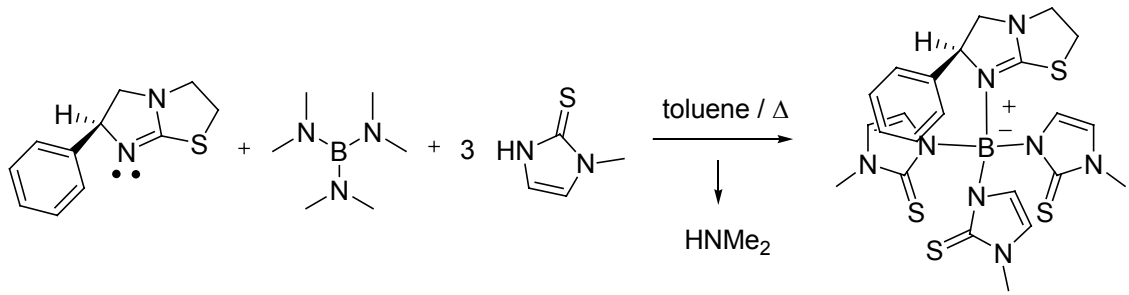

4.24

Scheme 4.7. *Tetramisole coordinates to $B(NMe_2)_3$ to form* **4.24** *in excellent yields.*

The mixture was filtered under nitrogen and the colourless solid was washed twice with dry ether. The ^{1}H-NMR spectrum shows a dramatic shift of – 0.98 ppm to high field for the hydrogen at the tetramisole 6-position. In all previous examples the protons of the activators were shifted downfield due to donation of electronic density to the borane. In this case the opposite tendency is observed and it could be ascribed to an edge to face interaction between the proton and the methimazole rings in solution. The proton at the tetramisole 6-position is therefore experiencing ring current shielding from the face of the proximate methimazole rings.

Molecular models were used to compare the tetramisole with the imidazoline **4.23**. It is possible to see in the Fig. **4.15** that the lone pair of the nitrogen is not shielded this time by the phenyl group at the 6-position due to the more flexible C_6–N bond that allows the phenyl group to be pushed away from the imine nitrogen.

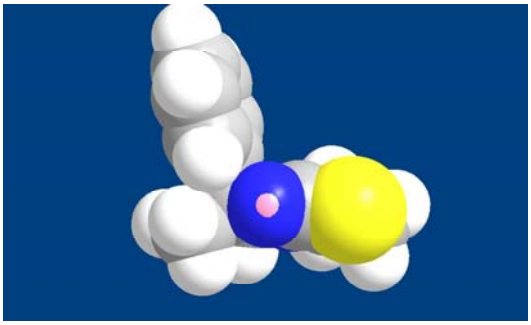

Fig. 4.16. *The lone pair of the tetramisole nitrogen atom is readily available.*

Complexation of **4.24** to [Ru(*p*-cymene)Cl_2]$_2$ dimer was performed following the standard conditions discussed previously for other ligands. To a solution of [Ru(*p*-cymene)Cl_2]$_2$ in dry MeCN, two equivalents of ligand **4.24** were added in small portions over 15 min. A colour change from orange-reddish to dark red indicated complex formation. After two hours no traces of starting materials were detected by mass spectrometry. The solvent was removed under vacuum and the deep red solid redissolved in dry MeOH. To this solution excess NH_4PF_6 was added causing immediate precipitation of a reddish crystalline solid. The solid was filtered off and washed with dry MeOH, dry Et_2O and dried under vacuum. The complex was formed in an excellent yield (89%). A region of the ^{1}H-NMR spectrum of the ruthenium complex is shown in Fig. **4.17**. All protons of the complex appear doubled meaning that a mixture of the two possible diastereomers (*S*,Δ) (**4.25**) and (*S*,Λ) (**4.26**) have been formed and integration of the signals shows that the diastereomer ratio is approximately 2:1.

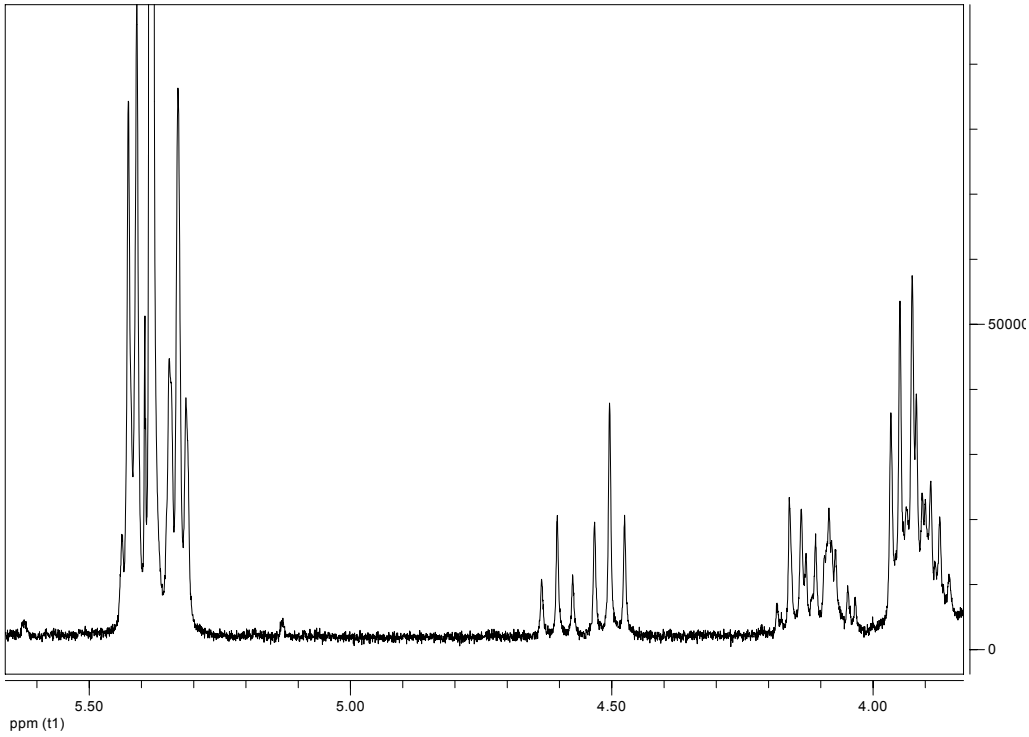

Fig. 4.17. *Selected ^{1}H-NMR region of* **4.25** *showing the H at 6-tetramisole position.*

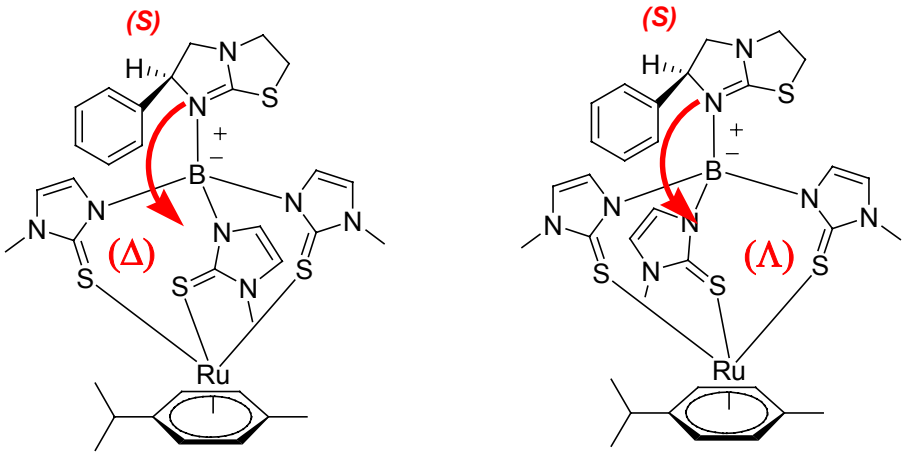

4.25 **4.26**

Fig. 4.18. *Both diastereomer (S,Λ) and (S,Δ) are formed upon metal complexation.*

The methimazolyl protons have undergone an average downfield shift of +0.61 ppm with respect to the free ligand following the expected tendency.

The chirality at the 6-position of the tetramisole affects the helical cage formed upon complexation but it is *not effective enough* to direct the formation of only one of the two possible diastereomers. For this reason (*R*- Λ) and (*R*-Δ) were formed although in unequal proportions. The energy of the diastereomers must be very similar forming both kinetic and thermodynamic products that do not interconvert in the NMR scale. All attempts to selectively crystallise one diastereomer over the other were unfortunately unsuccessful.

The reaction between tetramisole, $B(NMe_2)_3$ and pyrazole was also undertaken and the ligand (**4.27**) was formed in excellent yield (87%).

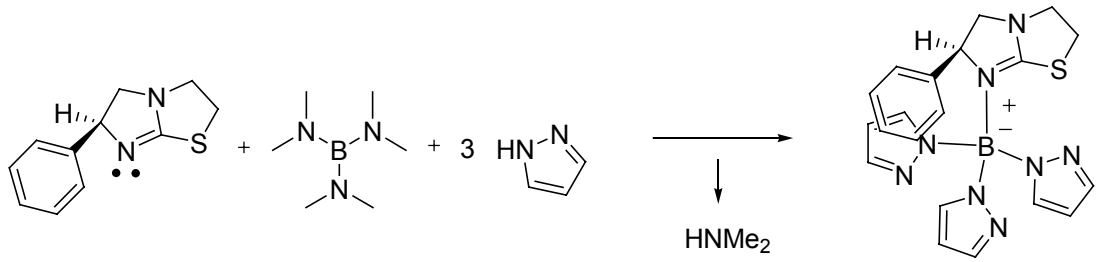

4.27

Scheme 4.8. *Synthesis of [(-) tetramisole]B(pyrazolyl)$_3$* **4.27**.

^{1}H-NMR and ^{13}C-NMR spectra confirm the formation of **4.27**. The proton at the 6-position of the tetramisole appears dramatically shifted to highfield (-1.3 ppm) upon formation of the ligand as observed for **4.24** which could again be ascribed to an edge to face interaction between the proton at the tetramisole 6-position and the pyrazole rings in solution. X-ray quality crystals of **4.27** were grown from an acetonitrile solution layered with ether. The structure is shown in Fig. **4.18**. The three-pyrazole nitrogen atoms are pointing towards the tetramisole group, one of them being in close proximity to the sulphur of the tetramisole (N-S distance is 3.134 Å). The N_{coord}-B distance is 1.564 Å, slightly longer than the N_{pyr}-B (mean 1.531 Å) due to the coordinating character of the bonding. The phenyl group of the chiral carbon at the 6-position is almost forming π–π stacking with one of the pyrazole rings (distance between centroids 3.776 Å). Selected bond distances and angles are

summarised in the Table **4.1.** From the X-ray figure it is possible to observe that the phenyl ring is perpendicular to the ligand *pseudo*-C_3-axis.

Upon metal complexation, for example in the synthesis of the ruthenium complex of **4.24**, this activator is not able to direct the helical twist to form a single diastereoisomer since it cannot interact with the metal-ligand bicyclo-cage. Using bulky groups at the heterocycle fifth position might improve the interaction between the chiral tetramisole and the heterocycles, but it could also prevent coordination to the borane due to steric interactions as will be discussed in the next section.

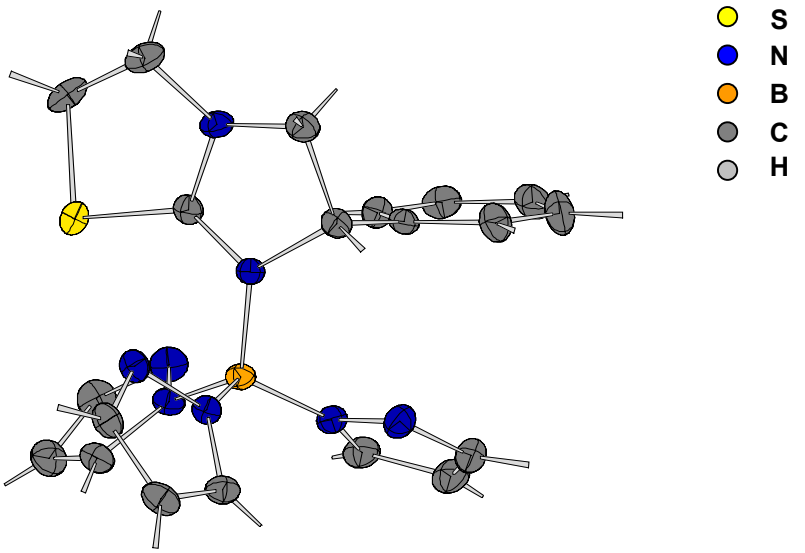

Fig. 4.19. *The phenyl ring is perpendicular to the C_3 axis of* **4.27**.

Table 4.1. SELECTED BOND LENGTHS (Å) AND ANGLES (°) FOR **4.27**.

B-N(1)	1.526(2)	N(11)-B-N(21)	117.62(13)
B-N(11)	1.536(2)	N(1)-B-N(31)	107.62(13)
B-N(21)	1.531(2)	N(11)-B-N(31)	108.66(13)
B-N(31)	1.564(2)	N(21)-B-N(31)	108.87(13)
N(1)-B-N(11)	110.16(13)	Ph_{centr}-pyr_{centr}	3.776
N(1)-B-N(21)	111.58(13)	N-S $_{H\text{-bond}}$	3.134

4.4.2 Chiral heterocycles

4.4.2.1 Oxazolidinethiones

The oxazolidinethione heterocycle **4.11** was formed in good yields from chiral norephedrine and C_2S following the reported protocol. One equivalent of *N*-methylimidazole, one equivalent of $B(NMe_2)_3$ and three of the azole were heated to reflux in toluene but no reaction was detected even after three days under these conditions.

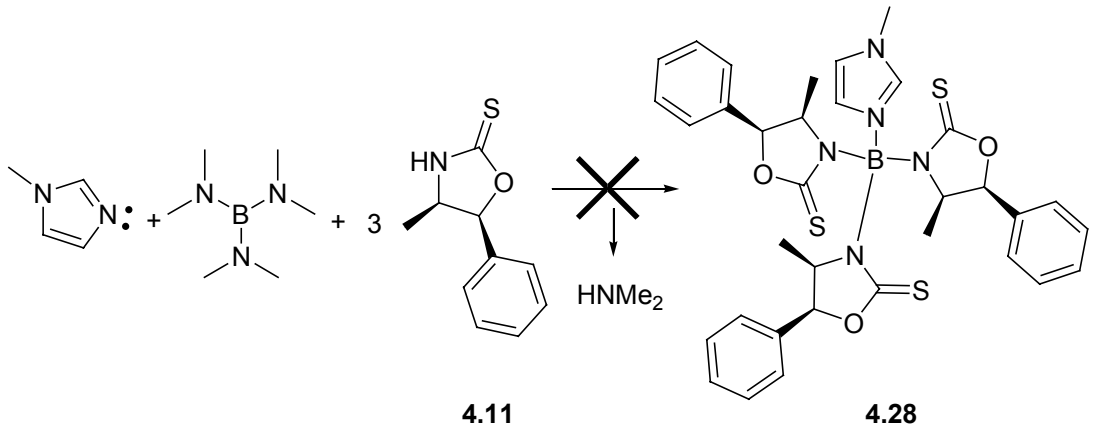

4.11 **4.28**

Scheme 4.9. *Oxazolidinethiones do not react with $B(NMe_2)_3$ even under forcing conditions.*

The heterocycle seems to be completely inert and could be recovered from the crude mixture. This is somewhat surprising given the high reactivity of the NMe_2 groups as discussed in Chapter II, but no traces of anything other than starting materials were detected by mass spectrometry. Since the acid pK_a´s of oxazolidinethiones are similar (pK_a = 13) to methimazole, we assume that steric factors impede the formation of the tripodal ligand (**4.28**). We considered that the formation of **4.28** is hampered by the methyl group at the oxazolidinethione 4-position.

4.4.2.2 Chiral Methimazole

The chiral methimazole **4.9** was reacted with *N*-methylimidazole and $B(NMe_2)_3$ under standard conditions to form the ligand [(*N*-methylimidazole)B {1-(*S*-)α-methylbenzyl-2-mercapto-imidazolyl}$_3$] (**4.29**) in 82% yield.

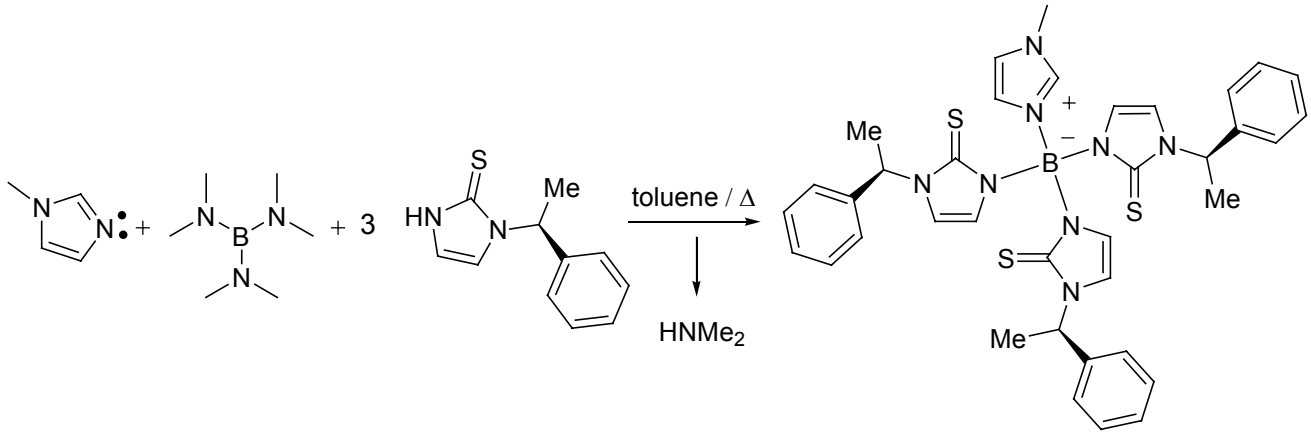

Scheme 4.10. *Formation of* **4.29** *using the standard procedure.*

The ^{11}B-NMR spectrum of this ligand shows a singlet at 3.54 due to the tetrahedral geometry at the boron. Selected peaks from the ^{1}H-NMR spectrum of **4.29** are the three singlets for the *N*-methylimidazolyl ring at 8.80, 7.51 and 7.42 ppm and the protons of the methimazolyl rings that appear as doublets at 6.95 and 6.32 ppm with a coupling constant of 2.35 Hz. The CH proton of the *α*-methyl-benzyl chiral group appears as a quartet at 6.12 ppm. Mass spectrometry shows a molecular ion peak at 703 m/z corresponding to the protonated ligand. The ligand **4.29** was used in the synthesis of the ruthenium complex (**4.30**) without further purification. Complexation of **4.29** to Ru(II) was achieved by reaction with $[Ru(p\text{-cymene})Cl_2]_2$ in dry ethanol solution to provide [{(*N*-methylimidazole)B(1-(*S*-)α-methylbenzyl-2-mercapto-imidazolyl)$_3$}Ru(*p*-cymene)][PF_6]$_2$ **4.30** following exchange of the chloride counter ions for PF_6^- by salt metathesis with NH_4PF_6.

The chirality of **4.30** is revealed in its ^{1}H-NMR spectrum which shows a pair of doublets for the diastereotopic *p*-cymene ^{i}Pr methyl groups and four doublets for the *p*-cymene arene CH protons which normally provide an $(AB)_2$ pattern in racemic systems as discussed in the Chapter II.

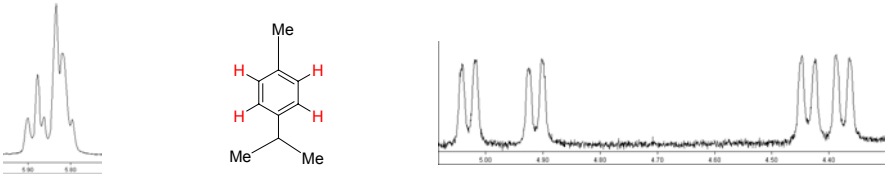

Fig. 4.20. *^{1}H-NMR p-cymene region of the racemic Ru complex* **3.10** *(left) and the chiral example* **4.30** *(right).*

A general tendency is that all protons corresponding to the ligand in **4.30** appear dramatically down-field shifted upon complexation. The protons of the *N*-methylimidazole ring are shifted by an average of +0.43 ppm, whilst the methimazole ones show a larger shift of +0.70 ppm. The protons of the α-methyl-benzyl groups are less affected showing an average downfield shift of + 0.32 ppm. X-ray quality crystals were grown from a concentrated solution of **4.30** in MeOH by slow diffusion with Et_2O. The X-ray structure of **4.30** (Fig. **4.21**) shows just one molecule per unit cell, which compares with the enantiomeric pair found for the analogous complex with the achiral ligand [(*N*-methylimidazole)B(methimazolyl)$_3$]. Each of the three ligand tripod arms has δ stereochemistry and the complex has a θ^{m} value (mean N-B-M-S torsion angles) of 50.7°. The other torsional parameter ω^{m} (51.7°) falls in the range observed for ZTm and Tm complexes of octahedral metals. The coordinate B-N (*N*-methylimidazole) bond (1.581 Å) is slightly longer than the covalent bonds to the azolyl rings (mean 1.549 Å). The C-S bond lengths (mean 1.728 Å) do not differ significantly from those found in the corresponding complex containing the Tm ligand [(Tm)Ru(*p*-cymene]Cl (mean C-S = 1.723 Å) and [ZTmRu(*p*-cymene]Cl_2 (mean 1.720 Å). However, the Ru-S distances (mean 2.440 Å) are slightly longer than in the Tm complex (mean 2.411 Å) and the ZTm complex (mean 2.425 Å) indicating that the steric bulk of the α-methylbenzyl substituents in **4.30** slightly hinders the coordination of the [Ru(*p*-cymene)]$^{2+}$ unit.

Two positions of disorder for the benzyl group close to the isopropyl moiety are observed due to the bulky isopropyl group. While the introduction of bulky substituents onto the 3- and 5-positions of poly(pyrazolyl)borates significantly alters the steric profile of the scorpionates as discussed with the case of the "second generation of scorpionates", this appears to be less apparent in the chemistry of Tm derivatives. The steric influence of a substituent in the 3-position of the heterocycle is felt less at the metal centre because the substituent points away from the coordination sphere. The central chiral groups at the 3-position of the methimazole heterocycle control the chiral cage formed upon coordination to the metal centre directing its helical twist. The other possible diastereomer (*S*-Δ) is not formed due to unfavourable interactions between both chiral moieties. It has previously been suggested that the energy barrier to racemisation of C_3-symmetric octahedral Tm complexes is in excess of 90 $kJmol^{-1}$. In **4.30** such twisting of the metal-ligand bicyclo[3.3.3]-cage structure would represent interconversion between diastereomers, and therefore not only is there a substantial barrier to this process, but the two forms will be of different energy, and the Λ stereochemistry of the tripod arms provides the lowest energy conformation of this cage with the *S*-configuration of the α-methylbenzyl substituents. Clearly Δ-stereochemistry may be anticipated in combination with the enantiomeric (*R*) α-methylbenzyl substituents.

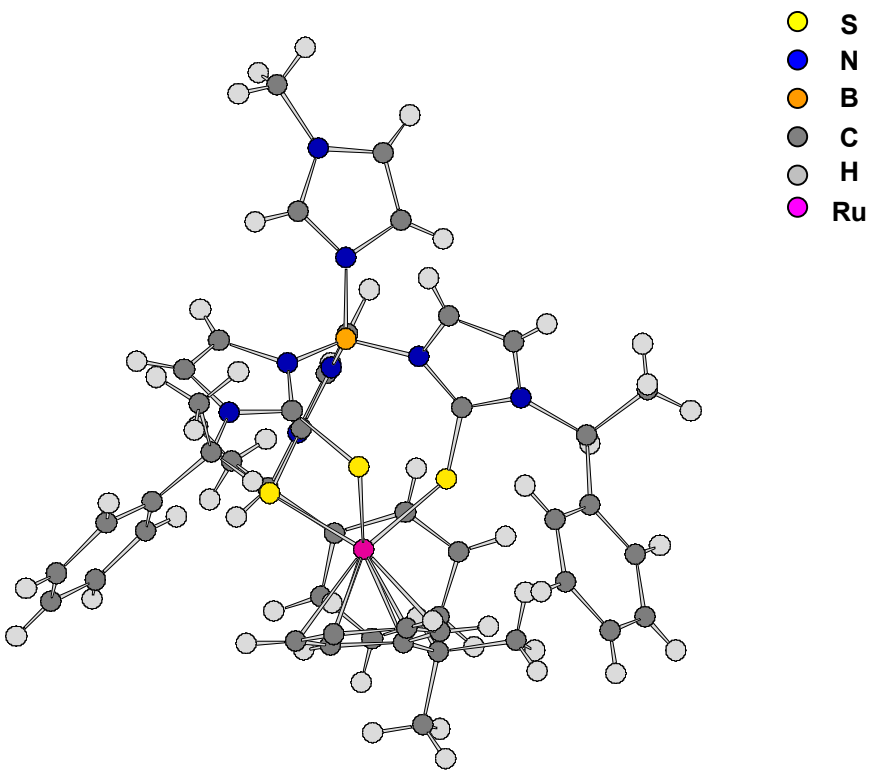

Fig 4.21. *First example of a chiral TmRu(p-cymene) complex* **4.30**.

Table 4.2. SELECTED BOND LENGHTS (Å) AND ANGLES (°) FOR **4.30**.

B-N(15)	1.580(7)	S(12)-Ru-C(22)	106.13(16)
B-N(32)	1.547(7)	S(13)-Ru-C(23)	110.46(16)
B-N(33)	1.551(7)	S(14)-Ru-C(24)	105.15(16)
B-N(34)	1.549(7)	N(32)-B-N(34)	112.1(4)
C(22)-S(12)	1.727(5)	N(32)-B-N(33)	109.3(4)
C(23)-S(13)	1.727(5)	N(33)-B-N(34)	114.1(4)
C(24)-S(14)	1.730(5)	N(15)-B-N(32)	110.0(4)
S(12)-Ru	2.453(12)	N(15)-B-N(34)	103.9(4)
S(13)-Ru	2.423(13)	N(15)-B-N(33)	107.2(4)
S(14)-Ru	2.446(13)		

4.4.3 CHIRAL COUNTERANION

The outer coordination sphere of the ruthenium and manganese compounds reported in Chapter III is usually occupied with PF_6^- counteranions to balance the complex charge. The replacement of the anions by the chiral phosphate TRISPHAT **4.12** was performed, following the experimental procedures reported by Lacour and

coworkers, to study the influence of the chirality of this anion in the behaviour of the ruthenium complexes introduced in Chapter II.

4.4.3.1 Enantioselective Extraction

The first of the experiments was the use of the Λ-TRISPHAT as selective extractor of the complex **3.10**.

The complex **3.10** was synthesised with chloride counteranions due to its higher solubility in water when compared to the PF_6^- salt which is completely insoluble. Λ-TRISPHAT **4.15** was chosen for this experiment due to its high solubility in chlorinated solvents compared to its Δ-form, which due to the chinchonidinium cation, requires the use of DMSO to solubilize the whole mixture. As discussed in Section **4.3.3.B**, polar solvents can weaken the contact between ion pairs, thus leading to a lower enantiodifferentiation in the process and therefore must be avoided in these experiments.

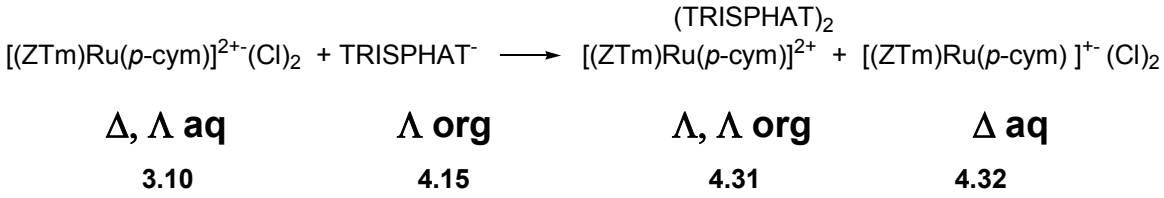

Scheme 4.11. *Selective extraction of* **3.10** *with Λ-TRISPHAT.*

The ruthenium complex **3.10** was dissolved in 25 ml of water and stirred for 20 min to give a reddish-coloured solution. In another flask the Λ-TRISPHAT was dissolved in 25 ml of chloroform and stirred for 20 min to give a colourless solution. After this time, the solution of the complex was added over 10 min to the TRISPHAT solution. Colour change was detected immediately in the organic phase. The mixture was allowed to stir for 15 min. After this time the organic layer was decanted, dried over $MgSO_4$ and the solvent removed under reduced pressure and dried to yield a reddish solid.

The water from the aqueous solution was also removed under vacuum at 50ºC over 12 hours to yield an orange solid. The ^{1}H- NMR analysis of the organic phase shows the formation of both diastereomeric salts (ΔΛ) and (ΛΛ) in equal proportions.

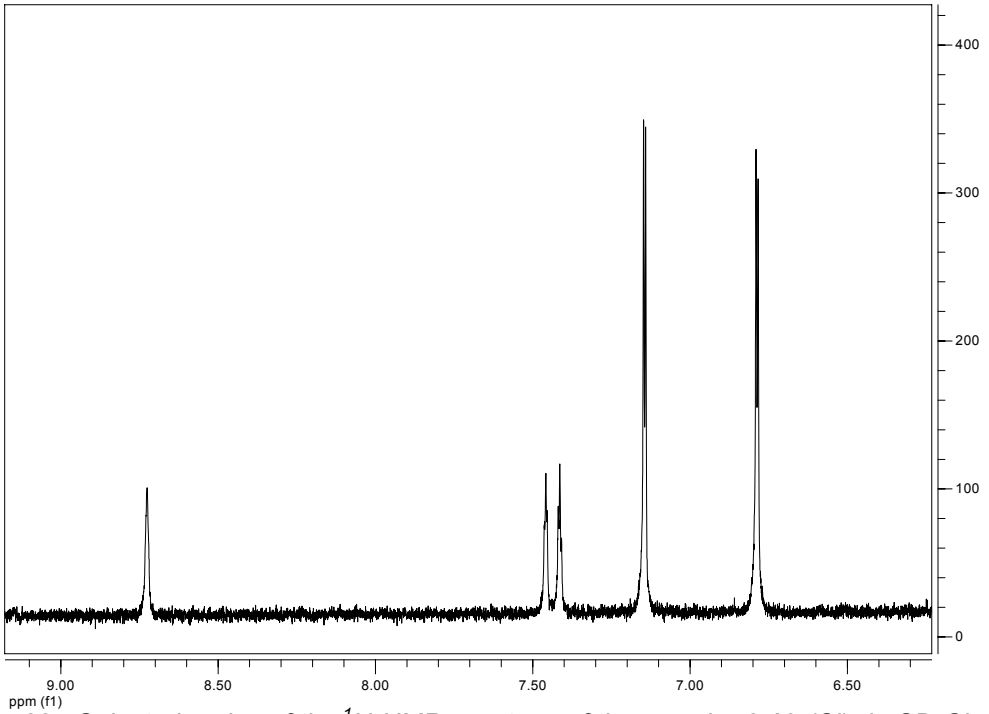

Fig. 4.22. *Selected region of the ^{1}H-NMR spectrum of the complex* **3.10** *$(Cl)_2$ in CD_2Cl_2.*

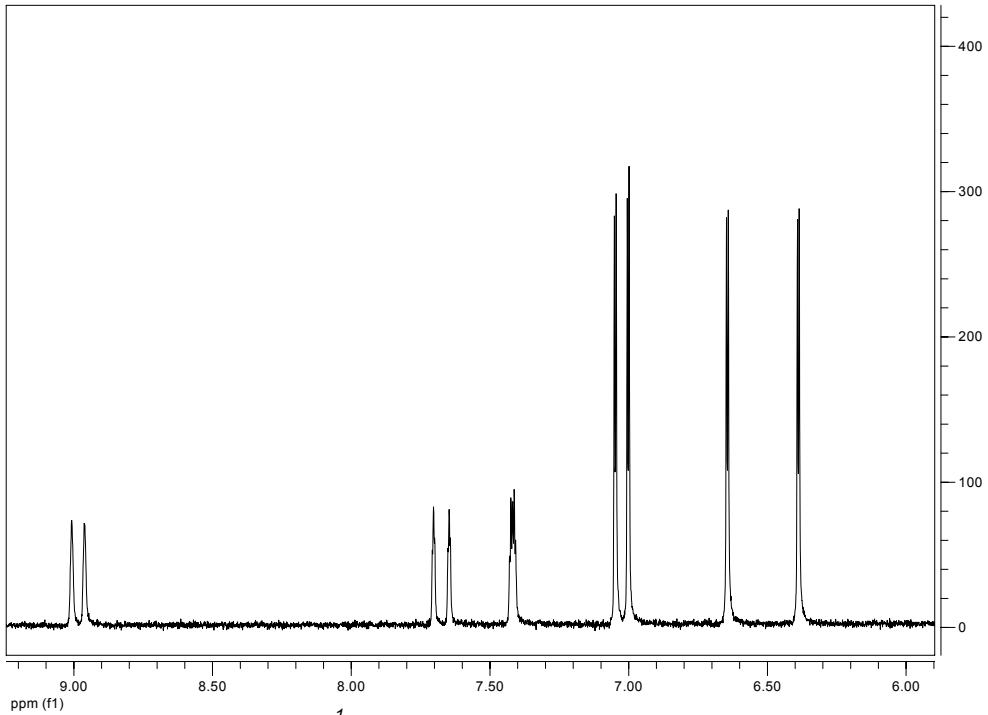

Fig. 4.23. *Selected region of the ^{1}H-NMR spectrum of the complex* **4.31** *$(TRISPHAT)_2$ in CD_2Cl_2.*

Comparing both spectra before and after addition of the chiral phosphate, the most perturbed signals are the protons of the *N*-methylimidazole ring that appear downfield shifted by almost +0.5 ppm. It is possible to postulate that the TRISPHAT anions in solution are located closer to this group in a similar position as the PF_6^- in the complexes **3.10** or **3.12**. These are the positions where the chiral anions are as close as possible to the C_3 axis, which is its preferential approach as has been observed for other ruthenium complexes. The *p*-cymene region of the Ru-TRISPHAT complex does not show chemical shift differences when compared with the spectrum of the chloride salt, therefore the formation of π–π stacking between the TRISPHAT cathechol rings and the Ru arene moiety does not occur, at least in solution. The ^{1}H-NMR spectrum of the aqueous phase shows exactly the same pattern of signals for the ruthenium complex upon addition of two equivalents of Λ-TRISPHAT. The absence of diastereoselectivity in the process can be explained as follows: if Λ-TRISPHAT shows a similar affinity for both enantiomers because homo- and heterochiral diastereomer interactions are evenly preferred, then both diastereomers are equally formed and extracted onto the organic phase at the same ratio. A reason for the same affinity might be due to the presence of the *N*-methylimidazole ring that is placed in the C_3-axis of the molecule, the exact direction from where the TRISPHAT anion is known to approach the molecule. This is further supported by the ^{1}H-NMR evidence discussed above. This group might prevent the effective interaction between the chiral ruthenium cage and the TRISPHAT to form selectively one diastereomer over the other, thus both are formed in the same proportion. The other explanation would be considering that the ruthenium TRISPHAT complexes are configurationally labile in solution and racemisation occurs immediately after the diastereoselective extraction takes place. However, since the energy of the racemisation is known to be higher than 90 kJmol^{-1} this phenomenon is quite unlikely to occur.

4.4.3.2 Column Chromatography

The second experiment performed with the chiral TRISPHAT was the resolution of the diastereomers by column chromatography on Al_2O_3. In this case the (Δ-TRISPHAT$^-$)(chinchonidinium) and the ruthenium complex **3.10** [(*N*-methylimidazole)B(methimazolyl)$_3$Ru(*p*-cymene)]PF_6 were used since it is known that the salt [chinchonidium]PF_6 is retained in the column under the experimental conditions. Δ-TRISPHAT and **3.10** were dissolved in acetone and stirred for 10 min. After this time the mixture was charged onto a column packed with alumina and dichloromethane was used as the eluent. An orange fraction was immediately detected running down the column. It was isolated and characterised upon removal of the solvent to yield a reddish solid. ^{1}H-NMR studies of the solid showed a similar spectrum to the one obtained by the selective extraction of **3.10** with Λ-TRISPHAT. Although both diastereomers are formed they seem to present similar retention times being eluted simultaneously. Different solvent combinations were tried in order to find the right conditions for the separation of the diastereomers but unfortunately no separation was achieved. This experiment shows that although the salt metathesis occurs there is no diastereoselectivity in the process.

4.5 CONCLUSIONS

Chiral tripodal borate ligands, which are rare in the literature due to the absence of appropriate synthetic routes, can be synthesised using the methodology introduced in Chapter II. Three different routes have been considered for the insertion of chiral groups into the ligand framework, either at the boron centre, at the azole heterocycles or in the outer coordination sphere of their metal complexes. The use of chiral oxazolines as activators of the $B(NMe_2)_3$ to reaction with methimazole was found to be limited by an intramolecular ring opening process of the oxazoline due to the nucleophilicity of the methimazolyl sulphur upon coordination to the borane. A chiral imidazoline, expected to be stable to the opening process, was also synthesised, but found to be unable to coordinate the $B(NMe_2)_3$ presumably due to

steric hindrance. Tetramisole, a chiral natural product, was found to act as a chiral activator of the borane to reaction with methimazole to form the chiral ligand [(tetramisole)B(methimazolyl)$_3$]. The chirality of this group is, however, not able to strongly direct the formation of a single diastereomer upon coordination to ruthenium and therefore both diastereomers *S,*Λ and *S,*Δ {[(Tetramisole)B(methimazolyl)$_3$] Ru(*p*-cymene)}$(PF_6)_2$ were formed. The fact that the diastereomers are formed in a 2:1 ratio does however indicate that some stereodirection is being achieved in this system. The chiral ligand [(tetramisole)B(pyrazolyl)$_3$] was also synthesised and characterised by X-ray spectroscopy. The three pyrazole ring nitrogen atoms are pointing in the direction of the tetramisole activator, although the flexibility of the B-N bonds allows free rotation to coordinate to metal centres. It is possible to observe in the X-ray structure how the plane of the phenyl group at the chiral C6-position is arranged perpendicular to the ligand pseudo-C_3-axis. This is the reason why this specific group cannot very effectively direct the helical twist of the chiral bicyclo-cage in the ruthenium complex **4.24** discussed before. A methimazole substituted at the 4- or 5-position could interact with the tetramisole phenyl ring to form only one of the two possible diastereomers upon complexation, but as seen for the oxazolidinethiones, the 4-position is considered to prevent the coordination to the borane, so the steric interactions would need to be carefully considered. No reaction was detected between oxazolidinethiones and the borane, even under forcing conditions. The use of a heterocycle with chiral groups at the 3-position, that places the chiral groups far from the boron atom, allows the first synthesis of a neutral chiral tris(methimazolyl)borate Tm ligand.[23] The chirality at these positions does not affect the coordination behaviour of this ligand and thus directs the helical twist of the bicyclo-cage upon metal complexation. Only one of the two possible diastereomers was formed as shown in the X-ray structure. The third approach that involved the metathesis of the PF_6^- anions with the chiral TRISPHAT$^-$ anion in the outer coordination sphere of the metal complexes was also considered. Selective extraction using Λ-TRISPHAT was attempted, however both diastereomers (ΛΛ) and (ΔΛ) were isolated in the same ratio.

The TRISPHAT anions in solution are located close to the *N*-methylimidazolyl ring as revealed by ^{1}H-NMR spectroscopy. A reason for the formation of both diastereomers could be that Λ-TRISPHAT cannot approach the C_3-symmetric chiral cage due to the presence of the *N*-methylimidazole ring thus impeding the formation of the homochiral diastereomer (ΛΛ). A second explanation could be that the ruthenium complex formed is labile in solution, racemising during the extraction process, although previous work in the group has shown that the racemisation of analogous complexes does not to occur at room temperature. The use of Δ-TRISPHAT in the diastereoselective column chromatography lead to similar results where both diastereomers were formed in the same ratio and the fact that they present similar retention times made their separation impossible to achieve.

PART II

4.6 TRANSFER HYDROGENATION OF KETONES

4.6.1 INTRODUCTION

Catalytic reduction of polar functional groups such as ketones and imines to alcohols and amines has become an interesting field of study in both academia and industry.[24] Among the catalytic processes known for these transformations, transfer hydrogenation has received recent attention due to its operational simplicity, high selectivity and avoidance of the use of hydrogen.[25]

Hydrogen transfer reactions in which two hydrogen atoms are formally transferred from an alcohol to a ketone have been known for more than 80 years since the development of the Meerwein-Ponndorf-Verlay (MPV) reduction of ketones was reported.[26] In this reaction aluminium isopropoxide is used to catalyse the transfer of hydrogen from isopropanol to a ketone. The reaction can be also run in the opposite direction, then known as the Oppenauer oxidation, where the acetone is acting as the hydrogen acceptor. The mechanism for both processes has been reported to proceed through a six-membered transition state where the metal acts as a template providing the reactants with the correct orientation for the hydride transfer as shown in Scheme **4.12**.

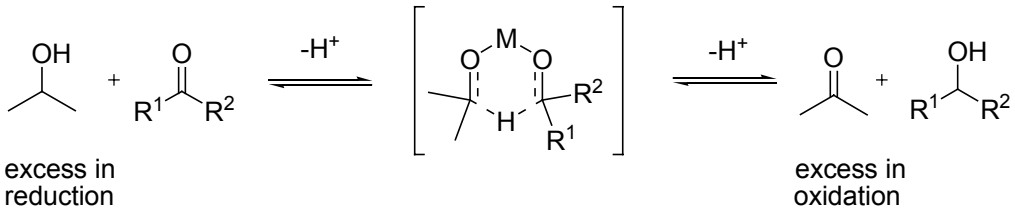

Scheme 4.12. *MVP reduction and Oppenauer oxidation catalised by Al(^{i}PrO)$_3$.*

The hydrogen transfer reactions are equilibrium processes that can be shifted to a certain side by controlling the starting reagents.

Thus, for the MPV reduction of ketones isopropanol is employed in excess, and for the Oppenauer oxidation of alcohols, acetone is used in excess. The aluminium salt in this reaction is required in stoichiometric ratios being transition metal catalysed hydrogenations therefore more attractive. Complexes of ruthenium, iridium and rhodium are known to catalyse the transfer hydrogenation of ketones following a mechanism that generally operates through a hydridic route where a metal-hydrogen bond is formed. Ruthenium has been found to be the most active transition metal for the process and will be covered in detail in the next section.

4.6.2 RUTHENIUM(II) CATALYSED TRANSFER HYDROGENATION

The first ruthenium-catalysed transfer hydrogentation reaction was reported by Sasson and Blum in 1971 using the ruthenium precursor $[Ru(Cl)_2(PPh_3)_2]$ at high temperatures but it provided only moderate turnover frequencies.[27] Later, Bäckvall and coworkers noted that the addition of a base to this ruthenium precursor lead to an enhancement of the reaction rate due to the formation of the highly reactive $[Ru(H_2)(PPh_3)_3]$ species.[28] Since then, the number of ruthenium complexes studied has increased substantially with the years and transfer processes have become a key step in many synthetic methodologies. Special attention has received the asymmetric version of the reaction known as asymmetric transfer hydrogenation (ATH). The importance of the ruthenium catalysed asymmetric transfer hydrogenation was recognised with the Nobel prize being awarded in 2001 to Ryoji Noyori for his studies in this field.[29]

4.6.3 MECHANISM OF THE ATH

For main group metals a direct hydrogen transfer mechanism is generally involved where the hydrogen is transferred to the substrate in a concerted process as shown in Scheme **4.13**.

For transition metals a hydridic route, that involves the formation of a metal hydride by interaction of the catalyst with the hydrogen donor is always observed. This hydride is subsequently transferred to the substrate. The hydridic route can follow two mechanisms depending on the ligand coordinated to the metal; a **dihydride mechanism** where a dihydride metal complex is formed, or a **monohydride mechanism** where only one Ru-H bond is involved in the catalytic process. In the dihydride mechanism (also known as the *inner sphere mechanism*), the formation of the metal-hydride may involve the formation of a transition metal alkoxide followed by β-elimination to give M-H.

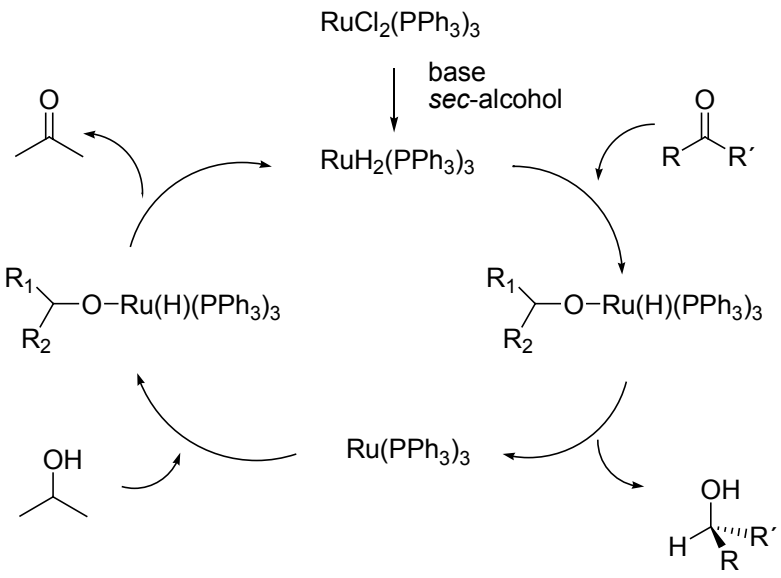

Scheme 4.13. *Catalytic cycle of Ru-dihydride mediated H-transfer (inner sphere mechanism).*

In the monohydride mechanism, or *outer sphere mechanism*, the alcohol does not coordinate to the metal and the hydrogen transfer proceeds in a concerted manner involving hydrogen bonds and dipolar interactions where both the hydrogen donor and the hydrogen acceptor are held together and in close proximity by the catalyst.

An astonishing example of a cooperative asymmetric hydride transfer process was introduced by Noyori with the so called "**metal–ligand bifunctional catalysts**".[30]

This term was coined for catalysts like **I** that present a group able to form a hydrogen bond with the ketone, thus facilitating the transfer process.

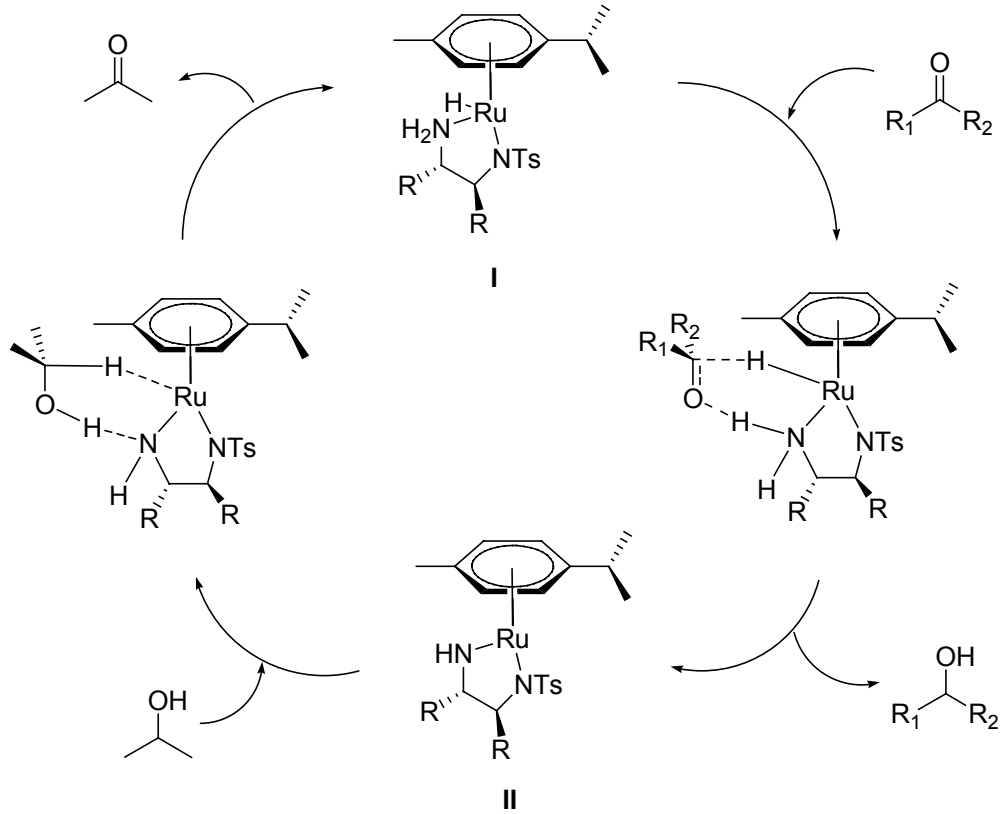

Scheme 4.14. *Catalytic cycle of catalyst* **I** *via a concerted six-membered transition state.*

A concerted transfer of the proton and the hydride from **I** to the substrate occurs following a cyclic six-membered transition state to give the alcohol and **II** which is considered as the catalyst active species. The hydride and the proton from 2-propanol are then delivered to the ligand and the metal respectively to form **I** and acetone. The basic amine group of the ethylene diimine derived ligand is responsible for the control of the disposition of the substrate by hydrogen bonding prior the hydride transfer.

4.6.4 SUBSTRATES AND REAGENTS FOR THE ATH

Prochiral ketones and imines can be reduced to the corresponding chiral alcohols or amines using transfer hydrogenation catalysts with high enantioselectivities. Usually aromatic substituted ketones like acetophenone, chloro- and methoxyacetophenone are the standard substrates to determine the activity and enantioselectivity of a given catalyst and the effect of electron releasing or withdrawing groups in the catalytic process. The hydrogen donor is usually isopropanol for the reduction of ketones and an azeotropic mixture of triethylamine/formic acid for the imine reduction processes. In both cases the hydrogen source also acts as the solvent medium, this minimising waste being these processes are therefore considered to be environmentally friendly.

4.6.5 LIGANDS USED IN ATH

The ligands used in ATH feature various combinations of different donor groups from oxygen, nitrogen, phosphorus, sulphur or arsenic. Bidentate, tridentate and even tetradentate ligands have been used. Some examples of the most successful ligands applied in ATH are shown in Fig. **4.24**.

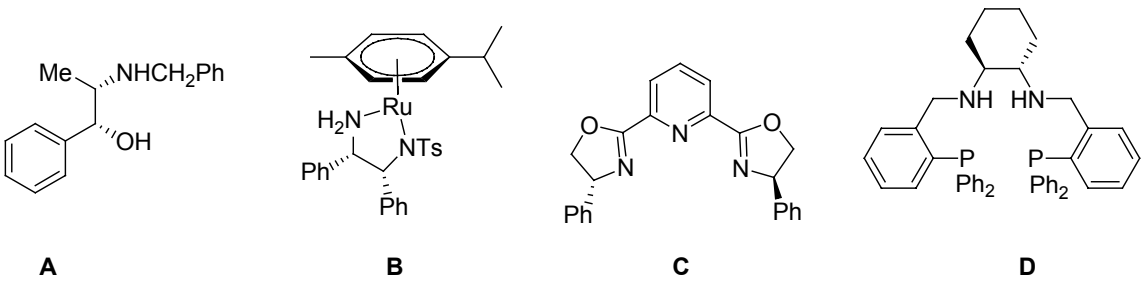

Fig. 4.24. *Ligands that provide enantioselectivities higher than 90 e.e. in the ATH.*

Amongst all of them, half sandwich *p*-cymene complexes of Ru(II) with chiral aminoalcohols or chiral diamine ligands have been extensively studied.[29] Noyori´s complex (**B**) is the most used catalyst because of its broad range of application. Prochiral ketones and imines are both reduced with high

enantioselectivities using this catalyst. Wills and coworkers have recently studied the structural factors that make these catalysts so active in the reduction process.[31]

Half-sandwich arene complexes provide unique reactivity and selectivity due to their interaction with the substrate via aromatic T-stacking type interactions. (Fig. **4.25**). The same group has also introduced the half-sandwich tethered ruthenium complex in which the chiral diamine is linked to the arene moiety to achieve improved enantiocontrol by locking the chiral elements of the ligand during the transition state.

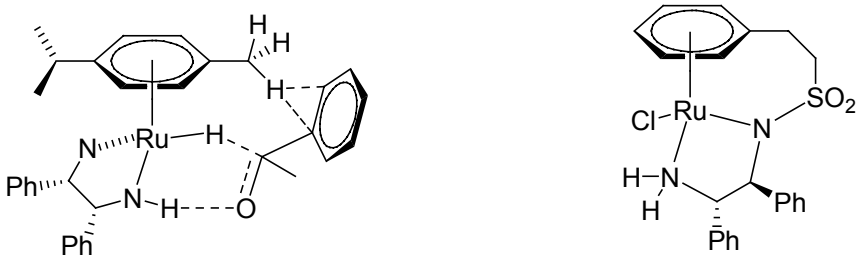

Fig. 4.25. *Half sandwich Ru arene are ideal as catalysts of the ATH.*

4.7 RESULTS

As shown in Fig. **4.24**, ruthenium complexes with C_1 and C_2-symmetric ligands providing a chiral environment, have been used in ATH with high enantioselectivities. However, the use of C_3-symmetric complexes in this process is yet to be reported. With the application of C_3-symmetric ligands in ATH we expect to be able to determine the effect that increasing the catalyst symmetry has upon the enantioselectivity of the ATH reaction. The tripodal ligand **4.29** was tested in the ruthenium(II)-catalysed ATH of acetophenone using isopropanol as the hydrogen source.

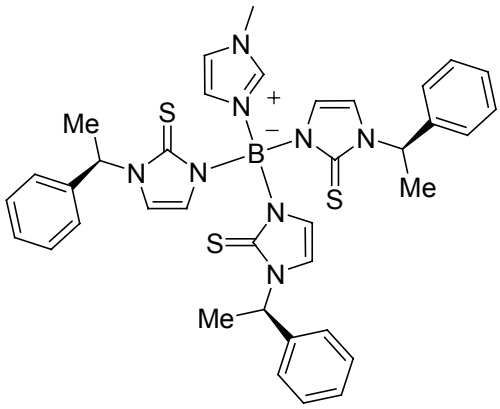

Fig. 4.26. *Ligand used in the study.*

In order to understand the behaviour of these ligands the reaction was studied using different catalyst pre-formation conditions, base loadings, temperatures, metal precursors and substrates. The general catalytic reaction is despicted in Scheme **4.15**.

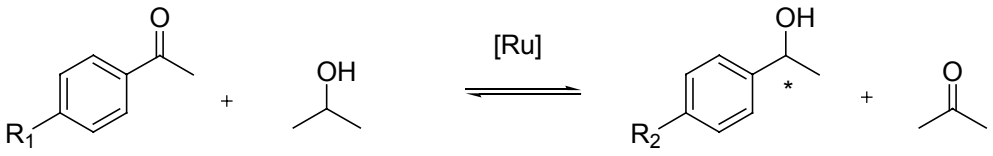

R_1 = H, Cl, MeO

Scheme 4.15. *ATH reduction of ketones.*

4.7.1 Ruthenium Precursors

The ruthenium precursors used were [Ru(*p*-cymene)Cl_2]$_2$ [(Ru_{cym})], Ru(DMSO)$_4Cl_2$, Ru(MeCN)$_4Cl_2$ [(Ru_{MeCN})], $RuCl_2(PPh_3)_3$ and [Ru(cod)Cl_2]$_x$.

4.7.2 Catalytic Studies

The catalytic behaviour was first explored with *in situ* catalysts generated from the Ru precursor and **4.29** in a 1:1 ratio with respect to Ru in isopropanol. As dicussed in the Chapter III, the complexation of the ligands with $[Ru(p\text{-cymene})Cl_2]_2$ dimer was found to take place in 1 hour, therefore the mixture was stirred at room temperature during this time. Afterwards the base ($KOBu^t$) and the substrate (acetophenone) were added in a 6:400 ratio with respect to the catalyst. The crude mixture was stirred at room temperature and the catalytic process was checked every 30 min.[31] With the $Ru(DMSO)_4Cl_2$, $RuCl_2(PPh_3)_3$ and $[Ru(cod)Cl_2]_x$ precursors no activity was found in any case, even under refluxing conditions. Therefore the studies were concentrated on the $[Ru(p\text{-cymene})Cl_2]_2$ and the $[Ru(MeCN)_4Cl_2]$ as Ru source.

Fig. **4.27** shows the time *vs* conversion plot for the ATH of acetophenone with ligand **4.29** and the $[Ru(p\text{-cymene})Cl_2]_2$ dimer. The control experiment where the ruthenium precursor was used as the catalyst showed some activity (entry **1**) meaning that the precursor is able to induce activity in the transfer process. However the recorded activity was very low even after increasing the temperature. With the catalyst formed by the ligand and the ruthenium precursor more activity was recorded at room temperature compared to the metal precursor on its own, being the equilibrium reached after 60 hours at room temperature. An overall decrease of 20% in the reaction time was observed if the temperature was raised to 55°C. Under reflux conditions the equilibrium was reached after only 24 h. In all cases no enantioselectivities were detected during the process being the 1-phenylethanol obtained always as a racemic mixture.

Table 4.3. Catalytic results of ligand **4.29** in ATH using Ru_{cymene}.

ENTRY	CATALYST	Time (h)	Conversion (%)
1	Ru_{cymene}	**24**	**5**
2	Ru_{cymene} – **4.29**	**2**	**2**
3	Ru_{cymene} – **4.29**	**12**	**10**
4	Ru_{cymene} – **4.29**	**24**	**30**
5	Ru_{cymene} – **4.29**	**48**	**45**
6	Ru_{cymene} – **4.29**	**60**	**50**

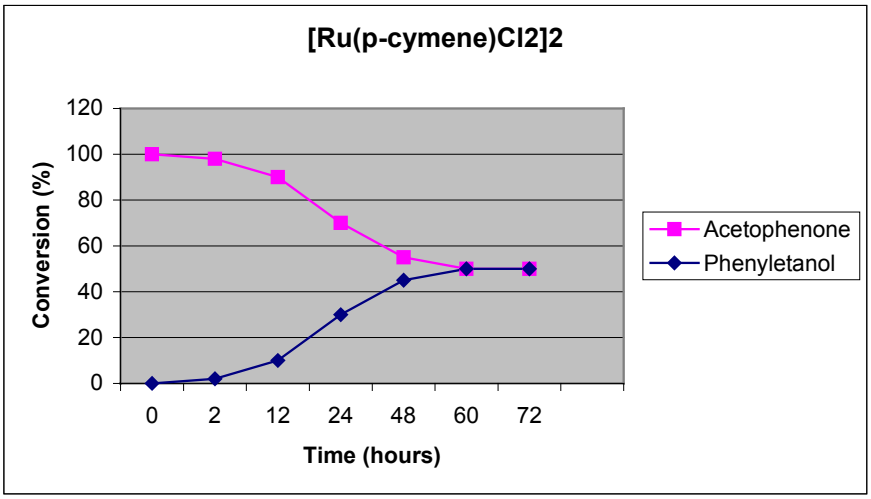

Fig. 4.27. *Catalytic results using for lig* **4.29** *and* Ru_{cymene}.

The catalyst formed by **4.29** and $Ru(MeCN)_4Cl_2$ showed a slightly lower activity as summarised in the Fig. **4.28**. The metal precursor on its own did not catalyse the reaction at all this time (entry **1**). Ligand **4.29** was found again to accelerate the reaction but no enantioselectivities were detected in the phenylethanol product. By increasing the temperature, the reaction times were again reduced by 20% as observed before.

Table 4.4. Catalytic results of ligand **4.29** in ATH using Ru_{MeCN}.

ENTRY	CATALYST	Time (h)	Conversion (%)
1	Ru_{MeCN}	**24**	**0**
2	Ru_{MeCN} – **4.29**	**2**	**1**
3	Ru_{MeCN} – **4.29**	**12**	**8**
4	Ru_{MeCN} – **4.29**	**24**	**25**
5	Ru_{MeCN} – **4.29**	**48**	**38**
6	Ru_{MeCN} – **4.29**	**60**	**50**

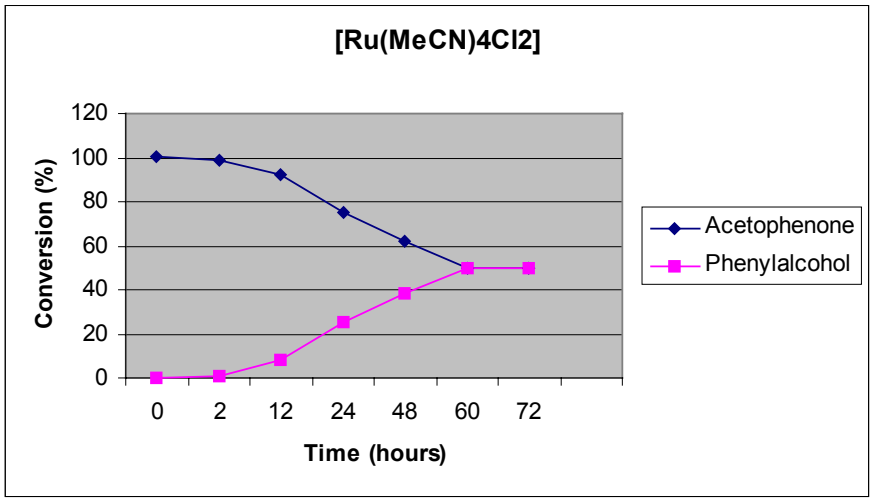

Fig. 4.28. *Catalytic results using for lig* **4.29** *and* Ru_{MeCN}.

4.8 CONCLUSIONS

This preliminary catalytic testing shows that the system composed by the ligand **4.29** and the ruthenium precursors Ru_{MeCN} and Ru_{pcym} present almost no activity in the transfer hydrogenation of ketones. Ligand **4.29** is not a good chiral inductor for the asymmetric transfer hydrogenation of ketones, the phenyethanol being always detected as a racemic mixture. Further work is required to complete this study, but unfortunately the time available was insufficient to undertake the

necessary experiments. Some of the issues which still need to be addressed are discussed next.

During the process, IPA is oxidised to acetone, therefore the reduction of ketones by IPA is a reversible process where the equilibrium is regulated by the oxidation potentials of the relevant carbinol/ketone couples. To shift the equilibrium, IPA is used not only as reactant, but also as a solvent. The reversibility of the reaction is one of the biggest drawbacks in the use of IPA and it is also known to be an important factor for racemisation to occur.[33] The mixture Et_3N / formic acid would avoid this reversibility because the use of this mixture as the hydride source forms CO_2 as the by-product thus making the process irreversible.

Regarding the base used, its role is to deprotonate the IPA and also to facilitate the formation of the ruthenium hydride species upon removal of the chloride from the metal centre. It would also be possible that this base is strong enough to deprotonate the ligand α-methylbenzyl groups leading to the catalyst decomposition. A screening of different bases like Et_3N or KOH would also give information in this regard. Another reason for the absence of enantioselectivity in the process could be due to coordination of the tripodal ligand to the metal centre blocking all the coordination positions. For [Ru(*p*-cymene)Cl_2]$_2$, it has been discussed in Chapter III that the ligand coordinates facially to the metal occupying three coordination sites whilst the arene moiety coordinates the remaining three. This saturated 18 electron complex does not present any free coordination site. Decoordination of either the *p*-cymene or the Tm ligand would therefore be required for activity to be observed.

Changes in the hapticity of the arene moiety are known to occur during the ATH process.[34] It is possible that the bulk of the α-methylbenzyl groups hinders the necessary processes at the metal centre, and that upon heating, new active species are formed in a system that does not contain the chiral ligand. The presence of significant steric hindrance at the metal centre is supported by the Ru-S bond lengths observed in the ruthenium complex **4.30** when compared with those in complexes

with less bulky Tm ligands (Chapter III). There is, however, no experimental evidence to confirm that the coordination behaviour of the ligand remains unchanged during the catalytic experiments.

In the complex of ligand **4.29** with $Ru(MeCN)_4Cl_2$, tripodal coordination of the ligand leaves two positions occupied by chloride, and a third one with an acetonitrile ligand. Due to the symmetry of the ligand these three positions are equivalent and certain enantioselectivity was expected. The fact that similar results to those obtained with $[Ru(p\text{-cymene})Cl_2]_2$ were found suggests the existence of an active catalytic species where the ligand is not able to induce any enantioselectivity to the process. Comparing the results obtained with the control experiments where only Ru_{pcym} or Ru_{MeCN} were used as the catalyst (Entries 1 in both Tables **4.3** and **4.4**), it seems that the ligand **4.29** is however, playing some role in the process accelerating the hydrogen transfer. To identify the active catalytic species a more detailed study must be undertaken.

Upon heating, decoordination of one of the ligand arms could also take place leaving a free position for the substrate to coordinate to the metal centre, or for the metal hydride to be formed. The hemi-lability of one of the ligands donor groups has been observed during the racemisation of Tm complexes of tetrahedral metals [Cu(I), Zn(II), Cd(II)], but the tendency for this to occur is expected to be less for the substitutionally inert Ru(II).[5] As discussed in the previous chapter, racemisation of the ligand will not occur due to unfavourable interactions between both the central metal-ligand cage and the α-methylbenzyl groups. Such twisting of the bicyclo[3.3.3]-cage structure would represent interconversion between diastereomers, and therefore not only is there a substantial barrier to this process, but the two forms will be of different energy.

Interestingly, examples where this type of ligand hemi-lability process has been demonstrated to be effective in catalysis was recently reported by Gade and coworkers in the asymmetric Mannich reaction of *β*-ketoesters catalysed by Cu(II).[35] (Scheme **4.16**.)

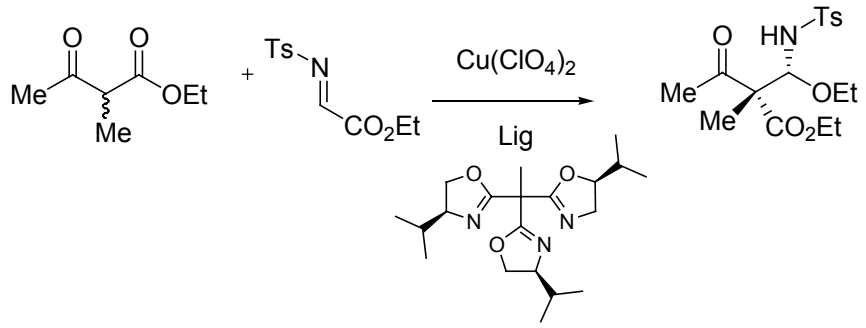

Scheme 4.16. *Asymmetric Mannich reaction catalysed by Cu(II).*

High catalytic loadings were generally needed for this reaction due to the kinetic lability of Cu(II). A C_3-symmetric tripodal ligand that stabilises the resting state of the catalyst has proved to be effective in reducing the catalyst loadings. The transformation into the active 17 electron species that requires the decoordination of one ligand arm, is provided stereoelectronically by the strong dynamic Jahn-Teller effect of the d^9-Cu(II) centre. As a consequence of the C_3-symmetry of the ligand, all three possible dicoordinated active species are homotopic and equivalent, therefore the enantioselectivities obtained in the process were very high.

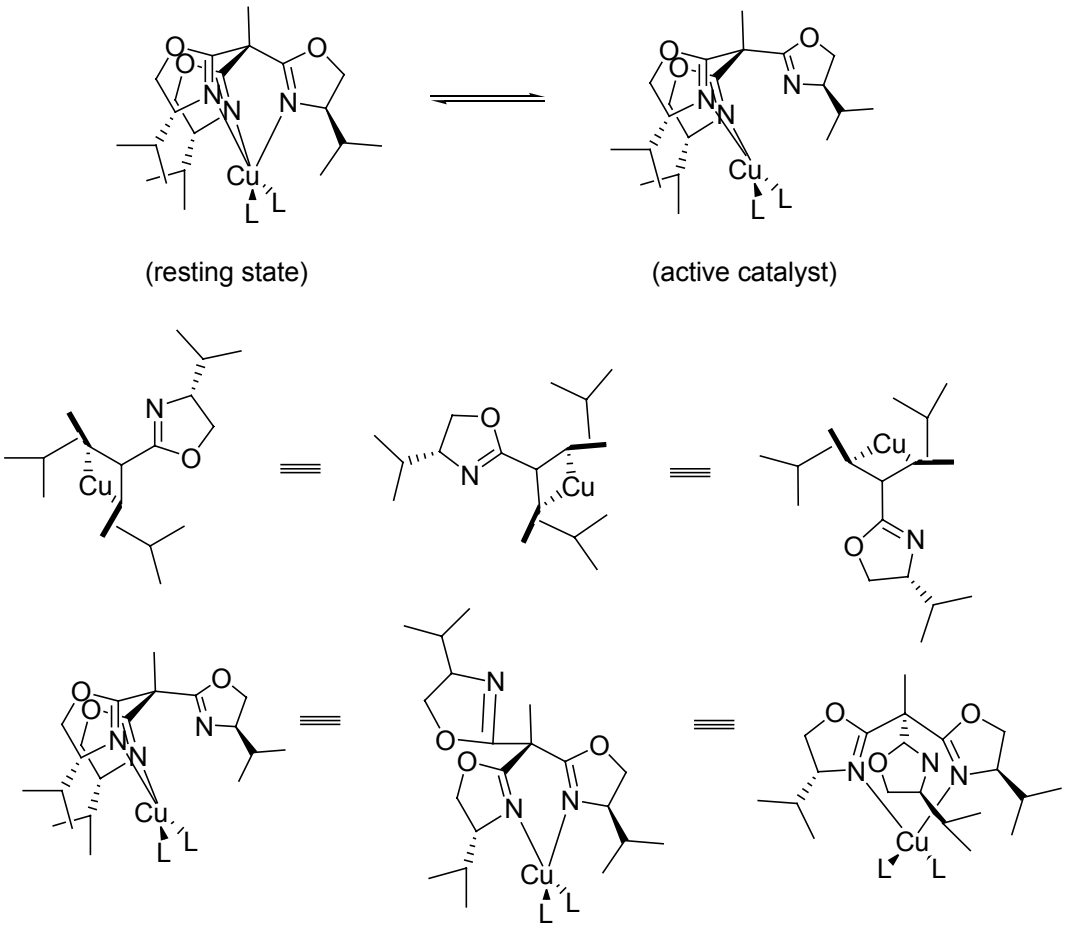

Fig. 4.29. *Coordination/decoordination between the active and the resting state proceed through equivalent intermediate geometries.*

4.9 REFERENCES CHAPTER IV

1. E. N. Jacobsen, A. Pfaltz, H. Yamamoto, (Eds.); *Comprehensive Asymmetric Catalysis,* Springer, New York; 1999.
2. J. K. Whitesell, *Chem .Rev.,* 1989, **89**, 1581.
3. C. Moberg, *Angew. Chem. Int. Ed.,* 1998, **37**, 248.
4. M. Garner, A. R. Kennedy, J. Reglinski, M. D. Spicer, *J. Chem. Soc. Chem. Commun.,* 1996, 1975.
5. P. J. Bailey, A. Dawson, C. McCormack, S. Moggach, I. Oswald, S. Parsons, D. Rankin, A, Turner, *Inorg. Chem.,* 2005, **44**, 8884.
6. R. R. Ernst, G. Bodenhausen, A. Wokaun, *Principles of Nuclear Magnetic Spectroscopy in One and Two Dimensions*; Clarenden Press, Oxford, U.K. 1987.
7. A. Pfaltz, *Proc. Natl. Acad. Sci. USA,* 2004, **101**, 5723.
8. W. R. Leonard, J. L. Romine, A. I. Meyers, *J. Org. Chem.,* 1991, **56**, 1961.
9. J. Tweddell, D. A. Hoic, G. Fu. *J. Org. Chem.,* 1997, **62**, 8286.
10. Y. Hsiao, L. S. Hegedus, *J. Org. Chem.,* 1997, **62**, 3586.
11. N. A. Boland, M. Casey, S. J. Hynes, J. W. Matthews, M. P. Smyth. *J. Org. Chem.,* 2002, **67**, 3919.
12. V. B. Birman, X. Li, *Org. Lett.,* 2006, **8**, 1351.
13. R. G. Jones, E. C. Kornfeld, K. C. McLaughlin, R. C. Anderson, *J. Am. Chem. Soc.,* 1949, **71**, 4000.
14. J. F. Ojo, P. A. Slavin, J. Reglinsky, M. Garner, M. D. Spicer, A. R. Kennedy, S. J. Teat, *Inorg. Chim. Acta,* 2001, **313**, 15.
15. M. T. Crimmins, A. C. DeBaillie, *J. Am. Chem. Soc.,* 2006, **128**, 4936.
16. A. Ortiz, L. Quintero, G. Mendoza, S. Bernés, *Tetrahedron. Lett.,* 2003, **44**, 5053.
17. J. Lacour, V. Hebbe-Viton, *Chem. Soc. Rev.,* 2003, **32**, 373.
18. R. Frantz, A. Pinto, S. Constant, G. Bernadielli, J. Lacour, *Angew. Chem. Int. Ed.,* 2005, **44**, 5060.
19. J. Lacour, C. Goujon-Ginglinger, S. Torche-Haldimann, J. J. Jodry, *Angew. Chem. Int. Ed.,* 2000, **39**, 3695.
20. J. Lacour, S. Torche-Haldimann, J. J. Jodry, C. Ginglinger, F. Favarger, *Chem. Commun.,* 1998, 1733.

21. L. Mimassi, C. Guyard, M. Noelle, H. Amouri. *Inorg. Chem.,* 2004, **43**, 6644.
22. M. J. Fazio, *J. Org. Chem.,* 1984, **49**, 4889.
23. P. J. Bailey, C. McCormack, S. Parsons, F. Rudolphi, A. Sanchez Perucha, P. Wood, *Dalton Trans.* 2007, 476.
24. G. Zassinovich, G. Mestroni, *Chem. Rev.,* 1992, **92**, 1051.
25. J. S. M. Samec, J. E. Bäckvall, P. G. Andersson, P. Brandt, *Coord. Chem. Rev.,* 2006, **35**, 237.
26. W. Ponndorf, *Angew. Chem.,* 1925, **39**, 138.
27. Y. Sasson, J. Blum, *Tetrahedron. Lett.,* 1971, 2167.
28. R. Howdhury, J. E. Bäckvall, *J. Chem. Soc., Chem. Commun.,* 1991, 1063.
29. http://nobelprize.org/nobel_prizes/chemistry/laureates/2001/noyori-lecture.html
30. R. Noyori, S. Hashiguchi, *Acc. Chem. Res.,* 1997, **30**, 97.
31. M. Hayes, D. J. Morris, G. J. Clarkson, M. Wills, *J. Am. Chem. Soc.,* 2005, **127**, 7318.
32. The conditions were optimised for trisoxazoline ligands by Dr. Caipa at the Eindhoven University
33. P. Jessop, T. Ikariya, R. Noyori, *Chem. Rev.,* 1995, **95**, 259.
34. A. Habib, R. S. Tanke, E. M. Holt, R. H. Crabtree, *Organometallics*, 1989, **8**, 225.
35. C. Foltz, B. Stecker, G. Marconi, S. Bellemin-Laponnaz, H. Wadepohl, L. H. Gade, *Chem. Commun.,* 2005, 5115.

CHAPTER V

EXPERIMENTAL PART

EXPERIMENTAL PART

General. All reactions were carried out under an atmosphere of dry, oxygen-free dinitrogen, using standard Schlenk techniques. Solvents were freshly distilled over an appropriate drying agent and further degassed before use where necessary. Mass spectra were recorded on Kratos MS50TC (FAB) and Micromass Platform II (ES-MS) spectrometers. NMR spectra were recorded on a Bruker 250AC spectrometer operating at room temperature. ^{1}H and ^{13}C chemical shifts are reported in ppm relative to $SiMe_4$ ($\delta = 0$) and were referenced internally with respect to the protic solvent impurity or the ^{13}C resonances respectively. Multiplicities and peak types are abbreviated: singlet, s; doublet, d; triplet, t; multiplet, m; broad, br; aromatic, ar. All chemicals were obtained from Sigma-Aldrich and used as received. $B(NMe_2)_3$ was used as received and stored under nitrogen atmosphere. [(1,8-diazabicyclo[5.4.0]undec-7-ene) (DBU) was used as received and stored under nitrogen. *N*-methylimidazole was dried over sodium, distilled under vacuum and stored under nitrogen. Pyrazole and imidazole were sublimed under vacuum prior to use and stored under nitrogen. KBH_4 was dried under vacuum during 12 hours and stored under nitrogen. $[Ru(p\text{-cymene})Cl_2]_2$, $[Mn(CO)_3(MeCN)_3]PF_6$, were prepared according to the literature procedures.[1,2] The oxazolines were prepared using the protocol reported by Meyers and coworkers.[3] The imidazoline was prepared following the route reported by Casey and coworkers.[4] TRISPHAT was synthesised following the experimental procedure reported by Lacour and coworkers.[5]

EXPERIMENTAL PART CHAPTER II

$[(HNMe_2)B(methimazolyl)_3]$ (2.2).

In a dry two-neck flask adapted with a reflux condenser, methimazole (0.978 g, 8.57 mmol) was suspended under nitrogen in 10 ml of benzene. To the mixture was added $B(NMe_2)_3$ (500 μl, 2.86 mmol) at room temperature in one portion and the mixture was set to reflux for 2h. During reflux a clear solution was first obtained (after a few minutes) followed by precipitation with time (approximately after 20 min). After 2h the reaction was cooled to room temperature and the solvent was filtrated by cannula leaving a colourless solid which was characterised as **2.2** (0.927 g, 2.14 mmol, 82%).

Crystals for X-ray were obtained by dissolving a small amount of the product in hot benzene and allowing the solution to slowly cool to room temperature.
^{1}H-NMR (250.1 MHz, $CDCl_3$), δ: 9.72 (br, 1H); 6.52 – 6.62 (m, 3H), 6.36 (s, 3H), 3.48 (s, 15H), ^{13}C-NMR (62.9 MHz, $CDCl_3$), δ: 165.4 (C=S), 120.6 (CH), 117.4 (CH), 34.9 (CH_3), 34.7 (CH_3); MS (FAB+) *m/z* = 396 (M^{+1}); Anal. Calcd. for $C_{14}H_{22}BN_7S_3 \cdot C_6H_6$: C, 50.73; H, 5.96; N, 20.71. Found: C, 50.67; H, 5.94; N, 20.79.

H[B(2-methylimidazolyl)$_4$] (2.10).

2-methylimidazole (0.703 g, 8.57 mmol) was added to a solution of $B(NMe_2)_3$ (500 μl, 2.86 mmol) in toluene (10 ml) and heated to reflux. The reaction was monitorized by mass spectrometry and after 8 h ions due to the reactants were absent. The solvent was removed under vacuum and the product washed twice with 10 ml of dry hexane and dried to give **2.10** (0.720 g, 2.14 mmol, 75%) as a colourless crystalline solid.
^{1}H-NMR: (250.1 MHz, CD_3OD), δ: 7.23 (d, 4H), 6.92 (d, 4H), 1.99 (s, 12H); ^{13}C-NMR (62.9 MHz, CD_3OD), δ: 147.53 (C_{quat}), 124.25 (4- or 5- CH), 121.88 (4- or 5- CH), 12.45 (CH_3); MS (ES +25 eV) *m/z* = 335 (M^+-H); Anal. Calcd. for $C_{16}H_{21}N_8B$: C, 57.15; H, 6.29; N, 33.32. Found: C, 56.97; H, 6.15; N, 33.04.

H[B(imidazolyl)$_4$] (2.12).

Freshly sublimed imidazole (0.585 g, 8.6 mmol) was added to a solution of $B(NMe_2)_3$ (500 μl, 2.86 mmol) in toluene (10 ml) and heated to reflux. After 8h the precipitated white powder was isolated by filtration. The crude product was purified by dissolving in the minimum amount of methanol followed by dropwise addition of ether until precipitation commenced and storage at -20°C. The product was filtered via cannula and the solid dried under vacuum to give **2.12** (0.60 g, 2.15 mmol, 75%) as a white powder. Spectroscopic data were consistent with the literature values.
^{1}H-NMR (250.1 MHz, $CDCl_3$), δ: 7.04 (s, 1H), 6.93 (d, 1H), 6.78 (d, 1H); MS (FAB+) *m/z* = 280.9 (M^{+1}).

H[B(benzimidazolyl)$_4$] (2.13).

Benzimidazole (1.01 g, 8.57 mmol) was added to a solution of $B(NMe_2)_3$ (500 μl, 2.86 mmol) in toluene (10 ml) and heated to reflux. Mass spectrometry indicated that the reaction was complete after 5h and the solvent was then removed under vacuum. The crude product was purified by dissolving it in the minimum amount of methanol and dropwise addition of ether until precipitation commenced, followed by storage at -20°C. The white solid product was filtered via cannula and dried under vacuum to give **2.13** (0.70 g, 1.45 mmol, 51%). A sample of the product was recrystallised by slow diffusion of pentane into a methanol solution to produce a crystal suitable for X-ray crystallography.

^{1}H-NMR (250.1 MHz, $CDCl_3$), δ: 7.73 (s, 1H), 7.64 (d, 1H), 7.09 (t, 1H), 6.90 (t, 1H), 6.57 (d, 1H); ^{13}C-NMR (62.9 MHz, $CDCl_3$), δ: 145.7 (C_{quat}), 144.6 (C_{quat}), 136.4 (CH), 121.8 (CH), 120.9 (CH), 118.9 (CH), 112.3 (CH); MS (FAB+) *m/z* = 479 (M^{+1}); Anal. Calcd. for $C_{28}H_{21}BN_8$ 0.5·C_5H_{12}·0.5·CH_3OH.; C, 69.93; H, 5.49; N, 21.04. Found: C, 69.89; H, 5.45; N, 21.09.

(2-chloroimidazole) (2.14).

1-tritylimidazole (2.0 g, 6.14 mmol) was mixed in a 250 ml Schlenk with 70 ml of dry THF. The suspension was stirred and cooled down to –78ºC. BuLi (4.9 ml, 3.06 mmol) was added dropwise over 15 min and the mixture stirred at this temperature for two hours. The pale yellow suspension turned to deep red once the deprotonation took place. After this time hexachloroethane (3.0 g, 12.28 mmol) was added in slow portions and the mixture stirred overnight. The reaction was quenched with saturated NH_4OH solution and extracted with ether. The organic phase was decanted and dried over $MgSO_4$ and the solvent reduced to yield a pale brown solid. This solid was dissolved in 5% of MeOH/AcOH (50 ml) and the mixture was refluxed for 30 min. After this time the solvent was reduced under vacuum and the solid recrystallised from ether three times to give **2.14** (0.426 g, 4.17 mmol, 68 %) as a colourless solid.

^{1}H-NMR (250.1 MHz, $CDCl_3$), δ: 7.39 (s, 2H); ^{13}C-NMR (62.9 MHz, $CDCl_3$), δ: 145.10 (C-Cl), 122.05 (CH); 120.87 (CH); MS (EI +25eV) *m/z* = 102.9 (M^{+1}); Anal. Calcd. $C_3H_3N_2Cl$; C, 35.15; H, 2.95; N, 27.32. Found: C, 34.92; H, 3.10; N, 28.63.

H[B(2-chloroimidazolyl)$_4$] (2.15).

2-chloroimidazole (0.878 g, 8.57 mmol) was added to a solution of $B(NMe_2)_3$ (500 µl, 2.86 mmol) in toluene (10 ml) and heated to reflux. After 1h mass spectrometry indicated that the reaction was complete. Half of the solvent was removed under vacuum precipitating a white solid which is filtered via cannula and washed twice with dry hexane and dried to give **2.15** (0.693 g, 1.66 mmol, 58%) as a white solid.
^{1}H-NMR (250.1 MHz, $CDCl_3$), δ: 6.84 (s, 1H), 6.63 (s, 1H); ^{13}C-NMR (62.9 MHz, $CDCl_3$), δ: 138.2 (C-Cl), 133.01 (CH); 129.92 (CH); MS (EI +25eV) *m/z* = 418.8 (M^{+1}); Anal. Calcd. $C_{12}H_9BN_8Cl_4 \cdot 3H_2O$; C, 34.87; H, 3.29; N, 25.42. Found: C, 34.82; H, 3.40; N, 25.63.

[(N-methylimidazole)B(methimazolyl)$_3$] (2.17).

Tris(dimethylamino)borane (128 µl, 0.73 mmol), *N*-methylimidazole (58 µl, 0.73 mmol) and methimazole (0.250 g, 2.20 mmol) were refluxed in toluene (5 ml) under nitrogen. After 3 h a colourless solid precipitated which was washed twice with dry hexane (10 ml) and dried under vacuum to yield **2.17** (0.280 g, 0.64 mmol, 88%).
^{1}H-NMR (250.1 MHz, $CDCl_3$), δ: 8.97 (s, 1H), 7.19 (s, 1H), 6.95 (s, 1H), 6.61-6.65 (m, 6H), 3.81 (s, 3H), 3.49 (s, 9H); ^{13}C-NMR (62.9 MHz, $CDCl_3$), δ: 164.70 (C=S); 142.66 (CH_{Imi}), 124.59 (CH_{Met}), 121.63 (CH_{Imi}), 117.94 (CH_{Met}), 114.36 (CH_{Imi}), 36.05 (CH_{3Imi}), 35.10 (CH_{3Met}); ^{11}B-NMR (80.3 MHz, $CDCl_3$), δ: 8.05; MS (EI +25eV) *m/z* = 433 (M^{+1}); Anal. Calcd. for $C_{16}H_{21}BN_8S_3 \cdot C_7H_8$; C, 52.66; H, 5.57; N, 21.36. Found: C, 52.57; H, 5.52; N, 21.39.

[(4-methoxypyridine)B(methimazolyl)$_3$] (2.18).

4-methoxypyridine (156 ml, 1.43 mmol), tris(dimethylamino)borane (250 ml, 1.43 mmol) and methimazole (0.444 g, 3.90 mmol) were refluxed in 10 ml of dry toluene. After 8h the reaction finished by precipitation of the adduct **2.18** as a colourless solid (0.506 g, 1.10 mmol, 85%).
^{1}H-NMR (250.1 MHz, $CDCl_3$), δ: 8.62 (br, 2H), 7.01 (t, 1H, J= 1.56 Hz), 6.97 (t, 1H, J= 1.56 Hz), 6.78 (br, 3H), 6.61 (d, 3H, J=2.34 Hz), 3.95 (s, 3H), 3.47 (s, 9H); ^{13}C-NMR

(62.9 MHz, $CDCl_3$), δ: 170.66 (C=S), 165.93 (C_{quat}), 147.99 (CH), 128.61 (CH), 118.16 (CH), 110.23 (CH), 57.26 (CH_3), 35.25 (CH_3); ^{11}B-NMR (80.3 MHz, $CDCl_3$), δ: 5.43; MS (EI +25eV) *m/z* = 459.88 (M^{+1}); Anal. Calcd. for $C_{18}H_{22}BN_7OS_3$; C, 47.06; H, 4,83; N, 21.34. Found: C, 46.87; H, 4,60; N, 21.69.

[(4-dimethylaminopyridine)B(methimazolyl)$_3$] (2.19).

4-dimethylaminopyridine (0.175 g, 1.42 mmol), tris(dimethylamino)borane (250 μl, 1.42 mmol) and methimazole (0.444 g, 3.90 mmol) were refluxed in 10 ml of dry toluene for 6h leading to precipitation of a colourless solid. The solution was cooled to room temperature and the solid was filtered and washed twice with dry ether (5 ml) and dried in vacuum to yield **2.19** (0.583 g, 1.23 mmol, 87%) as a colourless solid.
^{1}H-NMR (250.1 MHz, $CDCl_3$), δ: 8.12 (br, 2H), 6.59 (d, 3H, J= 2.34 Hz), 6.54 (t, 1H, J= 1.43 Hz), 6.51 (t, 1H, J= 1.43 Hz), 3.48 (s, 9H), 3.09 (s, 6H); ^{13}C-NMR (62.9 MHz, $CDCl_3$), δ: 165.77 (C=S), 156.70 (C_{quat}), 146.56 (CH), 123.10 (CH), 117.85 (CH), 105.86 (CH), 40.11 (CH_3), 35.21 (CH_3); ^{11}B-NMR (80.3 MHz, $CDCl_3$), δ: 5.08; MS (EI +25eV) *m/z* = 473.04 (M^{+1}); Anal. Calcd. for $C_{19}H_{25}BN_8S_3$; C, 48.30; H, 5.33; N, 23.72. Found: C, 48.09; H, 5.10; N, 23.91.

[(1,8-diazabicyclo[5.4.0]undec-7-ene)B(methimazolyl)$_3$] (2.20).

1,8-diazabicyclo[5.4.0]undec-7-ene, (218 μl, 1.42 mmol), tris(dimethylamino)borane (250 μl, 1.42 mmol), and methimazole (0.444 g, 3.90 mmol) were mixed together and refluxed for 1h. A colourless solid precipitated from the solution after this time, which was filtered via cannula, washed with Et_2O and recrystallised from hot methanol to yield **2.20** (0.596 g, 1.18 mmol, 92%) as a colourless solid.
^{1}H-NMR (250.1 MHz, DMSO-d_6), δ: 7.10 (d, 3H, J= 2.34Hz), 6.79 (d, 3H, J= 2.34Hz), 4.15 (m, 2H), 3.88 (m, 2H), 3.54 (s, 9H), 2,33 (m, 2H), 1.93 (m, 2H), 1.73 (m, 2H), 1.70 (m, 2H), 1.10 (m, 4H); ^{13}C-NMR (62.9 MHz, DMSO-d_6), δ: 165.70 ($C_{quatDBU}$), 161.35 (C=S); 119.81 (CH_{Met}), 114.59 (CH_{Met}), 55.35 (CH_{2DBU}) 53.71 (CH_{2DBU}) 48.25 (CH_{2DBU}) 33.92 (CH_{Met}), 31.72 (CH_{2DBU}) 28.69 (CH_{2DBU}) 26.41 (CH_{2DBU}) 23.79 (CH_{2DBU}) 19.38 (CH_{2DBU}); ^{11}B-NMR (80.3 MHz, DMSO-d_6), δ: 7.57; MS (EI +25eV)

m/z = 503.05 (M^{+1}), 389.07 (M-het); Anal. Calcd. for $C_{21}H_{31}BN_8S_3B \cdot MeOH$; C, 49.43; H, 6.60; N, 20.96. Found: C, 49.22; H, 6.42; N, 21.54.

[(N-methylimidazole)B(pyrazolyl)$_3$] (2.21).

N-methylimidazole, (118 µl, 1.43 mmol), tris(dimethylamino)borane (250 µl, 1.43 mmol), and pyrazole (0.290 g, 4.26 mmol) were mixed together in 10 ml of dry toluene and refluxed for five hours. After this time the solvent was removed under vacuum. 10 ml of dry ether were added and the mixture stirred for 30 min. After this time the resulting colourless solid was isolated and dried under vacuum to yield **2.21** (0.232 g, 0.78 mmol, 92%) as a colourless solid.

^{1}H-NMR (250.1 MHz, $CDCl_3$), δ: 8.52 (s, 1H), 7.65 (dd, 3H, J= 1.56Hz, J= 0.51Hz), 7.48 (t 1H, J= 1.53Hz), 6.88 (dd, 3H, J= 2.34Hz, J= 0.51Hz), 6.85 (t 1H, J= 1.53Hz), 6.17 (dd, 3H, J= 2.34Hz, 1.56Hz), 3.68 (s, 3H); ^{13}C-NMR (62.9 MHz, $CDCl_3$), δ:140.85 (CH_{Imi}), 137.43 (CH_{Imi}); 133.63 (CH_{Imi}), 125.48 (CH_{Pyr}), 119.55 (CH_{Pyr}), 104.10 (CH_{Pyr}), 34.44 (CH_{Imi}); ^{11}B-NMR (80.3 MHz, $CDCl_3$), δ: 3.76; MS (EI +25eV) *m/z* = 295.13 (M^{+1}); Anal. Calcd. for $C_{13}H_{15}N_8B$; C, 53.09; H, 5.14; N, 38.10. Found: C, 53.24; H, 5.03; N, 38.29.

[(N-methylimidazole)B(1-phenyl-4-imidazoline-2-one)]$_3$ (2.22).

N-methylimidazole (47µl, 0.57mmol), tris(dimethylamino)borane (100µl, 0.57mmol) and 1-phenyl-4-imidazoline-2-one (0.251 g, 1.56mmol) are refluxed together in 10 ml of toluene. After 3h a colourless solid precipitated which was filtered, washed twice with 5 ml of dry Et_2O and dried under vacuum to yield **2.22** (0.276 g, 0.48 mmol, 85%) as a colourless solid. The product is remarkably insoluble in most solvents so it was characterized by elementary analysis and FAB-NOM. Anal. Calcd. for $C_{31}H_{27}N_8O_3B$; C, 65.27; H, 4.77; N, 19.64. Found: C, 64.93; H, 5.00; N, 19.41; (FAB+) *m/z* = 571 (M^{+1}).

[(N-methylimidazole)B(1-ethyl-4-imidazoline-2-one)]$_3$ (2.23).

N-methylimidazole (47µl, 0.57mmol), tris(dimethylamino)borane (100µl, 0.57mmol) and 1-ethyl-4-imidazoline-2-one (0.193 g, 1.71mmol) were refluxed together in toluene (10 ml). After 3h no peaks due to starting materials were detected by mass spectrometry and the solvent was half removed. Dry ether (10 ml) was added and the mixture stored in the fridge at 5^0C overnight. The solid precipitated was filtered out, washed twice with 5 ml of dry Et_2O and dried under vacuum to yield **2.23** (0.217 g, 0.51 mmol, 89%) as a pale beige solid.

^{1}H-NMR (250.1 MHz, $CDCl_3$), δ: 9.14 (s, 1H), 7.77 (d, 1H, J= 1.69Hz), 6.76 (d, 1H, J= 1.69Hz), 6.13 (d, 3H, J= 2.86 Hz), 5.69 (d, 3H, J= 2.86 Hz), 3.66 (s, 3H), 3.55 (q, 6H, J= 7.43Hz), 1.17 (t, 9H, J= 7.43Hz); ^{13}C-NMR (62.9 MHz, $CDCl_3$), δ: 156.21 (C=O), 140.15 (CH_{Imi}); 127.90 (CH_{Imi}), 119.37 (CH_{Imi}), 112.93 (CH_{Het}), 110.59 (CH_{Het}), 37.90 (CH_{Het}), 35.71 (CH_{Imi}), 15.19 (CH_{Het}); ^{11}B-NMR (80.3 MHz, $CDCl_3$), δ: 3.87; MS (EI +25eV) *m/z* = 427.08 (M^{+1}); Compound highly hygroscopic.

Imidazabole (2.24).

Tris(dimethylamino)borane (100 µl, 0.57 mmol) and 1-phenyl-4-imidazoline-2-one (0.251 g, 1.56 mmol) were refluxed together in 10 ml of toluene. After 2h a colourless solid precipitated which was filtered, washed twice with 5 ml of dry Et_2O and dried under vacuum to yield **2.24** (0.276 g, 0.48 mmol, 85%) as a colourless solid.

^{1}H-NMR (250.1 MHz, $CDCl_3$), δ: 7.45 (dd, 12H, J = 8.43Hz, J = 1.23Hz), 7.28 (dd, 12H, J = 8.43Hz, J = 7.59Hz), 7.12 (dt, 6H, J = 7.59Hz, J = 1.23Hz), 6.67 (d, 6H, J= 2.57Hz), 6.38 (d, 6H, J= 2.57Hz); ^{13}C-NMR (62.9 MHz, $CDCl_3$), δ: 154.25 (C=O), 147.63 (C=O), 138.06 (C_{quat}); 134.77 (C_{quat}), 129.61 (CH), 129.19 (CH), 128.54 (CH), 125.11 (CH), 123.61 (CH), 122.35 (CH), 121.38 (CH), 115.23 (CH), 113.31 (CH), 110.27 (CH); ^{11}B-NMR (80.3 MHz, $CDCl_3$), δ: 3.75; MS (EI +25eV) *m/z* = 977 (M^{+1}), 816(M^{+1}-het); Anal. Calcd. for $C_{58}H_{54}N_{12}O_6B_2$; C, 67.19; H, 5.25; N, 16.21. Found: C, 66.87; H, 5.09; N, 16.43.

$(NHMe_2)B(2\text{-phenylimidazolin-2-one})_3$ (2.27).

2-phenylimidazolin-2-one (0.500 g, 3.12 mmol) was dissolved in dry toluene (10 ml). $B(NMe_2)_3$ (182 µl, 1.04 mmol) was added and the mixture heated at 100°C for two hours. After this time heating was discontinued and the volume reduced to half under vacuum. Dry ether (20 ml) was added and the flask stored in the fridge overnight. Small crystals were formed which were collected by filtration and dried under vacuum to yield **2.27**. (0.43 g, 0.80 mmol, 78%).
^{1}H-NMR (250.1 MHz, $CDCl_3$), δ: 8.62 (br, 1H), 7.69 (dd, 6H, J = 7.59Hz, J = 1.31Hz), 7.44 (dt, 6H, J = 8.58Hz, J = 7.59Hz), 7.25 (dt, 3H, J = 8.58Hz, J = 1.31Hz), 6.69 (d, 3H, J= 2.97Hz), 6.41 (d, 3H, J= 2.97Hz), 2.89 (s, 6H); ^{13}C-NMR (62.9 MHz, $CDCl_3$), δ: 156.15 (C=O), 138.41 (C_{quat}) 130.08 (CH), 126.52 (CH), 122.60 (CH), 115.02 (CH), 112.13 (CH), 41.09 (CH_3); ^{11}B-NMR (80.3 MHz, $CDCl_3$), δ: 3.55; MS (EI +25eV): *m/z* = 533.9 (M^{+1}); Anal. Calcd. for $C_{29}H_{28}N_7O_3B$; C, 65.30; H, 5.29; N, 18.38. Found: C, 66.17; H, 5.09; N, 18.55.

EXPERIMENTAL PART CHAPTER III

$[MnBr(CO)_5]$

To a solution of $[Mn_2(CO)_{10}]$ (2.00 g, 5.13 mmol) in dichloromethane (50 ml) was added a solution of bromine (0.26 ml, 5.13 mmol) in dichloromethane (20 ml). This solution was added dropwise over 30 min. The solution was stirred for 1h and then filtered. Dichloromethane was added to the filtrate to redissolve any precipitated product. Hexane was added (100 ml) and the volume of solution reduced to approximatelly 30 ml. The solid which precipitated was isolated by filtration, washed with cold pentane (20 ml) and dried under vacuum. (Yield 2.13 g, 76%) Analytical data are in agreement with literature values.

$[Mn(CO)_3(MeCN)_3]PF_6$

A solution of $[MnBr(CO)_5]$ (0.879 g 3.20 mmol) in acetonitrile (10 ml) was heated under reflux for 1 h. Upon cooling the solution was filtered and the volume of the filtrate reduced by half. A hot solution of ammonium hexafluorophosphate (0.527 g,

3.23 mmol) in an equimolar mixture of water and ethanol (10 ml) was added and the solution left in the freezer overnight. A small amount of product was collected by filtration. The filtrate was treated with water and the resulting crystals were collected by filtration. (Yield 1.03 g, 79%) Analytical data are in agreement with literature values.

$[Ru(\eta^6\text{-}p\text{-cymene})Cl_2]_2$

To a solution of ruthenium trichloride trihydrate (3.00 g, 14.5 mmol) in ethanol (200 ml) was added α-terpinine (25 ml, 85%). The solution was refluxed for 4 h. Upon cooling the crystals which settled were isolated by filtration, washed with cold methanol (30 ml) and dried under vacuum. The volume of the filtrate was reduced by half and the solution refrigerated at –20ºC overnight. The solid which had formed was isolated as with the first crop. (Yield 3.20 g, 72%). Analytical data are in agreement with literature values.

[(N-methylimidazole)B(methimazolyl)$_3$Ru(p-cymene][Cl]$_2$ (3.10).

[Ru(*p*-cymene)Cl_2]$_2$ (0.100 g, 0.16 mmol) and ligand **2.17** (0.141 g, 0.33 mmol) were stirred in dry ethanol (5 ml) overnight. Afterwards, the solution was stirred for 4h at 70°C. The solvent was removed in vacuum to give **3.10** (0.097 g, 0.13 mmol, 82%) as a red-brown solid. Crystals suitable for X-ray analysis were obtained by diffusion of hexane into a solution of the complex in dichloromethane.

^{1}H-NMR (250.1 MHz, DMSO-d_6), δ: 9.31 (s, 1H); 8.11 (d, 1H), 8.03 (d, 1H), 7.82 (d, 3H), 7.27 (d, 3H), 5.84-5.94 (m, 4H), 4.09 (s, 3H); 3.91 (s, 9H), 3.11 (sept, 1H), 2.38 (s, 3H), 1.39 (d, 6H); ^{13}C-NMR (62.9 MHz, DMSO-d_6), δ: 159.51 (C=S); 141.60 (C_{quatAr}), 139.48 (CH_{Imi}), 133.26 (C_{quatAr}), 128.50 (CH_{Ar}), 124.47 (CH_{Imi}), 122.95 (CH_{Imi}), 122.39 (CH_{Met}), 114.28 (CH_{Met}), 106.22 (CH_{Ar}), 95.31 (CH_{iPr}), 40.13 ($CH_{3\ iPr\ or\ Me}$), 39.78 ($CH_{3iPr\ or\ Me}$), 35.47 (CH_{3Imi}), 30.44 (CH_{3Met}); ^{11}B-NMR (80.3 MHz, DMSO-d_6), δ: 3.32; MS (EI +25eV) *m/z* = 334 ($M^{+1}/2$); Anal. Calcd. for $C_{26}H_{35}BN_8S_3Ru{\cdot}Cl_2{\cdot}(CH_2Cl_2)_2{\cdot}H_2O$; C, 36.29; H, 4.46; N, 12.09. Found: C, 37.13; H, 4.79; N, 13.27. Elemental analysis of this compound was hampered by gradual loss of CH_2Cl_2. The crystals used for the analysis were the same as those used in the X-ray analysis. The

calculated analysis for the compound with loss of one mole of CH_2Cl_2 is: C, 38.53; H, 4.67; N, 13.31.

[(N-methylimidazole)B(methimazolyl)$_3$Mn(triscarbonyl)][PF$_6$] (3.11).

Ligand **2.17** (0.100 g, 0.23 mmol) was added in small portions to a solution of $[Mn(CO)_3(MeCN)_3]PF_6$ (0.094 g, 0.23 mmol) in 10 ml of dry MeCN and the mixture was set under reflux for 2 hours providing a yellow solid precipitate. After cooling, the solid was filtered via cannula, washed with 10 ml of dry hexane and dried under high vacuum to yield **3.11** as a yellow solid (0.095 g, 0.17 mmol, 70%).
^{1}H-NMR (250.1 MHz, $CDCl_3$), δ: 8.83 (s, 1H), 7.70 (s, 1H), 7.67 (s, 1H), 7,38 (d, 3H, J= 2.34Hz), 6.82 (d, 3H, J= 2.34Hz), 3.83 (s, 3H), 3.55 (s, 9H); ^{13}C-NMR (62.9 MHz, $CDCl_3$), δ: 209.45 (C=O), 162.67 (C=S), 141.38 (CH_{Imi}); 125.64 (CH_{Imi}), 124.30 (CH_{Met}), 122.57 (CH_{Imi}), 121.54 (CH_{Met}), 40.40 (CH_{3Imi}), 35.06 (CH_{3Met}); ^{11}B-NMR (80.3 MHz, DMSO-d_6), δ: 4.07; MS (EI +25eV) *m/z* = 571.9 (M^{+1}); IR (MeCN solution) = 2007, 1914 cm^{-1}(CO); Anal. Calcd. for $C_{19}H_{21}BN_8S_3O_3MnPF_6$; C, 31.86; H, 2.95; N, 15.64. Found: C, 31.72; H, 2.89; N, 15.70.

[(N-methylimidazole)B(pyrazolyl)$_3$Ru(p-cymene][PF$_6$]$_2$ (3.12).

$[RuCl_2(p\text{-cymene})]_2$ (0.050 g, 0.08 mmol) was dissolved in 10 ml of dry MeCN and stirred at room temperature for 30 min. Ligand **2.21** (0.048 g, 0.16 mmol) was added in small portions and the mixture stirred for 2 hours. After this time the solvent was removed under vacuum and the residue redissolved in 10 ml of dry MeOH. NH_4PF_6 (0.130 g, 0.8 mmol) was added and the mixture stirred for 30 min. After this period the solvent was removed under vacuum. Dry acetone (10 ml) was added to dissolve the complex and separate it from excess NH_4PF_6. Compound **3.12** was obtained upon removal of the solvent under vacuum (0.61 g, 0.07 mmol, 93%). Crystals suitable for X-ray were obtained from a solution of **3.12** in acetone by slow diffusion of Et_2O.
^{1}H-NMR (250.1 MHz, MeCN-d_3), δ: 8.94 (s, 1H), 8.52 (d, 3H, J= 2.58 Hz), 7.81 (s, 2H), 7.54 (d, 3H, J= 2.58 Hz), 6.55 (t, 3H, J= 2.58), 6.17 (d, 2H, J= 6.31Hz), 6.04 (d, 2H, J= 6.31Hz), 4.24 (s, 3H), 3.11 (sept, 1H, J= 6.88Hz), 2.43 (s, 3H), 1.24 (d, 6H, J= 6.88Hz); ^{13}C-NMR (62.9 MHz, MeCN-d_3), δ: 147.52 (CH_{Imi}), 134.95 (CH_{Imi}); 125.05

(CH_{Imi}), 124.74 (CH_{Pyr}), 123.14 (CH_{Pyr}), 107.97(CH_{Pyr}), 107.74 (C_{quatAr}), 102.52 (C_{quatAr}), 86.53 (CH_{Ar}), 86.10 (CH_{Ar}), 35.96 (CH_{3Imi}), 30.05 (CH_{iPr}), 21.26 (CH_{3iPr}), 17.48 (CH_{3iPr}); ^{11}B-NMR (80.3 MHz, MeCN-d_3), δ: 1.29; MS (EI +25eV) *m/z* = 265.01 ($M^{+1}/2$); Anal. Calcd. for $C_{23}H_{29}BN_8BRuP_2F_{12}\cdot C_3H_6O$; C, 35.59; H, 4.02; N, 12.77. Found: C, 35.36; H, 3.87; N, 12.91.

[(N-methylimidazole)B(pyrazolyl)$_3$Mn(triscarbonyl)][PF$_6$] (3.13).

To a solution of $[Mn(CO)_3(MeCN)_3]PF_6$ (0.141 g, 0.34 mmol) in 10 ml of dry acetonitrile, Lig **2.21** (0.100 g, 0.34 mmol) was added in small portions. The reaction mixture was refluxed under N_2 and the reaction was monitorised by mass spectrometry. After 5h starting materials were no longer detected and the reaction was stopped and let it cool down to room temperature. Half of the solvent was removed under vacuum and the remaining solution was layered with 15 ml of dry Et_2O and stored at 5ºC overnight. A pale yellow solid precipitated, which was filtered off, washed with 10 ml of Et_2O and dried under vacuum to yield **3.13** as a pale yellow solid. (0.110 g, 0.25 mmol, 75%). Crystals suitable for X-ray were obtained by slow diffusion of Et_2O from a solution of **3.13** in acetone.

^{1}H-NMR (250.1 MHz, DMSO-d_6), δ: 9.69 (s, 1H), 8.36 (s, 1H), 8.23 (s, 1H), 8.17 (s, 3H), 8.09 (s, 3H), 6.55 (s, 3H), 3.86 (s, 3H); ^{13}C-NMR (62.9 MHz, $CDCl_3$), δ: 206.93 (C=O), 147.15 (CH_{Imi}), 141.48 (CH_{Imi}), 136.18 (CH_{Imi}), 125.42 (CH_{Pyr}), 125.08 (CH_{Pyr}), 107.97(CH_{pyr}), 36.43(CH_{Imi}); ^{11}B-NMR (80.3 MHz, DMSO-d_6), δ: 1.90; MS (EI +25eV) *m/z* = 433 (M+1); IR (MeCN): 2041, 1941 cm^{-1} (CO); Anal. Calcd. for $C_{16}H_{15}N_8BO_3MnPF_6$; C, 33.24; H, 2.62; N, 19.38. Found: C, 33.06; H, 2.50; N, 19.45.

[1-(1,8-diazabicyclo[5.4.0]undec-7-ene)B(methimazolyl)$_3$Ru(p-cymene][PF$_6$]$_2$ (3.14).

Ru(*p*-cymene)Cl_2 dimer (0.088 g, 0.14 mmol) was dissolved in 10 ml of dry EtOH and stirred at room temperature for 30 min. Ligand **2.20** (0.145 g, 0.28 mmol) was added in small portions and the mixture stirred for 2 hours. After this time the solution volume was reduced by half and NH_4PF_6 (0.117 g, 1.40 mmol) was added at once causing immediate precipitation of an orange-red solid. After filtration it was washed with 3 ml of dry EtOH and twice with 10 ml of dry Et_2O and dried under vacuum to yield **3.14**

(0.244 g, 0.23 mmol, 85%). Crystals suitable for X-ray were obtained from a solution of **3.14** in MeCN by slow diffusion with Et_2O.

^{1}H-NMR (250.1 MHz, DMSO-d_6), δ: 7.70 (d, 3H, J= 2.34 Hz), 7.25 (d, 3H, J= 2.34 Hz), 5.86 (d, 2H, J= 6.52 Hz), 5.76 (d, 2H, J= 6.52 Hz), 4.21 (m, 2H), 3.99 (m, 2H), 3.81 (s, 9H), 3.02 (sept, 1H, J= 7.43 Hz), 2.52 (m, 2H), 2.31 (s, 3H), 2.10 (m, 2H), 1.85 (m, 2H), 1.80 (m, 2H), 1.31 (d, 3H, J= 7.43Hz), 1.30(m, 4H); ^{13}C-NMR (62.9 MHz, DMSO-d_6), δ: 170.82 ($C_{quatDBU}$), 156.70 (C=S); 123.74 (CH_{Met}), 122.32 (CH_{Met}), 105.59 (C_{quatAr}), 101.23 (C_{quatAr}), 85.80 (CH_{Ar}), 85.6 CH_{Ar}), 84.52 (CH_{Ar}), 83.43 (CH_{Ar}), 55.40 (CH_{2DBU}) 49.69 (CH_{2DBU}) 45.37 (CH_{2DBU}) 35.87 (CH_{3Met}), 34.66 (CH_{2DBU}) 30.32 (CH_{2DBU}) 22.58 (CH_{2DBU}) 22.25 (CH_{2DBU}) 18.46 (CH_{2DBU}); ^{11}B-NMR (80.3 MHz, DMSO-d_6), δ: 4.32; MS (EI +25eV) *m/z* = 369.2 (M^{+1}/2); Anal. Calcd. for $C_{31}H_{45}BN_8S_3RuP_2F_{12}.H_2O$; C, 35.60; H, 4.53; N, 10.72. Found: C, 35.32; H, 4.30; N, 10.92.

EXPERIMENTAL PART CHAPTER IV

Oxazoline ring-opening product (4.16).

4(*R*)-methyl-5(*R*)-phenyl-2-oxazoline (0.118 g, 0.73 mmol), tris(dimethylamino)borane (128 μl, 0.73 mmol) and methimazole (0.250 g, 2.18 mmol) were heated to reflux in dry toluene (10 ml) for 12 h. A pale yellow solid precipitated, which was isolated by cannula filtration under N_2. The solid was washed twice with dry hexane and dried under high vacuum to give **4.16** (0.112 g, 0.25 mmol, 35%) as a pale yellow hygroscopic solid.

^{1}H-NMR (250.1 MHz, DMSO-d_6), δ: 8.60 (s, 1H), 7.46 (d, 1H, J= 2.2Hz), 7.35- 7.15 (m, 5H), 6.71 (d, 1H, J= 2.2Hz), 6.53 (d, 1H, J= 2.3Hz), 6.26 (d, 1H, J= 5.2Hz), 6.16 (d, 1H, J= 2.3Hz), 4.53 (dq, 1H, J= 5.2, 6.7Hz), 3.53 (s, 3H, CH_3), 3.49 (s, 3H, CH_3), 3.19 (s, 6H, CH_3), 0.67 (d, 3H, J = 6.7Hz); ^{13}C-NMR (62.9 MHz, DMSO-d_6), δ: 162.29 (C=S), 161.54 (N=C-S), 156.47 (CH), 138.93 ($C_{quatCHar}$), 127.02 (CH_{Ar}), 125.92 (CH_{Ar}), 125.07 (CH_{Ar}), 119.61 (CH_{Met}), 118.54 (CH_{Met}), 117.17 (CH_{Met}), 117.02 (CH_{Met}), 79.13 (CH), 55.90 (CH), 33.61 (CH_{3Met}), 33.48 (CH_{3Met}), 31.28 (CH_{3Imi}), 16.21 (CH_3); ^{11}B-NMR (80.3 MHz, DMSO-d_6), δ: 1.88; MS (EI +25eV) *m/z* = 443 (M^{+1}); IR(MeOH):

1675 cm^{-1} (formamide C=O). The air-sensitivity of **4.16** prevented its satisfactory elemental analysis.

[{(4R,5R)-4-methyl-5-phenyl-2-oxazoline}B(pyrazolyl)$_2$NMe$_2$] (4.22).

4(*R*)-methyl-5(*R*)-phenyl-2-oxazoline (0.118 g, 0.73 mmol), tris(dimethylamino)borane (128 μl, 0.73 mmol) and pyrazole (0.148 g, 2.18 mmol) were heated to reflux in dry toluene (10 ml) for 12 h. A colourless solid precipitated which was isolated, washed twice with dry ether and dried in vacuum to give **4.22** (0.180 g, 0.25 mmol, 30%) as a colourless solid.

^{1}H-NMR (250.1 MHz, $CDCl_3$), δ: 7.83 (d, 1H, J= 2.1Hz), 7.46 (d, 1H, J= 1.5Hz), 7.38-7.15 (m, 5H), 6.22 (t, 2H, J= 1.5Hz), 6.11 (t, 2H, J= 1.5Hz), 5.56 (d, 2H, J= 8.5Hz), 4.48 (ddq, 1H, J= 2.1, 6.6, 8.5Hz), 3.10 (br, 3H), 3.05 (br, 3H), 0.78 (d, 3H, J= 6.6Hz); ^{13}C-NMR (62.9 MHz, $CDCl_3$), δ: 154.53 (CH_{Ox}), 139.57 (C_{quatOx}), 128.52 (CH_{Ox}), 127.68 (CH_{Ox}), 126,88 (CH_{Ox}), 105.06 (CH_{Pyr}), 104.87 (CH_{Pyr}), 104.74 (CH_{Pyr}), 79.12 (CH_{Ox}), 57.33 (CH_{Ox}), 46.41 (CH_{3NMe}), 17.77 (CH_{3Ox}); ^{11}B-NMR (80.3 MHz, $CDCl_3$), δ: 7.8; MS (EI +25eV) *m/z* = 350 (M^{+1}); The air-sensitivity of **4.22** prevented its satisfactory elemental analysis.

(-) tetramisole] (4.8).

[(-) tetramisole hydrochloride] (0.500 g, 2.07 mmol) was dissolved in 50 ml of water and 10ml of 1M NaOH. 15 ml of AcOEt were then added and the mixture was stirred for 30 min. The organic phase was extracted, dried over $MgSO_4$ and the solvent was removed under vacuum to yield a colourless oil. This oil was immediatelly distilled off using a Kugelrohr apparatus. At 175^{0}C under vacuum (1.5 mbar) **4.8** was distilled off as a crystalline colourless highly hygroscopic oil (in contact with air it gets protonated immediatelly solidifying at once).

^{1}H-NMR (250.1 MHz, $CDCl_3$), δ: 7.36- 7.26 (m, 5H), 5.45 (t, 1H, J= 8.75Hz), 3.70-3.58 (m, 2H), 3.52-3.46 (m, 1H), 3.36-3.31 (m, 1H), 3.11 (q, 1H, J= 8.75Hz), 2.98 (t, 1H, J= 8.75Hz); ^{13}C-NMR (62.9 MHz, $CDCl_3$), δ: 178.16 (C_{quat}), 142.54 (C_{quat}), 132,27 (CHar), 128,54 (CHar), 71.34 (CH), 57.12 (CH_2), 52.76 (CH_2), 39.43 (CH_2). Highly hygroscopic colourless oil.

[(-) tetramisole)B(methymazolyl)]$_3$ (4.24).

(-) Tetramisole (0.116 g, 0.57 mmol), tris(dimethylamino)borane (100 μl, 0.57 mmol) and methimazole (0.195 g, 1.71 mmol) were refluxed in 10 ml of dry toluene for six hours. After this time no peaks from the starting materials were detected by mass spectrometry. Heating was discontinued and the solvent was half removed. 30 ml of dry ether were added to precipitate **4.24** as a colourless solid. (0.262 g, 0.47 mmol, 83%).

^{1}H-NMR (250.1 MHz, $CDCl_3$), δ: 7.48–7.23 (m, 5H), 7.17 (d, 3H, J= 2.31Hz), 6.71 (d, 3H, J= 2.31Hz), 4.47 (t, 1H, J= 9.08Hz), 3.81-3.72 (m, 4H), 3.62 (s, 9H), 3.50-3.44 (m, 2H); ^{13}C-NMR (62.9 MHz, $CDCl_3$), δ: 160.19 (C=S), 140.52 (C_{quat}), 131.06 (CH_{Ar}), 127.90 (CH_{Ar}), 126.32 (CH_{Ar}), 119.12 (CH_{Met}), 116.95 (CH_{Met}), 71.73 (CH), 58.50 (CH_2), 48.25 (CH_2), 36.30 (CH_3), 35.73 (CH_2); MS (EI +25eV) *m/z* = 555 (M^{+1}), 441 (M^{+1}-het); Anal. Calcd. for $C_{23}H_{27}BN_8S_4$; C, 49.81; H, 4.91; N, 20.20. Found: C, 49.12; H, 4.80; N, 21.45.

[(-) tetramisole)B(methimazolyl)]$_3$ Ru(p-cymene)](PF$_6$)$_2$ (4.25).

[Ru(*p*-cymene)Cl_2]$_2$ (0.056 g, 0.09 mmol) were dissolved in 10 ml of dry acetonitrile and stirred for 30 min at room temperature. Lig **4.24** (0.101 g, 0.18 mmol) was added in small portions and the crude stirred at room temperature for 5 hours. Complexation was followed by mass spectrometry and also visually since the redish solution of the ruthenium precursor gradually turned to deep red upon complexation. After this time the solvent was removed under vacuum and redissolved in 10 ml of dry MeOH. The crude was stirred for 30 min and NH_4PF_6 (0.150 g, 0.91 mmol) was added at once. Immediate precipitation of **4.24** took place and the mixture was stirred vigorously for 15 min. After this time the solvent was filtered under N_2 and the red solid was washed with 3 ml of dry MeOH and 20 ml of dry Et_2O, and dried under vacuum to yield **4.25** as a redish solid (0.086 g, 0.08 mmol, 89%). Both diastereomers were synthesised in a 2:1 ratio.

^{1}H-NMR (250.1 MHz, CD_2Cl_2), δ: 7.56- 7.26 (m, 7.5H), 7.20- 7.01 (m br, 4.5H), 5.90 (d, 0.5H, J= 2.31Hz), 5.88 (d, 1H, J= 2.31Hz), 5.41- 5.33 (dq, 6H, J= 5.78Hz), 4.60 (t,

0.5H, J= 10.50), 4.50 (t, 1H, J= 10.50Hz), 4.19-4.02 (m, 2H), 3.98-3.83 (m, 4H), 3.73 (s, 9H), 3.72 (s, 4.5H), 3.69-3.66 (m, 3H), 2.96 (d sept, 1.5H, J= 6.71Hz), 2.25 (s, 3H), 2.22 (s, 1.5H), 1.25 (dd, 9H, J= 6.71Hz); ^{13}C-NMR (62.9 MHz, CD_2Cl_2), δ: 140.27 ($C_{quatTetr}$), 140.23 ($C_{quatTetr}$), 131.27 (C_{ArTetr}), 130.83 (C_{ArTetr}), 130.49 (CH_{ArTetr}), 130.38 (CH_{ArTetr}), 126.58 (CH_{ArTetr}), 126.37 (CH_{ArTetr}), 108.28 (CH_{Met}), 107.98 (CH_{Met}), 102.36 (CH_{Met}), 102.22 (CH_{Met}), 85.85 (CH_{pcym}), 85.71 (CH_{pcym}), 85.44 (CH_{pcym}), 85.17 (CH_{pcym}), 85.13 (CH_{pcym}), 85.10 (CH_{pcym}), 84.13 (CH_{pcym}), 84.02 (CH_{pcym}), 73.33 (CH_{Tetr}), 72.98 (CH_{Tetr}), 57.63 (CH_{2Tetr}), 57.15 (CH_{2Tetr}), 49.04 (CH_{2Tetr}), 47.98 (CH_{2Tetr}), 37.99 (CH_{2Tetr}), 36.80 (CH_{2Tetr}), 36.62 (CH_{3Met}), 36.53 (CH_{3Met}), 31.52 (CH_{pcym}), 31.49 (CH_{pcym}), 23.50 (CH_{3pcym}), 23.40 (CH_{3pcym}), 23.10 (CH_{3pcym}), 23.02 (CH_{3pcym}), 19.73 (CH_{3pcym}), 19.63 (CH_{3pcym}); MS (EI +25eV) *m/z* = 394.5 (M^{+1}/2); Anal. Calcd. for $C_{33}H_{41}BN_8S_4RuP_2F_{12}$; C, 36.71; H, 3.83; N, 10.38. Found: C, 35.89; H, 3.78; N, 9.41.

[(-) tetramisole)B(pyrazolyl)]$_3$ (4.27).

(-) Tetramisole (0.116 g, 0.57 mmol), tris(dimethylamino)borane (100 μl, 0.57 mmol) and pyrazole (0.116 g, 1.71 mmol) were refluxed in 10 ml of dry toluene for two hours. After this time no peaks from the starting materials were detected by mass spectrometry. Heating was discontinued and the solvent was removed. The colourless powder obtained was washed carefully three times with 10 ml of dry ether to yield upon filtration **4.27** as a colourless solid. (0.201 g, 0.48 mmol, 85%).

^{1}H-NMR (250.1 MHz, $CDCl_3$), δ: 7.63 (d, 3H, J= 1.65Hz), 7.27–7.10 (m, 5H), 7.05 (d, 3H, J= 2.31Hz), 6.11 (dd, 3H, J= 2.31, J= 1.65Hz), 4.13 (t, 1H, J= 9.08Hz), 3.65 (m, 4H), 3.48 (dd, 2H, J= 9.08Hz); ^{13}C-NMR (62.9 MHz, $CDCl_3$), δ: 142.07 (C_{quat}), 141.31 (C_{quat}); 135.70 (CH_{Pyr}), 129.01 (CH_{Ar}), 128.13 (CH_{Ar}), 126.38 (CH_{Ar}), 105.98 (CH_{Pyr}), 105.94 (CH_{Pyr}), 71.40 (CH), 57.92 (CH_2), 48.63 (CH_2), 35.87 (CH_2); MS (EI +25eV) *m/z* = 417.09 (M^{+1}); Anal. Calcd. for $C_{20}H_{21}BN_8S$; C, 57.70; H, 5.08; N, 26.92. Found: C, 56.96; H, 4.78; N, 28.11.

[(N-methylimidazole)B{1-(S-)α-methylbenzyl-2-mercapto-imidazolyl}$_3$ (4.29).

Tris(dimethylamino)borane (71.5 µl, 0.41 mmol), *N*-methylimidazole (33 µl, 0.41 mmol), and 1-(*S*-)α-methylbenzyl-2-mercapto-imidazole (0.250 g, 1.23 mmol) were heated to reflux in dry toluene (8 ml) for 12 h to give a clear solution. Evaporation of the solvent resulted in a brown solid which was washed twice with dry hexane (5 ml) to yield **4.29** (0.236 g, 0.34 mmol, 82%) as a pale brown powder.
^{1}H-NMR (250.1 MHz, DMSO-d$_6$), δ: 8.80 (s, 1H), 7.51 (s, 1H), 7.42 (s, 1H); 7.40-7.22 (m, 15H), 6.95 (d, 3H, J= 2.35Hz), 6.32 (d, 3H, J= 2.35Hz), 6.12 (q, 3H, J= 5.85Hz), 3.65 (s, 3H), 1.77 (d, 9H, J= 5.85Hz); ^{13}C-NMR (62.9 MHz, DMSO-d$_6$), δ: 160.66 (C=S), 141.43 ($C_{quat\ \alpha\text{-}MeBzMet}$), 129.03 ($CH_{NIm}$), 128.59 ($CH_{Ar\ \alpha\text{-}MeBzMet}$), 128.34 ($CH_{NIm}$), 127.58 ($CH_{NIm}$), 126.73 ($CH_{Ar\ \alpha\text{-}MeBzMet}$), 125.45 ($CH_{Ar\ \alpha\text{-}MeBzMet}$), 115.57 ($CH_{Met}$), 114.96 ($CH_{Met}$), 53.43 ($CH_{\alpha\text{-}MeBzMet}$), 35.24 ($CH_{3NIm}$), 21.17 ($CH_{3\ \alpha\text{-}MeBzMet}$); ^{11}B-NMR (80.3 MHz, DMSO-d$_6$), δ: 3.54; MS (EI +25eV) *m/z* = 703 (M^{+1}); Anal. Calcd. for $C_{37}H_{39}BN_8S_3$: C, 63.23; H, 5.59; N, 15.94. Found: C, 63.19; H, 5.54; N, 15.98.

[{(N-methylimidazole)B(1-(S-)α-methylbenzyl-2-mercapto-imidazolyl)$_3$}Ru(p-cymene)][PF$_6$]$_2$ (4.30).

[Ru(*p*-cymene)Cl$_2$]$_2$ (0.052 g, 0.085 mmol) and the ligand **4.30** (0.120 g, 0.17 mmol) were stirred in dry ethanol (8 ml) at room temperature overnight. The solution was then stirred for 4h at 70°C. The solvent was half removed under vacuum and ammonium hexafluorophosphate (0.140 g, 0.85 mmol) was added resulting in immediate precipitation of **4.30** (0.177 g, 0.14 mmol, 85%) as a red solid. After filtration crystals suitable for X-ray analysis were obtained by diffusion of ether into a solution of the complex in methanol.
^{1}H-NMR (250.1 MHz, DMSO-d$_6$), δ: 9.26 (s, 1H), 8.05 (s, 1H), 7.75 (s, 1H), 7.72-7.41 (m, 15H), 7.38 (d, 3H, J= 2.35Hz), 7.36 (d, 3H, J= 2.35Hz), 6.55 (q, 3H, J= 5.85Hz), 5.04 (d, 1H, J= 5.42Hz), 5.02 (d, 1H, J= 5.85Hz), 4.93 (d, 1H, J= 5.42Hz), 4.91 (d, 1H, J= 5.85Hz), 4.08 (s, 3H), 2.20 (sept, 1H, J= 6.9Hz), 1.98 (d, 9H, J= 7.0Hz), 1.6 (s, 3H), 0.98 (d, 3H, J= 6.9Hz), 0.95 (d, 3H, J= 6.9Hz); ^{13}C-NMR (62.9 MHz, DMSO-d$_6$), δ: 158.64 ($C{=}S_{Met}$), 141.43 ($C_{quat\ \alpha\text{-}MeBzMet}$), 140.23 ($C_{quat\ Ar\ pcym}$),

128.79 ($C_{quatAr\ pcym}$), 128.73 (CH_{NIm}), 127.89 ($CH_{Ar\ \alpha\text{-}MeBzMet}$), 126.75 ($CH_{Ar\ \alpha\text{-}MeBzMet}$), 126.47 ($CH_{Ar\ \alpha\text{-}MeBzMet}$), 125.91 ($CH_{NIm}$), 124.13 ($CH_{NIm}$), 123.44 ($CH_{Met}$), 120.10 ($CH_{Met}$), 105.71 ($CH_{Ar\ pcym}$), 103.58 ($CH_{Ar\ pcym}$), 102.46 ($CH_{Ar\ pcym}$) 101.46 ($CH_{Ar\ pcym}$), 84.30 ($CH_{i\text{-}Pr\ pcym}$), 55.78 ($CH_{\alpha\text{-}MeBzMet}$), 48.78 ($CH_{3\ iPr\text{-}pcym}$), 47.81 ($CH_{3\ iPr\text{-}pcym}$), 45.26 ($CH_{3\ Me\text{-}pcym}$), 35.77 ($CH_{3\ NIm}$), 22.15 ($CH_{3\ \alpha\text{-}MeBzMet}$); ^{11}B-NMR (80.3 MHz, DMSO-d_6), δ: 3.32; MS (EI +25eV) *m/z* = 469(M^{+1}); Anal. Calcd. for $C_{47}H_{53}BN_8S_3{\cdot}Ru\ (PF_6)_2$: C, 45.97; H, 4.35; N, 9.13. Found: C, 45.93; H, 4.38; N, 9.14.

[{(N-methylimidazole)B(methimazolyl)$_3$}Ru(p-cymene)][TRISPHAT]$_2$ (4.31).

Method A. EXTRACTIVE PROCESS.

[{(*N*-methylimidazole)B(methimazolyl)$_3$}Ru(*p*-cymene)][Cl]$_2$ (0.025 g, 0.033 mmol) was dissolved in 10 ml of water and stirred for 20 min. (^{n}Bu)$_3$NH TRISPHAT (0.033 g, 0.033 mmol) were dissolved in 10 ml of $CHCl_3$ and stirred for 20 min. The ruthenium solution was added slowly over the organic one and the mixture was stirred for 10 min. Immediate colour change took place, the organic phase turning orange. The organic phase was isolated, dried over $MgSO_4$ and the solvent removed to yield **4.31** as an orange powder (0.029 g, 0.013 mmol, 78%).

Method B. CHROMATOGRAPHIC RESOLUTION.

[{(*N*-methylimidazole)B(methimazolyl)$_3$}Ru(*p*-cymene)][PF_6] (0.010 g, 0.01 mmol) and TRISPHAT chinchonidinium (0.010 g, 0.01 mmol) were mixed in 10 ml of acetone and stirred for 10 min. The crude was charged in silica and passed through a silica column with CH_2Cl_2 as eluyent. A broad band was observed and collected to yield **4.31** as a redish solid after removal of the solvent in the rotavaporator.

^{1}H-NMR (250.1 MHz, CD_2Cl_2), δ: 8.99 (s, 1H, *N-Imi*), 8.93 (s, 1H, **N-Imi*), 7.68 (t, 1H, J= 1.57Hz *N-Imi*), 7.62 (t, 1H, J= 1.57Hz **N-Imi*), 7.39 (dt, 2H, J= 1.57Hz *N-Imi**), 7.02 (d, 3H, J= 2.43Hz, *Met*), 6.97 (d, 3H, J= 2.43Hz, *Met**), 6.62 (d, 3H, J= 2.43Hz, *Met*), 6.36 (d, 3H, J= 2.43Hz, *Met**), 5.46-5.43 (m, 4H, *pcym*), 5.41-5.34 (m, 4H, *pcym**), 4.20 (s, 3H, *NImi*), 4.11 (s, 3H, *NImi**), 3.73 (s, 18H, *Met´**), 2.98

(dsept, 2H, J= 6.88Hz, *pcym´**), 2.25 (s, 6H, *pcym´**), 1.29- 1.23 (dd, 12H, J= 6.88Hz, *pcym´**); ^{13}C-NMR (62.9 MHz, DMSO-d_6), δ: 160.43 (C=S); 159.91 (C=S*), 142.13 (C_{quatAr}), 141.90 ($C_{quat\ Ar*}$), 140.09 (CH-$_{2Imi}$), 139.76 (CH-$_{2Imi*}$), 134.21 (C_{quatAr}), 133.65 ($C_{quat\ Ar*}$), 129.54 (CH $_{Ar}$), 129.04 (CH $_{Ar*}$), 125.65 (CH $_{Imi}$), 125.12 (CH $_{Imi*}$), 124.34 (CH $_{Imi}$), 124.03 (CH $_{Imi*}$), 123.32 (CH $_{Met}$), 123.01 (CH $_{Met*}$), 115.23 (CH $_{Met}$), 114.78 (CH $_{Met*}$), 107.05 (CH $_{Ar}$), 106.89 (CH $_{Ar*}$), 96.36 (CH_{iPr}), 96.12 (CH_{iPr*}), 41.24 (CH_3 $_{iPr\ or\ Me}$), 41.03 (CH_3 $_{iPr\ or\ Me*}$), 40.25 (CH_3 $_{iPr\ or\ Me}$), 40.12 (CH_3 $_{iPr\ or\ Me*}$), 36.74 (CH_3 $_{Imi}$), 36.32 (CH_3 $_{Imi*}$), 31.57 (CH_3 $_{Met}$), 31.24 (CH_3 $_{Met*}$); ^{11}B-NMR (80.3 MHz, DMSO-d_6), δ: 3.52; ^{31}P NMR (101.3 MHz, CD_2Cl_2): δ = -79.0 ppm; MS (ES +25eV) *m/z* =334 ($M^{+1}/2$), (ES –25eV): *m/z* = 769 (TRISPHAT); Anal. Calcd. for $C_{62}H_{35}BCl_{24}N_8O_{12}S_3RuP_2$: C, 33.77; H, 1.60; N, 5.08. Found: C, 35.03; H, 1.90; N, 5.24.

REFERENCES CHAPTER V

1. S. B. Jensen, S. J. Rodger, M. D. Spicer, *J. Organomet. Chem.,* 1998, **556**, 151.
2. R. H. Reimann, E. Singleton, *J. Chem. Soc., Dalton Trans.,* 1974, 808.
3. W. R. Leonard, J. L. Romine, A. I. Meyers, *J. Org. Chem.,* 1991, **56**, 1961.
4. N. A. Boland, M. Casey, S. J. Hynes, J. W. Matthews, M. P. Smyth. *J. Org. Chem.,* 2002, **67**, 3919.
5. F. Favarger, C. Goujon-Ginglinger, D. Monchaud, J. Lacour, *J. Org. Chem.,* 2004, **69**, 8521.